2019

Therapeutic efficacy of small molecule inhibitors of human respiratory syncytial virus (hRSV) in neonatal lambs

Panchan Sitthicharoenchai
Iowa State University

Therapeutic efficacy of small molecule inhibitors of human respiratory syncytial virus (hRSV) in neonatal lambs

by

Panchan Sitthicharoenchai

A dissertation submitted to the graduate faculty

in partial fulfillment of the requirements for the degree of

DOCTOR OF PHILOSOPHY

Major: Veterinary Pathology

Program of Study Committee:
Mark R. Ackermann, Co-major Professor
Jesse M. Hostetter, Co-major Professor
Rachel J. Derscheid
Michael J. Yaeger
Marian L. Kohut

The student author, whose presentation of the scholarship herein was approved by the program of study committee, is solely responsible for the content of this dissertation. The Graduate College will ensure this dissertation is globally accessible and will not permit alterations after a degree is conferred.

Iowa State University

Ames, Iowa

2019

DEDICATION

This dissertation is dedicated to the late King of Thailand,

His Majesty King Bhumibol Adulyadej.

TABLE OF CONTENTS

LIST OF FIGURES

Page

CHAPTER 4 EFFICACY AND TIME WINDOW FOR TREATMENT WITH COMBINATION THERAPY OF THE HUMAN RESPIRATORY SYNCYTIAL VIRUS (HRSV) FUSION INHIBITOR AND NON-FUSION PROTEIN INHIBITOR IN HRSV INFECTED LAMB MODEL

LIST OF TABLES

Page

ACKNOWLEDGMENTS

I would like to extend my thanks to the most important person contributing to this work, my major advisor, Dr. Mark R. Ackermann, for accepting this foreign visiting scholar that walked into his office one day asking if she could do her PhD research with him and be part of his lab. Without him, the lamb projects would never have been possible. To every current and former Ackermann Lab members, whom with or without knowing it, have contributed one way or another to the making of this dissertation.

I would also like to give my appreciation to all the committee members; Dr. Jesse Hostetter, for accepting and stepping in as the co-major advisor, Dr. Mike Yaeger, for his humor and care over my research work, future career and correct English language usage, Dr. Rachel Derscheid, for all her pre-existing work on the lamb projects and Dr. Marian Kohut, for her positive attitude and support.

In addition, I would like to express thanks to my family for their long distance encouragements as well as my fellow colleagues and resident mates at the Department of Veterinary Pathology, Sarhad Alnajjar, Alyona Michael, Eric Cassmann, Jeba Jesudoss Chelladurai, Tyler Harm, Ariel Nenninger, Ya-Mei Chen and Saleh Albarrak, for their assistance throughout the course of my study and made coming to work feeling like going to a party even on the worst days.

Lastly, I would like to give my most profound gratitude to Anandamahidol Foundation for sponsoring the entire duration of this graduate study.

ABSTRACT

Human respiratory syncytial virus (hRSV) is a common cause of respiratory infection in human infants worldwide. Direct therapeutic methods for the prevention and treatment such as vaccination and antiviral therapy are limited. In studies within this dissertation, we determined the efficacy of orally administered small molecule fusion inhibitor and replication inhibitor in hRSV-infected neonatal lambs which model hRSV infection in infants. Furthermore, we evaluated the efficacy and treatment time window for administration of a combination treatment using both compounds. We determined that daily oral administration of small molecule fusion protein inhibitor (JNJ-53718678) and replication inhibitor (JNJ-64166037) first administered to hRSV-infected within 24 hpi, reduced the viral load and lung lesion in a dose-dependent manner. The combination treatment of both hRSV fusion inhibitor and replication inhibitor given at 24 hpi decreased the amount of virus and pulmonary lesion in a more profound manner than monotherapeutic administration of each compound. Interestingly, the delayed combination treatment starting at day 3 post infection demonstrated significant reduction of viral load and pulmonary lesion compared to monotherapy administered at similar time indicating a prolonged treatment time window. The small molecule inhibitor compounds used in this study are good therapeutic candidates for future tests in human clinical trials.

In addition, we were able to quantify and localize the hRSV viral RNA with RNA *in situ* hybridization in the infected lung tissue as well as effectively quantify the amount of RNA expression by modification of RNAscope® H scoring evaluation method using an image analyzer software. A new approach for assessment of cytokine expression in lung of infected lambs was performed by creating a baseline of cytokine expression of Memphis

37 hRSV infected and non-infected lambs at 6 dpi through combining data from multiple lamb model studies.

CHAPTER 1. GENERAL INTRODUCTION

Statement of the Problem

Human respiratory syncytial virus (hRSV) is a common cause of respiratory infection in infants and children worldwide [1]. This ubiquitous virus affects mainly the respiratory system causing rhinitis, bronchiolitis, pneumonia and occasionally otitis media. The most commonly susceptible individuals are children younger than 5 years old and over the age of 65. Disease surveillance of hRSV determined that >57,000 children under the age of 5 years were hospitalized annually due to RSV-associated acute respiratory illness (ARI) [2]. The disease outcome can be severe and fatal in preterm infants and children younger than 1 year of age [1, 3, 4]. Approaches to prevent and treat hRSV includes vaccination, therapeutic antibodies, and antiviral drugs. Development of such therapeutic compounds and vaccines require extensive laboratory testing, animal trials in the preclinical stage and multiple phases of clinical trials. Our laboratory has established an hRSV-infected lamb model that has been proven suitable for many types of therapeutic and vaccination trials as well as pathogenesis studies [5-7]. The goal of this dissertation is to demonstrate the therapeutic efficacy of small molecule inhibitors of hRSV via intragastric administration in our neonatal lamb model of hRSV infection.

Central Hypothesis and Specific Aims

By administering different types of therapeutic compounds, including monotherapy of fusion protein inhibitor, monotherapy of non-fusion protein inhibitor and combination of both, to groups of hRSV infected lambs, our central hypothesis is that these compounds will reduce the clinical signs, amount of hRSV pulmonary viral load and lesions in hRSV infected lambs.

To test this hypothesis, the following were determined in hRSV-infected lambs: 1) the efficacy of fusion protein inhibitor (JNJ-53718678), 2) the efficacy of non-fusion protein, replication inhibitor (JNJ-64166037), and 3) the efficacy and treatment time window when administrating combination of a fusion protein inhibitor and a non-fusion protein inhibitor.

Dissertation Organization

This dissertation is divided into five chapters organized in the journal paper format. The first chapter (Chapter 1) describe the general knowledge and literature review related to the study. The following four chapters (Chapter 2-4) are individual manuscripts with references cited at the end of each chapter. The last chapter (Chapter 5) is the general conclusion. The first manuscript was published as part of an article in *Nature Communications*. The second and third manuscripts are prepared for submission to appropriate journal including *Antiviral Research, Journal of Virology, Antimicrobial Agents and Chemotherapy, Plos One,* and other related journals.

Literature Review

Human Respiratory Syncytial Virus (hRSV)

Viral classification and characteristics of hRSV

Human respiratory syncytial virus (hRSV), first discovered in 1956, is an enveloped non-segmented negative sense single stranded RNA virus. The virus belonged in the subfamily Pneumovirinae under Paramyxoviridae family, but have recently been reclassified into the family Pneumoviridae, genus Orthopneumovirus [8]. The hRSV virus is pleomorphic and covered by large glycoprotein spiked and herringbone-shaped nucleocapsid. The genome is 15.2 kbp with 2 open reading frames, composed of 10 genes encoding for 11 proteins;

transmembrane proteins (G, F and SH), nucleocapsid protein (N), phosphoprotein (P), large polymerase protein (L), matrix protein (M), transcription factors (M2-1 and M2-2) and two non-structural proteins (NS1 and NS2). Infection of the virus is through the attachment of G and F protein and the entry is promoted by fusion of F protein with the host plasma membrane. Syncytial formation of infected cells initiated by F protein is a characteristic feature of this virus that mediates the spread of viral infection.

Epidemiology of hRSV infection

Respiratory syncytial virus mainly targets and infects the epithelial cells of the respiratory tract, and most commonly causes mild disease symptoms. However, in infants and older individuals, the disease can be severe and fatal resulting in hRSV associated bronchiolitis, hospitalization and death in some cases [9]. Infection at a young age, especially among infants less than 6 months of age, and in preterm infants are independent risk factors for hospitalization by hRSV due to severe bronchiolitis and pneumonia with an intense acute inflammatory response in the lower respiratory tract [2, 10]. Furthermore, this virus is the most common cause of hospitalized bronchiolitis in infants and children (60-80% of all cases) [2, 11, 12], and along with human rhinoviruses, is one of the most common cause of acute respiratory infection (ARI) in infants [13, 14]. Most individuals (80-90%) are infected with hRSV at least once by two years of age [15]. Reinfections of the virus are common throughout life due to the short duration and partial protection of hRSV neutralizing antibody, though typically with milder clinical symptoms in uncomplicated cases [16, 17]. In addition to ARI, there is much evidence that support long-term respiratory problems, such as persistent or recurrent wheezing and asthma, associated with infants and children with history of hRSV lower respiratory tract infection and bronchiolitis [18-23].

Another group of individuals susceptible to severe disease from hRSV infection is elderly adults and especially those of more than 65 years of age [24]. Initial outbreaks were reported in nursing homes in the late 1970s resulting in cases of pneumonia and deaths [25, 26]. Further epidemiological and clinical data indicated elderly individuals with history of chronic heart and lung diseases are among high risk factors contributing to illness in this age group [27, 28].

Similar to influenza virus, seasonality is an important factor for hRSV infection with patterns of infection during specific times of the year. Epidemiological data have demonstrated a peaked pattern of hRSV activity during winter months in the temperate zone, but more variability of timing and durations in the tropical climate [29-31]. The knowledge of seasonality of hRSV infection is not only essential for epidemiologic predictions, but also has implications for prophylaxis, prevention and control program especially in individuals with high risks of hRSV infection including preterm infants and children under 6 months of age at peak hRSV season [32-34].

Pathogenesis of hRSV: Viral load and host immune response

The degree of severity with hRSV infection is related to many factors including the virus, host genetics contributing to the immune responses and environmental factors. Studies on hRSV viral loads revealed an association of higher level of hRSV with increased period of hospitalization, requirement of intensive care and respiratory failure in infants [35-37]. In addition, the host immune system also has a significant role in the hRSV disease severity. The components and balance of the host immune responses include the innate, cell-mediated and humoral immunity can result in different clinical manifestation of individuals infected with hRSV. Also, other factors that contribute to disease severity include immunocompromised

individuals [38, 39], immunomodulatory alterations associated Th1 and Th2 responses [40-43] and immune dysregulation [44, 45].

Once the hRSV virus enters the airways of the lung, its main viral target are respiratory epithelial cells with cell entry mediated through the attachment of G and F proteins. In response to the infection, the first line of defense to the virus are the host physical barriers and innate immunity. The respiratory tract mucociliary apparatus traps and removes pathogens and particulate matter from the airways. Furthermore, the respiratory mucosa produces surfactant proteins (SP), SP-A and SP-D, which enhances hRSV uptake by opsonization [46] and inhibits viral infection also through activation of macrophages [47]. Infection with hRSV triggers innate immune responses through binding of pattern recognition receptors (PRRs); TLR3, TLR4, TLR2, TLR7 and TLR9. Studies have shown that the double stranded RNA of hRSV can activate and upregulate TLR3 in lung epithelial cells and lung fibroblasts resulting in the activation of NK cells and several chemokines; CCL5 (RANTES), CXCL10 (IP-10) and CXCL8 (IL-8) [48, 49]. In addition, there are interactions between hRSV F proteins with TLR4 and its accessory protein, CD14, in human monocytes [50]. This interaction triggers the signal transduction pathway through STAT and NF-κB resulting in transcription of various cytokines (e.g., GM-CSF, TNF-α, CCL2 (MCP-1), CCL3 (MIP-1α), etc.) and α and β interferons [51]. A few studies have also demonstrated hRSV interaction with TLR2 [52], intracellular TLR7 and TLR9 [53], although the mechanisms of viral binding and downstream responses have not been thoroughly evaluated. Overall, the responses of the innate immune system not only protect the host against hRSV and provide time for adaptive immune development, but also establish the pathway of adaptive immune response and influence the disease outcome.

Various cellular components of the immune system respond to hRSV infection, and these include neutrophils, macrophages, eosinophils, dendritic cells, natural killer (NK) cells and lymphocytes. Neutrophils are recruited into the airway by cytokines and chemokines released from viral infected cells and are the predominant cell type associated with hRSV bronchiolitis [54-56]. The neutrophils induce damage and detachment of hRSV infected epithelial cells through degranulation and release of lytic enzymes [57]. The virus can infect or be opsonized by macrophage and monocytes which mediate antigen presentation and trigger inflammatory responses through the production various cytokines (e.g., proinflammatory cytokines (IL-6, TNF-α, IL-1β, GM-CSF, IL-16) and anti-inflammatory mediators (IL-10 and prostaglandin E (PGE)) [58]. Eosinophils are associated with bronchiolitis in hRSV infection and respond by degranulation and release of antiviral ribonucleases, such as eosinophil cationic protein and eosinophil-derived neurotoxin [59, 60]. These products may have positive effect on destroying the virus and infected cells, but also can contribute to pulmonary pathology [61]. Dendritic cells (DCs) contribute to defense by antigen presentation and cytokine release to stimulate and regulate the immune system response. Murine models of hRSV infection have demonstrated increases of both myeloid and plasmacytoid dendritic cells (pDCs) in the airways [62]. The pDC enhanced hRSV clearance suggesting an antiviral and protective role against hRSV [63] and increased myeloid DCs likely contribute to an inflammatory response during and after bronchiolitis [64]. NK cells and one of their main products, IFN-γ, are present at early stages of hRSV infection. Even though NK cells have important antiviral activity, few studies have characterized NK activity with hRSV infection and results are still inconclusive. Some studies have demonstrated higher NK cells and IFN-γ associated with less severe hRSV disease

in some individuals [65, 66], while other studies suggest NK cell involvement with acute lung injury in early RSV infection [67].

Infection by hRSV can stimulate the cell-mediated immune system through both $CD8^+$ and $CD4^+$ T lymphocytes by antigen presentation of DC in the draining lymph nodes. The stimulation of $CD8^+$ effector T cells is critical for the hRSV viral clearance [68-70]. In contrast, studies have also identified immune responses with pathological effects by effector and memory $CD8^+$ T cells in response to viral reinfection [69, 71]. The differentiation of $CD4^+$ T cells into Th1 or Th2 cells depends on the cytokines released during the innate immune response with the main cytokine, IL-12, stimulating differentiation to Th1 and IL-4, IL-5 and IL-13 stimulating the differentiation to Th2.

There is much evidence demonstrating a balance between Th1/Th2 responses that result in different pathological outcomes of the hRSV infection. Increased expression of Th2-type humoral response including IL-4, IL-5, IL-13 and IgE was seen in many studies of infants and children with severe hRSV infection [42, 72-74]. Furthermore, reduction in the Th1 effector cytokine, IFN-γ, and elevation of IL-4/IFN-γ ratio were demonstrated in cases of infants with acute bronchiolitis [42, 65]. Many investigators have tried to explain the cause of skewed Th2 response with severe disease of hRSV infection. Some of the hypotheses include the host immune status and immune modulatory effect from certain viral components. Immune response of infants tends to have stronger Th2 response than Th1 [75, 76]. Certain amino acid domains of hRSV G glycoprotein are involved in Th2 biased response in many pathogenesis studies and vaccine testing with cell cultures and animal models [77-79]. The infection of hRSV with a Th2 biased response is also associated with the development of allergy, asthma and wheezing [80, 81].

The humoral immune response is essential for protection of hRSV reinfection. Viral neutralizing antibodies are made against F and G proteins. Studies have shown detection of hRSV specific IgM, IgG, IgA in the serum and IgE and secreted IgA in the respiratory secretions of infant patients [82]. The first antibody response after infection, IgM, can be first detected around 5-10 days post infection and lasts as long as three months post infection. The peaked response of IgG is somewhat delayed for the first response to hRSV. The IgG titer reaches its peak around 20-30 days after the start of symptoms. The IgG response is produced faster and with higher magnitude upon the second exposure to the virus [83, 84]. IgA can be detected in both secreted and cell bound form in nasopharyngeal secretions. It is first present at 2 to 5 days after infection and peaks between 8-13 days after infection. Additionally, hRSV-specific IgE has been detected in infected children. In children less than 6 months of age, only about 50% had an antibody response to hRSV [85, 86]. This is likely due to the presence of passive maternal antibody and the weak responses of the immune system [87]. In one study , three quarters of adults infected with hRSV displayed a 4-fold decrease in neutralizing anti-hRSV IgG antibody one year after infection [88]. Thus, hRSV infection often produces a short duration of protective antibodies, which permits subsequent reinfection. Reinfections typically produce milder clinical symptoms in uncomplicated RSV upper respiratory tract infection [16, 17].

Regulation of immune responses to hRSV

Regulatory $Foxp3^{+}CD4^{+}CD25^{+}$ T cells (Treg) have an important role in regulating the inflammatory responses to hRSV. A number of studies were performed in laboratory rodents that identified a role of Treg cells in limiting immunopathology during the hRSV infection. Increases of pro-inflammatory cytokines, including IFN-γ and TNF-α, and number of $CD8^{+}$ T

cells were associated with enhanced disease severity in Treg-depleted mice [89]. Another study suggested that Treg contributes to the resolution of hRSV by reducing eosinophilia and Th2 response [41]. Modulation of B cell activity associated with Treg was seen in an hRSV-infected mice model, particularly through the decreased production of anti-F protein neutralizing antibody [90]. In cases of hRSV-infected hospitalized infants, there were reduced levels of circulating Treg and Foxp3+ mRNA for 3 weeks following acute infection [44, 91], although a different study did not show correlation between the number of Treg and disease severity [92]. Immunoregulatory cytokines such as IL-10 have also been demonstrated to have a role in the severity of hRSV infection. Higher expression of IL-10 regulate and inhibit the inflammatory response of mice infected with hRSV [93]. Certain single nucleotide polymorphisms of IL-10 gene also contribute to hRSV disease outcome [94].

Animal Models for hRSV and the Neonatal Lamb Model

Animal models for hRSV infection have been established for the purpose of studying the pathogenesis, immunological response and pharmaceutical testing with the objective of finding novel therapies and preventive measures [95, 96]. These include: 1) rodent models such as mice and cotton rats, 2) non-human primates (NHPs), such as rhesus macaques, baboons, and chimpanzees; 3) ruminants, such as cattle and neonatal lambs, and 4) ferrets. The ideal animal model would replicate key features of the disease in humans, including having similar anatomical structure, similar immunologic responses, clinical signs and respiratory tract lesions to hRSV infection. Nevertheless, many concerns and limitations are unavoidable with animal studies including animal husbandry, handling, housing, costs and ethical issues. Thus, understanding the strengths and weaknesses is crucial for constructing research experiments, performing laboratory tests and evaluation of the results of each animal study.

This section will briefly describe and update the advantages and disadvantages of animal models for hRSV with focus on the neonatal lamb model. Further details of other animal models had been reviewed elsewhere [95, 97, 98].

Cotton rats (*Sigmodon hispidus*) have become a standard model for evaluation of preventive and therapeutics agents for hRSV [97, 99, 100]. Cotton rats are relatively small and hRSV has a moderate degree of permissive viral replication. Specialized training in handling cotton rats is needed due to excitability, agility and aggressiveness towards handling of this species. Limited molecular tools for cotton rats can be an issue for selecting this model for hRSV studies, but recently there are more available immunological reagents specific for cotton rats. Another rodent species for hRSV are mice [98, 101]. The laboratory mouse is an exemplary model for gene target studies due to the wide use of transgenic mice and implication of genetic knockouts in this species. In addition, experiments using the mouse model are easier to conduct due to the relatively small size of the animal, low costs, and extensive molecular tools and assays available. Nevertheless, conducting hRSV studies in mice comes with disadvantages including the high genetic, immunological and anatomical structural differences from humans as well as low replication of hRSV in mice.

More closely related species to humans are non-human primates (NHPs). Even though these animal species have the most advantages in the similarity of genetic, anatomic, immunologic response to humans, the extensive husbandry care, ethical issues and expensive costs hinder the advancement of NHPs as model for hRSV. Studies of experimental hRSV infection have been performed in NHPs species including owl monkeys [102-104], baboons [105], cebus monkeys [106], African green monkeys [107, 108], bonnet monkeys [109-111], cynomolgus monkeys [112, 113], rhesus macaques [114-118], and most notably, the

chimpanzee. Chimpanzees are permissive to viral replication and develop clinical symptoms with hRSV infection [114, 119]. This model has been proven useful for vaccine studies [120, 121].

An experimental lamb model for hRSV infection was developed and this model has been more increasingly accepted in recent years. Lambs infected with hRSV mimic hRSV infection in human infants [122]. Lambs have similarities of lung development, structure, cellular components in airways, immunological responses, and bronchiolar lesions compared to human infants. The lamb lung undergoes prenatal alveologenesis as do human infants and there are also similarities in lung size, the airway branching pattern, the amount of submucosal glands in the airways and percentage of club cells (20-30%) to that of human infants [122-124]. The overall decrease of immune response including the pulmonary neutrophilic response to hRSV in the preterm lamb is similar to that of preterm infants. Other immunological factors that mimic the human includes the presence of dendritic cells (DCs) responses to hRSV [122], genetic expression of IL-8 (rodents lack IL-8 gene) [125-127], and presence of Duox/LPO system in the airways [128-130]. The lesions of hRSV-infected lamb are similar to human infection including necrotizing bronchiolitis, neutrophilic and lymphoplasmacytic infiltration with syncytial cell formation [131-135]. The viral antigen is present in bronchial and bronchiolar epithelial cells as well as infection in type II pneumocytes. Enhanced hRSV disease severity was demonstrated in preterm lambs compared to newborn lambs and in lambs vaccinated with formalin-inactivated hRSV vaccine [136]. Also, lambs are susceptible to at least three strains of hRSV (Memphis, A and Long strains) [122, 131] as well as bovine respiratory syncytial virus (bRSV) [137], ovine and human parainfluenza viruses [138]. Thus, the lamb model of hRSV infection can be used for modeling hRSV infection in newborn

infants, preterm infants, and also vaccine, therapeutic and potentially asthma studies. The ability to eliminate maternal passive immunity interference by use of colostrum-deprived lambs is another advantage of using this animal model. Lambs are easy to handle and restraint with large and accessible blood vessels for sampling or placement of an intravascular drug delivery system. The disadvantages of using lamb studies is finding the source of large-scale sheep breeding facilities to produce and customize the lamb for experimental use. A middle-size to large housing facility is needed with lamb studies compared to rodents, though not as specialized and extensive as NHPs. Another concern with using sheep experimental model is the limited molecular tools and genomic data for this animal species which can be more difficult to perform certain experimental assays, although key types of information are routine and proteomics as well as genetic assays are readily available.

Development of Vaccine and Therapeutic Agents for hRSV

Advancement in treatment, prevention and control methods is necessary for the fight against hRSV infection. For the past half a century, numerous studies have been designed to identify suitable vaccine and pharmaceutical agents for controlling hRSV infection. The development of vaccine and therapeutic agents of hRSV has been challenging for researchers and scientists, and competitive in the pharmaceutical world. Currently, there are no vaccines available for commercial use and commercially approved therapeutic agents are limited. The following section will give a brief review on the ongoing process and challenges of hRSV vaccine and therapeutic drugs development.

Vaccine development of hRSV

History of RSV vaccine development

The first human hRSV vaccine developed was a formalin-inactivated hRSV vaccine (FI-RSV) in the 1960s and the result was unsatisfactory. The vaccine did not protect against infection, but instead exacerbated the inflammation from subsequent hRSV infection in children [139]. The problem with vaccine-enhanced immunopathology of hRSV has led to many studies on and investigations of the virus, advanced techniques in hRSV vaccine development, and alternative tools for treatment and prevention. Several studies were conducted to answer why hRSV immunization caused vaccine-induced enhancement. Studies have suggested the mechanisms of this immunopathological outcome were from the production of hRSV non-neutralizing antibody [140, 141] and imbalance of Th1/Th2 responses associated with Th2 bias [80, 112, 142, 143], but the precise mechanism still remains unclear. Other than the formalin-inactivated vaccine, there are reports of other hRSV vaccine types resulting in the same vaccine-induced disease enhancement. Recombinant vaccinia virus (rVV) vaccine with expression of different hRSV proteins was tested in mice followed by challenge with hRSV. Results indicated that the rVV recombinant with G protein (rVV-G) induced eosinophilia and disease enhancement subsequent to viral challenge [144]. The route of inoculation is another factor in determining the disease enhancement. Inoculation of rVV-G intranasally or intraperitoneally appeared to induce protection against challenging with hRSV [145]. Host factors including age and genetic could additionally determining the post-vaccination outcome. There is evidence that the severity of symptoms is age dependent with younger children exhibiting more severe clinical signs [146, 147] and genetic predisposition to a Th2 response [148] is associated with vaccine-enhancement disease of hRSV.

Current RSV vaccine development strategies

The current goal is to develop hRSV vaccine that exhibit protection against hRSV and lack adverse effects. Many attempts in designing different types of RSV vaccines were undertaken (e.g. subunit vaccine, vector vaccine, live attenuated vaccine, etc.), but none has been licensed for human usage due to many factors, most importantly the safety concern associated with infants and children.

The subunit vaccines previously evaluated were based on the G and F proteins, the neutralization target. Newer vaccines are based on multivalent recombinant proteins and conformation change F protein epitope. As stated earlier, G protein could be integral in mediating the induction of vaccine-induced disease. Interestingly, studies have been made to pinpoint the G protein coding gene sequence site responsible for induction of pulmonary eosinophilia and disease enhancement [149]. With that in mind, a recombinant G protein fragment subunit vaccine was designed, and it had protection against hRSV challenge without inducing lung lesions in animal models [150-152]. However, this did not induce sufficient duration of protection from hRSV [153]. F subunit vaccines have been tested in many preclinical trials, some of which were safe and generated protection against hRSV challenge in children over the age of 1 year, adults and elderly [154-157]. Others have demonstrated evidence of same vaccine-enhanced immunopathology as those with FI-RSV. This may be associated with the formulated adjuvants in the vaccine [158, 159]. Studies of different conformation changes in F protein during cell attachment have led to a new candidate for F subunit vaccine. Results showed that pre-fusion F protein epitopes induces strong neutralizing antibody response [160]. The conformation metastability of the pre-fusion F protein compound that tends to spontaneously fold to the post-fusion F protein conformation is a challenge for

vaccine developers and biochemists [161, 162], and multiple studies were conducted and currently in pursuit to find the solution in stabilizing the protein construct and characterize the neutralizing epitopes [161, 163].

Intranasal immunization of live attenuated hRSV vaccines has shown no association with priming of disease enhancement [164]. Construction of live-attenuated hRSV vaccines are from two platforms; 1) attenuation of virus through viral cold passage or chemical mutagenesis [165, 166], 2) reverse genetically engineered virus [167]. Some recombinant live attenuated vaccines have advanced into phases of human and infant clinical trials with the aim to identify the level of attenuation to balance the effectiveness and the safety of the vaccine [167-170].

Combined application of subunit hRSV antigen with different Th1 promoting adjuvants was tested in order to overcome the vaccine-induced immunopathological enhancement from Th2 biased immune response. Monophosphoryl lipid A (MPL), QS21 or both, in combination with FG chimeric protein [171], single subunit protein [172] and even with FI-RSV, elicited better Th1-biased responses and reduced pulmonary inflammation. Addition of unmethylate CpG oligodeoxynucleotides (ODNs) to F protein subunit vaccine induces the production of IL-12 enhanced Th1 biased immune responses resulting in reduction of pulmonary eosinophilia and increased viral clearance efficacy from the lung of animal models [173, 174]. Administration of CpG prior to hRSV infection in neonate mice protected against disease enhancement [175]. When formulating CpG ODN with formalin-inactivated bovine respiratory syncytial virus (bRSV), this resulted in stimulation of high levels of antibody, IFN-γ expression and viral clearance after bRSV challenge [176]. Currently, human clinical trials

of CpG-ODNs hRSV vaccine have not been initiated and little is known about the effect of the vaccine in human infants with maternal-derived antibody and deviation of antibody responses.

The ISCOMS vaccine delivery system was also designed and tested for RSV surface protein with Th1 promoting adjuvant. The results were effective in both neonates and adult mice, including the development of good Th1/Th2 balance, high cell-mediated immune responses and protection from viral challenge, although there was evidence of pulmonary eosinophilia and a high level of IL-4 production in neonates [177]. To avoid the maternal antibody and stimulate the mucosal immune system, ISCOMS was also used for delivery of hRSV subunit mucosal vaccine. Other combination of adjuvants and hRSV antigens for mucosal administration includes FI-RSV with influenza virosomes and *E. coli* heat-labile toxin and fragment G subunit vaccine with cholera toxin B. Newer mucosal vaccine designs involve hRSV virosomes containing different Th1 promoting adjuvants (e.g., MPL, TLR2 and/or NOD-2 ligands) achieved protection against infection with hRSV without disease enhancement in animal models [178, 179].

Many vectored vaccines have been in trials for protection against hRSV. These have advantages to induce immune responses similar to that of natural infection and can produce antibodies against multiple pathogens. Additionally, adenovirus vectors are capable of inducing antibody even in the presence of maternal antibody. For hRSV, replicating vaccinia vector vaccines expressing hRSV proteins have been tested with little success due to safety concern of disease induced by the vector itself in infants and children [180-182]. More recent studies using a recombinant influenza virus vector vaccine with hRSV proteins protected against hRSV virus without priming of enhanced disease in mice and cotton rats [183]. Other vector hRSV vaccines tested were Sendai virus vector [184, 185], measles virus vector,

Newcastle disease virus vector with F protein [186] and modified Bacillus Calmette-Guerin (BCG) expressing multivalent RSV proteins [187].

Virus-like particles (VLPs) vaccines using different proteins have been developed. VLPs for hRSV were developed from an influenza virus matrix protein core with hRSV-F or G on the surface. The immunization of VLPs protected and reduced RSV viral load post challenge [188]. Mixed VLP of hRSV F and G proteins can provide high level of protection without vaccine-enhanced disease after hRSV infection. However, the use of VLP from G protein alone could cause vaccine-enhanced disease similar to FI-RSV [189]. More recently, smaller size VLP called nanoparticles, were designed from F protein and tested for efficiency. Purified hRSV F nanoparticles induces neutralizing serum antibodies and inhibition of viral replication in the lung without signs of disease enhancement in cotton mice [190]. Another nanoparticle vaccine used RSV G protein with CX3C chemokine motif induces similar results [191]. Additional tests were performed by immunizing animal models with combination of nanoparticles VLP of hRSV with DNA vaccine. These induced a significant Th1 immune response with high viral clearance, suggesting good potential as a hRSV vaccine candidate and further investigation on its effectiveness is warranted [192].

Therapeutic agents for prevention and treatment of hRSV

The general goal in developing hRSV therapeutic agents is to design compounds that inhibit viral entry into the respiratory epithelial cells and/or interfere with the viral replication. Two broad groups of therapeutic agents have been developed for hRSV; immunotherapy and small molecule inhibitor compound. Many of the hRSV therapeutics are in preclinical phase of development through *in vitro* testing and animal trials. The most common target for these therapeutic compounds is the F protein that functions in viral fusion and entry into the

respiratory epithelium. Some anti-fusion protein antibodies and fusion protein inhibitors have advanced to human clinical phases with only a few licensed for commercial use. Other targets for hRSV therapies include inhibition of viral RNA polymerase, nucleocapsid mRNA and hRSV nucleoprotein (N).

Immunotherapy against hRSV

Immunotherapy and the implication of monoclonal antibodies as therapeutics have been used extensively in human medicine and the advancement in this area has led to novel production of monoclonal antibodies that can manipulate the outcome of many diseases and disorders. The only approved immunotherapeutic compound against hRSV is palivizumab (Synagis®), a humanized monoclonal antibody against the F protein. It has shown to have good success in prophylactic treatment and was recommended for patients with higher risk of hRSV infection [193]. The mechanism of palivizumab is through the binding of viral F protein and neutralizing the virus, preventing it from entry into the host cells. Previous data indicated the use of palivizumab resulted in the reduction of hRSV-associated hospitalization rates by 55% in premature infants, when compared to a placebo [194]. Few studies have reported the use of palivizumab as an hRSV treatment [195]. However, due to the short half-life, the inconsistent effectiveness between individuals and the high cost, this treatment in no longer recommended for routine usage [196].

Other forms of F protein antibodies are currently in various phases of animal and clinical trials including polyclonal hRSV neutralizing antibody, RI-001 and RI-002 [197-199]; monoclonal antibody, REGN222 [200], MEDI8897 [201] and trimeric nanobody, ALX-0171 [7, 202, 203]. The polyclonal antibody RI-001 and RI-002 are derived from plasma donors

with high hRSV titers. The use of RI-001 was tested on children and adults who underwent an organ transplant, but the efficacy was difficult to assess due to lack of a control group [198, 199, 204]. REGN222 is a fully humanized monoclonal IgG1 antibody that specifically target viral F protein. MEDI8897 is a recombinant human IgG1k monoclonal antibody with modified Fc region that prolongs the antibody half-life. MEDI8897 acts by neutralizing the pre-fusion F protein and is intended for use in the prevention of hRSV infection. Trimeric nanobody ALX-0171 is designed to bind and neutralized the antigenic site of the F protein. This compound can be delivered through an aerosol route with high treatment effectiveness in animal trials, including the lamb model [7], and has advanced to phases of clinical trials.

Small molecule inhibitors of hRSV

Currently treatment in most cases for hRSV consists largely of supportive care for the disease symptoms. The only FDA approved specific treatment for severe cases of hRSV is the broad-spectrum antiviral drug Ribavirin, a guanosine analog, which inhibits inosine-5'-monophosphate dehydrogenase (IMPDH) resulting in reduced formation of mRNA and viral polymerase. This aerosolized drug has been used to treat hRSV infection, but the results still remain controversial due to the failure to have a significant therapeutic effect, high cost and the direct and indirect side effects [205]. Other drugs that inhibit the viral replication and assembly have been tested for hRSV with various outcomes. The largest group of hRSV small molecule inhibitors therapy are the fusion inhibitors. Numerous fusion inhibitors have been developed and some are currently in different phases of clinical trials, such as AK-0529 [206], Enzaplatovir (BTA-C585) [207], JNJ-53718678 [6, 208, 209], Presatovir (GS-5806) [210-213], RV521 [214]. The general mechanism of fusion inhibitors is to prevent viral infection of

the host respiratory epithelial cells by targeting the F protein which facilitate viral entry and membrane fusion [215]. Thus, resulting in decreased viral load and pulmonary lesions.

Another group of hRSV therapies are is the non-fusion protein inhibitors that are designed to target components other than viral fusion protein which are associated with viral entry and replication. Some non-fusion protein inhibitors have advanced into phases of clinical trials. Lumicitabine (ALS-008176) is a nucleoside analog that inhibits the viral RNA polymerase [216, 217]. RSV-604 is a compound benzodiazepine derivative that inhibits nucleocapsid (N) protein, which is a necessary component for viral replication [218, 219]. Small interfering RNA, ALN-RSV01, has also been developed to prevent the formation of nucleocapsid by targeting nucleocapsid mRNA. Interestingly, administration of ALN-RSV01 reduced the risk of bronchiolitis obliterans development in hRSV-infected lung transplant patients in clinical trial [220]. There are a large number of hRSV therapeutics that are in preclinical phase of development through *in vitro* testing and animal trials that is beyond the scope of this review. Some of these compounds will be mentioned in greater details in subsequent chapters including fusion inhibitor, JNJ-53718678, and replication inhibitor, JNJ-64166037.

References

1. Hall CB, Weinberg GA, Blumkin AK, Edwards KM, Staat MA, Schultz AF, et al. Respiratory syncytial virus-associated hospitalizations among children less than 24 months of age. Pediatrics. 2013;132(2):e341-8. Epub 2013/07/22. doi: 10.1542/peds.2013-0303. PubMed PMID: 23878043.

2. Hall CB, Weinberg GA, Iwane MK, Blumkin AK, Edwards KM, Staat MA, et al. The burden of respiratory syncytial virus infection in young children. N Engl J Med. 2009;360(6):588-98. doi: 10.1056/NEJMoa0804877. PubMed PMID: 19196675; PubMed Central PMCID: PMCPMC4829966.

3. Sommer C, Resch B, Simões EA. Risk factors for severe respiratory syncytial virus lower respiratory tract infection. Open Microbiol J. 2011;5:144-54. Epub 2011/12/30. doi: 10.2174/1874285801105010144. PubMed PMID: 22262987; PubMed Central PMCID: PMCPMC3258650.

4. Rossi GA, Medici MC, Arcangeletti MC, Lanari M, Merolla R, Paparatti UD, et al. Risk factors for severe RSV-induced lower respiratory tract infection over four consecutive epidemics. Eur J Pediatr. 2007;166(12):1267-72. Epub 2007/02/17. doi: 10.1007/s00431-007-0418-y. PubMed PMID: 17308898; PubMed Central PMCID: PMCPMC2042510.

5. Ackermann MR. Lamb model of respiratory syncytial virus-associated lung disease: insights to pathogenesis and novel treatments. ILAR J. 2014;55(1):4-15. doi: 10.1093/ilar/ilu003. PubMed PMID: 24936027; PubMed Central PMCID: PMCPMC4158344.

6. Roymans D, Alnajjar SS, Battles MB, Sitthicharoenchai P, Furmanova-Hollenstein P, Rigaux P, et al. Therapeutic efficacy of a respiratory syncytial virus fusion inhibitor. Nat Commun. 2017;8(1):167. Epub 2017/08/01. doi: 10.1038/s41467-017-00170-x. PubMed PMID: 28761099.

7. Larios Mora A, Detalle L, Gallup JM, Van Geelen A, Stohr T, Duprez L, et al. Delivery of ALX-0171 by inhalation greatly reduces respiratory syncytial virus disease in newborn lambs. MAbs. 2018;10(5):778-95. doi: 10.1080/19420862.2018.1470727. PubMed PMID: 29733750.

8. Rima B, Collins P, Easton A, Fouchier R, Kurath G, Lamb RA, et al. ICTV Virus Taxonomy Profile: Pneumoviridae. J Gen Virol. 2017;98(12):2912-3. Epub 2017/10/31. doi: 10.1099/jgv.0.000959. PubMed PMID: 29087278; PubMed Central PMCID: PMCPMC5775899.

9. Thompson WW, Shay DK, Weintraub E, Brammer L, Cox N, Anderson LJ, et al. Mortality associated with influenza and respiratory syncytial virus in the United States. JAMA. 2003;289(2):179-86. PubMed PMID: 12517228.

10. Constantopoulos AG, Kafetzis DA, Syrogiannopoulos GA, Roilides EJ, Malaka-Zafiriu EE, Sbyrakis SS, et al. Burden of respiratory syncytial viral infections on paediatric hospitals: a two-year prospective epidemiological study. Eur J Clin Microbiol Infect Dis. 2002;21(2):102-7. PubMed PMID: 11939389.

11. Hall CB. Respiratory syncytial virus and parainfluenza virus. N Engl J Med. 2001;344(25):1917-28. doi: 10.1056/NEJM200106213442507. PubMed PMID: 11419430.

12. Nair H, Nokes DJ, Gessner BD, Dherani M, Madhi SA, Singleton RJ, et al. Global burden of acute lower respiratory infections due to respiratory syncytial virus in young children: a systematic review and meta-analysis. Lancet. 2010;375(9725):1545-55. doi: 10.1016/S0140-6736(10)60206-1. PubMed PMID: 20399493; PubMed Central PMCID: PMCPMC2864404.

13. Kumar P, Medigeshi GR, Mishra VS, Islam M, Randev S, Mukherjee A, et al. Etiology of Acute Respiratory Infections in Infants: A Prospective Birth Cohort Study. Pediatr Infect Dis J. 2017;36(1):25-30. doi: 10.1097/INF.0000000000001359. PubMed PMID: 27753796.

14. Denny FW. The clinical impact of human respiratory virus infections. Am J Respir Crit Care Med. 1995;152(4 Pt 2):S4-12. doi: 10.1164/ajrccm/152.4_Pt_2.S4. PubMed PMID: 7551411.

15. Glezen WP, Taber LH, Frank AL, Kasel JA. Risk of primary infection and reinfection with respiratory syncytial virus. Am J Dis Child. 1986;140(6):543-6. PubMed PMID: 3706232.

16. Hall CB, Walsh EE, Long CE, Schnabel KC. Immunity to and frequency of reinfection with respiratory syncytial virus. J Infect Dis. 1991;163(4):693-8. PubMed PMID: 2010624.

17. Henderson FW, Collier AM, Clyde WA, Denny FW. Respiratory-syncytial-virus infections, reinfections and immunity. A prospective, longitudinal study in young children. N Engl J Med. 1979;300(10):530-4. doi: 10.1056/NEJM197903083001004. PubMed PMID: 763253.

18. Sigurs N, Bjarnason R, Sigurbergsson F, Kjellman B, Björkstén B. Asthma and immunoglobulin E antibodies after respiratory syncytial virus bronchiolitis: a prospective cohort study with matched controls. Pediatrics. 1995;95(4):500-5. PubMed PMID: 7700748.

19. Stein RT, Sherrill D, Morgan WJ, Holberg CJ, Halonen M, Taussig LM, et al. Respiratory syncytial virus in early life and risk of wheeze and allergy by age 13 years. Lancet. 1999;354(9178):541-5. doi: 10.1016/S0140-6736(98)10321-5. PubMed PMID: 10470697.

20. Sigurs N, Bjarnason R, Sigurbergsson F, Kjellman B. Respiratory syncytial virus bronchiolitis in infancy is an important risk factor for asthma and allergy at age 7. Am J Respir Crit Care Med. 2000;161(5):1501-7. doi: 10.1164/ajrccm.161.5.9906076. PubMed PMID: 10806145.

21. Sigurs N, Gustafsson PM, Bjarnason R, Lundberg F, Schmidt S, Sigurbergsson F, et al. Severe respiratory syncytial virus bronchiolitis in infancy and asthma and allergy at age 13. Am J Respir Crit Care Med. 2005;171(2):137-41. Epub 2004/10/29. doi: 10.1164/rccm.200406-730OC. PubMed PMID: 15516534.

22. Sigurs N, Aljassim F, Kjellman B, Robinson PD, Sigurbergsson F, Bjarnason R, et al. Asthma and allergy patterns over 18 years after severe RSV bronchiolitis in the first year of life. Thorax. 2010;65(12):1045-52. Epub 2010/06/27. doi: 10.1136/thx.2009.121582. PubMed PMID: 20581410.

23. Simões EA, Carbonell-Estrany X, Rieger CH, Mitchell I, Fredrick L, Groothuis JR, et al. The effect of respiratory syncytial virus on subsequent recurrent wheezing in atopic and nonatopic children. J Allergy Clin Immunol. 2010;126(2):256-62. Epub 2010/07/10. doi: 10.1016/j.jaci.2010.05.026. PubMed PMID: 20624638.

24. Han LL, Alexander JP, Anderson LJ. Respiratory syncytial virus pneumonia among the elderly: an assessment of disease burden. J Infect Dis. 1999;179(1):25-30. doi: 10.1086/314567. PubMed PMID: 9841818.

25. Hart RJ. An outbreak of respiratory syncytial virus infection in an old people's home. J Infect. 1984;8(3):259-61. PubMed PMID: 6736667.

26. Sorvillo FJ, Huie SF, Strassburg MA, Butsumyo A, Shandera WX, Fannin SL. An outbreak of respiratory syncytial virus pneumonia in a nursing home for the elderly. J Infect. 1984;9(3):252-6. PubMed PMID: 6527041.

27. Walsh EE, Peterson DR, Falsey AR. Risk factors for severe respiratory syncytial virus infection in elderly persons. J Infect Dis. 2004;189(2):233-8. Epub 2004/01/09. doi: 10.1086/380907. PubMed PMID: 14722887.

28. Falsey AR, Hennessey PA, Formica MA, Cox C, Walsh EE. Respiratory syncytial virus infection in elderly and high-risk adults. N Engl J Med. 2005;352(17):1749-59. doi: 10.1056/NEJMoa043951. PubMed PMID: 15858184.

29. Stensballe LG, Devasundaram JK, Simoes EA. Respiratory syncytial virus epidemics: the ups and downs of a seasonal virus. Pediatr Infect Dis J. 2003;22(2 Suppl):S21-32. doi: 10.1097/01.inf.0000053882.70365.c9. PubMed PMID: 12671449.

30. Bloom-Feshbach K, Alonso WJ, Charu V, Tamerius J, Simonsen L, Miller MA, et al. Latitudinal variations in seasonal activity of influenza and respiratory syncytial virus (RSV): a global comparative review. PLoS One. 2013;8(2):e54445. Epub 2013/02/14. doi: 10.1371/journal.pone.0054445. PubMed PMID: 23457451; PubMed Central PMCID: PMCPMC3573019.

31. Haynes AK, Manangan AP, Iwane MK, Sturm-Ramirez K, Homaira N, Brooks WA, et al. Respiratory syncytial virus circulation in seven countries with Global Disease Detection Regional Centers. J Infect Dis. 2013;208 Suppl 3:S246-54. doi: 10.1093/infdis/jit515. PubMed PMID: 24265484.

32. Paes BA, Craig C, Pigott W, Latchman A. Seasonal respiratory syncytial virus prophylaxis based on predetermined dates versus regional surveillance data. Pediatr Infect Dis J. 2013;32(9):e360-4. doi: 10.1097/INF.0b013e31829479d3. PubMed PMID: 23546534.

33. Diseases AAoPCoI, Committee AAoPBG. Updated guidance for palivizumab prophylaxis among infants and young children at increased risk of hospitalization for respiratory syncytial virus infection. Pediatrics. 2014;134(2):415-20. doi: 10.1542/peds.2014-1665. PubMed PMID: 25070315.

34. Hsu CH, Lin CY, Chi H, Chang JH, Hung HY, Kao HA, et al. Prolonged seasonality of respiratory syncytial virus infection among preterm infants in a subtropical climate. PLoS One. 2014;9(10):e110166. Epub 2014/10/21. doi: 10.1371/journal.pone.0110166. PubMed PMID: 25333346; PubMed Central PMCID: PMCPMC4204860.

35. DeVincenzo JP, El Saleeby CM, Bush AJ. Respiratory syncytial virus load predicts disease severity in previously healthy infants. J Infect Dis. 2005;191(11):1861-8. Epub 2005/04/21. doi: 10.1086/430008. PubMed PMID: 15871119.

36. El Saleeby CM, Devincenzo JP. Respiratory syncytial virus load and disease severity in the community. J Med Virol. 2011;83(5):904-5. doi: 10.1002/jmv.22039. PubMed PMID: 21412798.

37. El Saleeby CM, Bush AJ, Harrison LM, Aitken JA, Devincenzo JP. Respiratory syncytial virus load, viral dynamics, and disease severity in previously healthy naturally infected children. J Infect Dis. 2011;204(7):996-1002. doi: 10.1093/infdis/jir494. PubMed PMID: 21881113; PubMed Central PMCID: PMCPMC3203391.

38. Hall CB, Powell KR, MacDonald NE, Gala CL, Menegus ME, Suffin SC, et al. Respiratory syncytial viral infection in children with compromised immune function. N Engl J Med. 1986;315(2):77-81. doi: 10.1056/NEJM198607103150201. PubMed PMID: 3724802.

39. Couch RB, Englund JA, Whimbey E. Respiratory viral infections in immunocompetent and immunocompromised persons. Am J Med. 1997;102(3A):2-9; discussion 25-6. PubMed PMID: 10868136.

40. Openshaw PJ, Chiu C. Protective and dysregulated T cell immunity in RSV infection. Curr Opin Virol. 2013;3(4):468-74. Epub 2013/06/25. doi: 10.1016/j.coviro.2013.05.005. PubMed PMID: 23806514; PubMed Central PMCID: PMCPMC4295022.

41. Durant LR, Makris S, Voorburg CM, Loebbermann J, Johansson C, Openshaw PJ. Regulatory T cells prevent Th2 immune responses and pulmonary eosinophilia during respiratory syncytial virus infection in mice. J Virol. 2013;87(20):10946-54. Epub 2013/08/07. doi: 10.1128/JVI.01295-13. PubMed PMID: 23926350; PubMed Central PMCID: PMCPMC3807299.

42. Legg JP, Hussain IR, Warner JA, Johnston SL, Warner JO. Type 1 and type 2 cytokine imbalance in acute respiratory syncytial virus bronchiolitis. Am J Respir Crit Care Med. 2003;168(6):633-9. Epub 2003/05/28. doi: 10.1164/rccm.200210-1148OC. PubMed PMID: 12773328.

43. Caballero MT, Serra ME, Acosta PL, Marzec J, Gibbons L, Salim M, et al. TLR4 genotype and environmental LPS mediate RSV bronchiolitis through Th2 polarization. J Clin Invest. 2015;125(2):571-82. Epub 2015/01/02. doi: 10.1172/JCI75183. PubMed PMID: 25555213; PubMed Central PMCID: PMCPMC4319428.

44. Raiden S, Pandolfi J, Payasliàn F, Anderson M, Rivarola N, Ferrero F, et al. Depletion of circulating regulatory T cells during severe respiratory syncytial virus infection in young children. Am J Respir Crit Care Med. 2014;189(7):865-8. doi: 10.1164/rccm.201311-1977LE. PubMed PMID: 24684360.

45. Korppi M, Nuolivirta K, Lauhkonen E, Holster A, Teräsjärvi J, Vuononvirta J, et al. IL-10 gene polymorphism is associated with preschool atopy and early-life recurrent wheezing after bronchiolitis in infancy. Pediatr Pulmonol. 2017;52(1):14-20. Epub 2016/05/26. doi: 10.1002/ppul.23489. PubMed PMID: 27228545.

46. Hickling TP, Malhotra R, Bright H, McDowell W, Blair ED, Sim RB. Lung surfactant protein A provides a route of entry for respiratory syncytial virus into host cells. Viral Immunol. 2000;13(1):125-35. doi: 10.1089/vim.2000.13.125. PubMed PMID: 10733174.

47. Hickling TP, Bright H, Wing K, Gower D, Martin SL, Sim RB, et al. A recombinant trimeric surfactant protein D carbohydrate recognition domain inhibits respiratory syncytial virus infection in vitro and in vivo. Eur J Immunol. 1999;29(11):3478-84. doi: 10.1002/(SICI)1521-4141(199911)29:11<3478::AID-IMMU3478>3.0.CO;2-W. PubMed PMID: 10556802.

48. Rudd BD, Burstein E, Duckett CS, Li X, Lukacs NW. Differential role for TLR3 in respiratory syncytial virus-induced chemokine expression. J Virol. 2005;79(6):3350-7. doi: 10.1128/JVI.79.6.3350-3357.2005. PubMed PMID: 15731229; PubMed Central PMCID: PMCPMC1075725.

49. Gern JE, French DA, Grindle KA, Brockman-Schneider RA, Konno S, Busse WW. Double-stranded RNA induces the synthesis of specific chemokines by bronchial epithelial cells. Am J Respir Cell Mol Biol. 2003;28(6):731-7. Epub 2002/12/30. doi: 10.1165/rcmb.2002-0055OC. PubMed PMID: 12600836.

50. Kurt-Jones EA, Popova L, Kwinn L, Haynes LM, Jones LP, Tripp RA, et al. Pattern recognition receptors TLR4 and CD14 mediate response to respiratory syncytial virus. Nat Immunol. 2000;1(5):398-401. doi: 10.1038/80833. PubMed PMID: 11062499.

51. Haeberle HA, Takizawa R, Casola A, Brasier AR, Dieterich HJ, Van Rooijen N, et al. Respiratory syncytial virus-induced activation of nuclear factor-kappaB in the lung involves alveolar macrophages and toll-like receptor 4-dependent pathways. J Infect Dis. 2002;186(9):1199-206. Epub 2002/10/11. doi: 10.1086/344644. PubMed PMID: 12402188.

52. Murawski MR, Bowen GN, Cerny AM, Anderson LJ, Haynes LM, Tripp RA, et al. Respiratory syncytial virus activates innate immunity through Toll-like receptor 2. J Virol. 2009;83(3):1492-500. Epub 2008/11/19. doi: 10.1128/JVI.00671-08. PubMed PMID: 19019963; PubMed Central PMCID: PMCPMC2620898.

53. Schlender J, Hornung V, Finke S, Günthner-Biller M, Marozin S, Brzózka K, et al. Inhibition of toll-like receptor 7- and 9-mediated alpha/beta interferon production in human plasmacytoid dendritic cells by respiratory syncytial virus and measles virus. J Virol. 2005;79(9):5507-15. doi: 10.1128/JVI.79.9.5507-5515.2005. PubMed PMID: 15827165; PubMed Central PMCID: PMCPMC1082779.

54. McNamara PS, Ritson P, Selby A, Hart CA, Smyth RL. Bronchoalveolar lavage cellularity in infants with severe respiratory syncytial virus bronchiolitis. Arch Dis Child. 2003;88(10):922-6. PubMed PMID: 14500316; PubMed Central PMCID: PMCPMC1719332.

55. Everard ML, Swarbrick A, Wrightham M, McIntyre J, Dunkley C, James PD, et al. Analysis of cells obtained by bronchial lavage of infants with respiratory syncytial virus infection. Arch Dis Child. 1994;71(5):428-32. PubMed PMID: 7826113; PubMed Central PMCID: PMCPMC1030058.

56. Bataki EL, Evans GS, Everard ML. Respiratory syncytial virus and neutrophil activation. Clin Exp Immunol. 2005;140(3):470-7. doi: 10.1111/j.1365-2249.2005.02780.x. PubMed PMID: 15932508; PubMed Central PMCID: PMCPMC1809401.

57. Wang SZ, Xu H, Wraith A, Bowden JJ, Alpers JH, Forsyth KD. Neutrophils induce damage to respiratory epithelial cells infected with respiratory syncytial virus. Eur Respir J. 1998;12(3):612-8. PubMed PMID: 9762789.

58. Becker S, Quay J, Soukup J. Cytokine (tumor necrosis factor, IL-6, and IL-8) production by respiratory syncytial virus-infected human alveolar macrophages. J Immunol. 1991;147(12):4307-12. PubMed PMID: 1753101.

59. Colocho Zelaya EA, Orvell C, Strannegård O. Eosinophil cationic protein in nasopharyngeal secretions and serum of infants infected with respiratory syncytial virus. Pediatr Allergy Immunol. 1994;5(2):100-6. PubMed PMID: 8087188.

60. Domachowske JB, Bonville CA, Dyer KD, Rosenberg HF. Evolution of antiviral activity in the ribonuclease A gene superfamily: evidence for a specific interaction between eosinophil-derived neurotoxin (EDN/RNase 2) and respiratory syncytial virus. Nucleic Acids Res. 1998;26(23):5327-32. PubMed PMID: 9826755; PubMed Central PMCID: PMCPMC147995.

61. Su YC, Townsend D, Herrero LJ, Zaid A, Rolph MS, Gahan ME, et al. Dual proinflammatory and antiviral properties of pulmonary eosinophils in respiratory syncytial virus vaccine-enhanced disease. J Virol. 2015;89(3):1564-78. Epub 2014/11/19. doi: 10.1128/JVI.01536-14. PubMed PMID: 25410867; PubMed Central PMCID: PMCPMC4300751.

62. Schwarze J. Lung dendritic cells in respiratory syncytial virus bronchiolitis. Pediatr Infect Dis J. 2008;27(10 Suppl):S89-91. doi: 10.1097/INF.0b013e318168b6f0. PubMed PMID: 18820586.

63. Smit JJ, Rudd BD, Lukacs NW. Plasmacytoid dendritic cells inhibit pulmonary immunopathology and promote clearance of respiratory syncytial virus. J Exp Med. 2006;203(5):1153-9. Epub 2006/05/08. doi: 10.1084/jem.20052359. PubMed PMID: 16682497; PubMed Central PMCID: PMCPMC2121199.

64. Beyer M, Bartz H, Hörner K, Doths S, Koerner-Rettberg C, Schwarze J. Sustained increases in numbers of pulmonary dendritic cells after respiratory syncytial virus infection. J Allergy Clin Immunol. 2004;113(1):127-33. doi: 10.1016/j.jaci.2003.10.057. PubMed PMID: 14713917.

65. Aberle JH, Aberle SW, Dworzak MN, Mandl CW, Rebhandl W, Vollnhofer G, et al. Reduced interferon-gamma expression in peripheral blood mononuclear cells of infants with severe respiratory syncytial virus disease. Am J Respir Crit Care Med. 1999;160(4):1263-8. doi: 10.1164/ajrccm.160.4.9812025. PubMed PMID: 10508817.

66. Bont L, Heijnen CJ, Kavelaars A, van Aalderen WM, Brus F, Draaisma JM, et al. Local interferon-gamma levels during respiratory syncytial virus lower respiratory tract infection are associated with disease severity. J Infect Dis. 2001;184(3):355-8. Epub 2001/06/26. doi: 10.1086/322035. PubMed PMID: 11443563.

67. Li F, Zhu H, Sun R, Wei H, Tian Z. Natural killer cells are involved in acute lung immune injury caused by respiratory syncytial virus infection. J Virol. 2012;86(4):2251-8. Epub 2011/12/14. doi: 10.1128/JVI.06209-11. PubMed PMID: 22171263; PubMed Central PMCID: PMCPMC3302418.

68. Taylor G, Stott EJ, Hayle AJ. Cytotoxic lymphocytes in the lungs of mice infected with respiratory syncytial virus. J Gen Virol. 1985;66 (Pt 12):2533-8. doi: 10.1099/0022-1317-66-12-2533. PubMed PMID: 2866227.

69. Graham BS, Bunton LA, Wright PF, Karzon DT. Role of T lymphocyte subsets in the pathogenesis of primary infection and rechallenge with respiratory syncytial virus in mice. J Clin Invest. 1991;88(3):1026-33. doi: 10.1172/JCI115362. PubMed PMID: 1909350; PubMed Central PMCID: PMCPMC295511.

70. Morabito KM, Erez N, Graham BS, Ruckwardt TJ. Phenotype and Hierarchy of Two Transgenic T Cell Lines Targeting the Respiratory Syncytial Virus KdM282-90 Epitope Is Transfer Dose-Dependent. PLoS One. 2016;11(1):e0146781. Epub 2016/01/11. doi: 10.1371/journal.pone.0146781. PubMed PMID: 26752171; PubMed Central PMCID: PMCPMC4708989.

71. Schmidt ME, Knudson CJ, Hartwig SM, Pewe LL, Meyerholz DK, Langlois RA, et al. Memory CD8 T cells mediate severe immunopathology following respiratory syncytial virus infection. PLoS Pathog. 2018;14(1):e1006810. Epub 2018/01/02. doi: 10.1371/journal.ppat.1006810. PubMed PMID: 29293660; PubMed Central PMCID: PMCPMC5766251.

72. Román M, Calhoun WJ, Hinton KL, Avendaño LF, Simon V, Escobar AM, et al. Respiratory syncytial virus infection in infants is associated with predominant Th-2-like response. Am J Respir Crit Care Med. 1997;156(1):190-5. doi: 10.1164/ajrccm.156.1.9611050. PubMed PMID: 9230746.

73. Sung RY, Hui SH, Wong CK, Lam CW, Yin J. A comparison of cytokine responses in respiratory syncytial virus and influenza A infections in infants. Eur J Pediatr. 2001;160(2):117-22. PubMed PMID: 11271383.

74. Pala P, Bjarnason R, Sigurbergsson F, Metcalfe C, Sigurs N, Openshaw PJ. Enhanced IL-4 responses in children with a history of respiratory syncytial virus bronchiolitis in infancy. Eur Respir J. 2002;20(2):376-82. PubMed PMID: 12212970.

75. Kovarik J, Siegrist CA. Immunity in early life. Immunol Today. 1998;19(4):150-2. PubMed PMID: 9577089.

76. Mahon BP. The rational design of vaccine adjuvants for mucosal and neonatal immunization. Curr Med Chem. 2001;8(9):1057-75. PubMed PMID: 11472241.

77. Elliott MB, Tebbey PW, Pryharski KS, Scheuer CA, Laughlin TS, Hancock GE. Inhibition of respiratory syncytial virus infection with the CC chemokine RANTES (CCL5). J Med Virol. 2004;73(2):300-8. doi: 10.1002/jmv.20091. PubMed PMID: 15122808.

78. Schwarze J, Schauer U. Enhanced virulence, airway inflammation and impaired lung function induced by respiratory syncytial virus deficient in secreted G protein. Thorax. 2004;59(6):517-21. PubMed PMID: 15170038; PubMed Central PMCID: PMCPMC1747027.

79. Arnold R, König B, Werchau H, König W. Respiratory syncytial virus deficient in soluble G protein induced an increased proinflammatory response in human lung epithelial cells. Virology. 2004;330(2):384-97. doi: 10.1016/j.virol.2004.10.004. PubMed PMID: 15567433.

80. Knudson CJ, Varga SM. The relationship between respiratory syncytial virus and asthma. Vet Pathol. 2015;52(1):97-106. Epub 2014/02/10. doi: 10.1177/0300985814520639. PubMed PMID: 24513802.

81. Wu P, Hartert TV. Evidence for a causal relationship between respiratory syncytial virus infection and asthma. Expert Rev Anti Infect Ther. 2011;9(9):731-45. doi: 10.1586/eri.11.92. PubMed PMID: 21905783; PubMed Central PMCID: PMCPMC3215509.

82. Meurman O, Ruuskanen O, Sarkkinen H, Hänninen P, Halonen P. Immunoglobulin class-specific antibody response in respiratory syncytial virus infection measured by enzyme immunoassay. J Med Virol. 1984;14(1):67-72. PubMed PMID: 6747613.

83. Kaul TN, Welliver RC, Wong DT, Udwadia RA, Riddlesberger K, Ogra PL. Secretory antibody response to respiratory syncytial virus infection. Am J Dis Child. 1981;135(11):1013-6. PubMed PMID: 7294005.

84. Welliver RC, Kaul TN, Putnam TI, Sun M, Riddlesberger K, Ogra PL. The antibody response to primary and secondary infection with respiratory syncytial virus: kinetics of class-specific responses. J Pediatr. 1980;96(5):808-13. PubMed PMID: 7365579.

85. Brandenburg AH, Groen J, van Steensel-Moll HA, Claas EC, Rothbarth PH, Neijens HJ, et al. Respiratory syncytial virus specific serum antibodies in infants under six months of age: limited serological response upon infection. J Med Virol. 1997;52(1):97-104. PubMed PMID: 9131465.

86. Murphy BR, Alling DW, Snyder MH, Walsh EE, Prince GA, Chanock RM, et al. Effect of age and preexisting antibody on serum antibody response of infants and children to the F and G glycoproteins during respiratory syncytial virus infection. J Clin Microbiol. 1986;24(5):894-8. PubMed PMID: 3771779; PubMed Central PMCID: PMCPMC269059.

87. Kasel JA, Walsh EE, Frank AL, Baxter BD, Taber LH, Glezen WP. Relation of serum antibody to glycoproteins of respiratory syncytial virus with immunity to infection in children. Viral Immunol. 1987;1(3):199-205. doi: 10.1089/vim.1987.1.199. PubMed PMID: 3509676.

88. Falsey AR, Singh HK, Walsh EE. Serum antibody decay in adults following natural respiratory syncytial virus infection. J Med Virol. 2006;78(11):1493-7. doi: 10.1002/jmv.20724. PubMed PMID: 16998887.

89. Fulton RB, Meyerholz DK, Varga SM. Foxp3+ CD4 regulatory T cells limit pulmonary immunopathology by modulating the CD8 T cell response during respiratory syncytial virus infection. J Immunol. 2010;185(4):2382-92. Epub 2010/07/16. doi: 10.4049/jimmunol.1000423. PubMed PMID: 20639494; PubMed Central PMCID: PMCPMC2923480.

90. Shao HY, Huang JY, Lin YW, Yu SL, Chitra E, Chang CK, et al. Depletion of regulatory T-cells leads to moderate B-cell antigenicity in respiratory syncytial virus infection. Int J Infect Dis. 2015;41:56-64. Epub 2015/11/10. doi: 10.1016/j.ijid.2015.10.026. PubMed PMID: 26555647.

91. Li B, Wu FL, Feng XB, Sun DK, Cui QQ, Zhao ZX. [Changes and the clinical significance of $CD4^+$ $CD25^+$ regulatory T cells and Th17 cells in peripheral blood of infants with respiratory syncytial virus bronchiolitis]. Xi Bao Yu Fen Zi Mian Yi Xue Za Zhi. 2012;28(4):426-8. PubMed PMID: 22482417.

92. Bacharier LB, Coverstone A, Schweiger T, Gregory G, Yin-DeClue H, Sajol G, et al. Regulatory T cells in Acute Severe RSV Bronchiolitis. American Thoracic Society 2013 International Conference; Philadelphia, Pennsylvania: American Journal of Respiratory and Critical Care Medicine; 2013.

93. Loebbermann J, Schnoeller C, Thornton H, Durant L, Sweeney NP, Schuijs M, et al. IL-10 regulates viral lung immunopathology during acute respiratory syncytial virus infection in mice. PLoS One. 2012;7(2):e32371. Epub 2012/02/29. doi: 10.1371/journal.pone.0032371. PubMed PMID: 22393401; PubMed Central PMCID: PMCPMC3290561.

94. Wilson J, Rowlands K, Rockett K, Moore C, Lockhart E, Sharland M, et al. Genetic variation at the IL10 gene locus is associated with severity of respiratory syncytial virus bronchiolitis. J Infect Dis. 2005;191(10):1705-9. Epub 2005/04/05. doi: 10.1086/429636. PubMed PMID: 15838798.

95. Taylor G. Animal models of respiratory syncytial virus infection. Vaccine. 2017;35(3):469-80. Epub 2016/11/29. doi: 10.1016/j.vaccine.2016.11.054. PubMed PMID: 27908639; PubMed Central PMCID: PMCPMC5244256.

96. Bem RA, Domachowske JB, Rosenberg HF. Animal models of human respiratory syncytial virus disease. Am J Physiol Lung Cell Mol Physiol. 2011;301(2):L148-56. Epub 2011/05/13. doi: 10.1152/ajplung.00065.2011. PubMed PMID: 21571908; PubMed Central PMCID: PMCPMC3154630.

97. Boukhvalova MS, Blanco JC. The cotton rat Sigmodon hispidus model of respiratory syncytial virus infection. Curr Top Microbiol Immunol. 2013;372:347-58. doi: 10.1007/978-3-642-38919-1_17. PubMed PMID: 24362698.

98. Openshaw PJ. The mouse model of respiratory syncytial virus disease. Curr Top Microbiol Immunol. 2013;372:359-69. doi: 10.1007/978-3-642-38919-1_18. PubMed PMID: 24362699.

99. Prince GA, Jenson AB, Horswood RL, Camargo E, Chanock RM. The pathogenesis of respiratory syncytial virus infection in cotton rats. Am J Pathol. 1978;93(3):771-91. PubMed PMID: 362946; PubMed Central PMCID: PMCPMC2018360.

100. Boukhvalova MS, Yim KC, Blanco J. Cotton rat model for testing vaccines and antivirals against respiratory syncytial virus. Antivir Chem Chemother. 2018;26:2040206618770518. doi: 10.1177/2040206618770518. PubMed PMID: 29768937; PubMed Central PMCID: PMCPMC5987903.

101. Prince GA, Horswood RL, Berndt J, Suffin SC, Chanock RM. Respiratory syncytial virus infection in inbred mice. Infect Immun. 1979;26(2):764-6. PubMed PMID: 546793; PubMed Central PMCID: PMCPMC414679.

102. Richardson LS, Belshe RB, London WT, Sly DL, Prevar DA, Camargo E, et al. Evaluation of five temperature-sensitive mutants of respiratory syncytial virus in primates: I. Viral shedding, immunologic response, and associated illness. J Med Virol. 1978;3(2):91-100. PubMed PMID: 104004.

103. Prince GA, Suffin SC, Prevar DA, Camargo E, Sly DL, London WT, et al. Respiratory syncytial virus infection in owl monkeys: viral shedding, immunological response, and associated illness caused by wild-type virus and two temperature-sensitive mutants. Infect Immun. 1979;26(3):1009-13. PubMed PMID: 118925; PubMed Central PMCID: PMCPMC414720.

104. Hemming VG, Prince GA, Horswood RL, London WJ, Murphy BR, Walsh EE, et al. Studies of passive immunotherapy for infections of respiratory syncytial virus in the respiratory tract of a primate model. J Infect Dis. 1985;152(5):1083-7. PubMed PMID: 4045247.

105. Papin JF, Wolf RF, Kosanke SD, Jenkins JD, Moore SN, Anderson MP, et al. Infant baboons infected with respiratory syncytial virus develop clinical and pathological changes that parallel those of human infants. Am J Physiol Lung Cell Mol Physiol. 2013;304(8):L530-9. Epub 2013/02/15. doi: 10.1152/ajplung.00173.2012. PubMed PMID: 23418091; PubMed Central PMCID: PMCPMC3625990.

106. Richardson LS, Belshe RB, Sly DL, London WT, Prevar DA, Camargo E, et al. Experimental respiratory syncytial virus pneumonia in cebus monkeys. J Med Virol. 1978;2(1):45-59. PubMed PMID: 210254.

107. Kakuk TJ, Soike K, Brideau RJ, Zaya RM, Cole SL, Zhang JY, et al. A human respiratory syncytial virus (RSV) primate model of enhanced pulmonary pathology induced with a formalin-inactivated RSV vaccine but not a recombinant FG subunit vaccine. J Infect Dis. 1993;167(3):553-61. PubMed PMID: 8440926.

108. Eyles JE, Johnson JE, Megati S, Roopchand V, Cockle PJ, Weeratna R, et al. Nonreplicating vaccines can protect african green monkeys from the memphis 37 strain of respiratory syncytial virus. J Infect Dis. 2013;208(2):319-29. Epub 2013/04/17. doi: 10.1093/infdis/jit169. PubMed PMID: 23596321.

109. Babu PG, Selvan A, Christuraj S, David J, John TJ, Simoes EA. A primate model of respiratory syncytial virus infection. Indian J Exp Biol. 1998;36(8):758-62. PubMed PMID: 9838875.

110. Simoes EA, Hayward AR, Ponnuraj EM, Straumanis JP, Stenmark KR, Wilson HL, et al. Respiratory syncytial virus infects the Bonnet monkey, Macaca radiata. Pediatr Dev Pathol. 1999;2(4):316-26. PubMed PMID: 10347274.

111. Ponnuraj EM, Hayward AR, Raj A, Wilson H, Simoes EA. Increased replication of respiratory syncytial virus (RSV) in pulmonary infiltrates is associated with enhanced histopathological disease in bonnet monkeys (Macaca radiata) pre-immunized with a formalin-inactivated RSV vaccine. J Gen Virol. 2001;82(Pt 11):2663-74. doi: 10.1099/0022-1317-82-11-2663. PubMed PMID: 11602778.

112. De Swart RL, Kuiken T, Timmerman HH, van Amerongen G, Van Den Hoogen BG, Vos HW, et al. Immunization of macaques with formalin-inactivated respiratory syncytial virus (RSV) induces interleukin-13-associated hypersensitivity to subsequent RSV infection. J Virol. 2002;76(22):11561-9. PubMed PMID: 12388717; PubMed Central PMCID: PMCPMC136757.

113. Grandin C, Lucas-Hourani M, Clavel M, Taborik F, Vabret A, Tangy F, et al. Evidence for an intranasal immune response to human respiratory syncytial virus infection in cynomolgus macaques. J Gen Virol. 2015;96(Pt 4):782-92. Epub 2014/12/23. doi: 10.1099/vir.0.000039. PubMed PMID: 25537374.

114. Belshe RB, Richardson LS, London WT, Sly DL, Lorfeld JH, Camargo E, et al. Experimental respiratory syncytial virus infection of four species of primates. J Med Virol. 1977;1(3):157-62. PubMed PMID: 416176.

115. Weltzin R, Traina-Dorge V, Soike K, Zhang JY, Mack P, Soman G, et al. Intranasal monoclonal IgA antibody to respiratory syncytial virus protects rhesus monkeys against upper and lower respiratory tract infection. J Infect Dis. 1996;174(2):256-61. PubMed PMID: 8699052.

116. McArthur-Vaughan K, Gershwin LJ. A rhesus monkey model of respiratory syncytial virus infection. J Med Primatol. 2002;31(2):61-73. PubMed PMID: 12110049.

117. Vaughan K, Rhodes GH, Gershwin LJ. DNA immunization against respiratory syncytial virus (RSV) in infant rhesus monkeys. Vaccine. 2005;23(22):2928-42. doi: 10.1016/j.vaccine.2004.10.046. PubMed PMID: 15780742.

118. Grunwald T, Tenbusch M, Schulte R, Raue K, Wolf H, Hannaman D, et al. Novel vaccine regimen elicits strong airway immune responses and control of respiratory syncytial virus in nonhuman primates. J Virol. 2014;88(8):3997-4007. Epub 2014/01/22. doi: 10.1128/JVI.02736-13. PubMed PMID: 24453366; PubMed Central PMCID: PMCPMC3993754.

119. BLOUNT RE, MORRIS JA, SAVAGE RE. Recovery of cytopathogenic agent from chimpanzees with coryza. Proc Soc Exp Biol Med. 1956;92(3):544-9. PubMed PMID: 13359460.

120. Crowe JE, Collins PL, London WT, Chanock RM, Murphy BR. A comparison in chimpanzees of the immunogenicity and efficacy of live attenuated respiratory syncytial virus (RSV) temperature-sensitive mutant vaccines and vaccinia virus recombinants that express the surface glycoproteins of RSV. Vaccine. 1993;11(14):1395-404. PubMed PMID: 8310760.

121. Collins PL, Purcell RH, London WT, Lawrence LA, Chanock RM, Murphy BR. Evaluation in chimpanzees of vaccinia virus recombinants that express the surface glycoproteins of human respiratory syncytial virus. Vaccine. 1990;8(2):164-8. PubMed PMID: 2336876.

122. Derscheid RJ, Ackermann MR. Perinatal lamb model of respiratory syncytial virus (RSV) infection. Viruses. 2012;4(10):2359-78. Epub 2012/10/23. doi: 10.3390/v4102359. PubMed PMID: 23202468; PubMed Central PMCID: PMCPMC3497056.

123. Barth PJ, Wolf M, Ramaswamy A. Distribution and number of Clara cells in the normal and disturbed development of the human fetal lung. Pediatr Pathol. 1994;14(4):637-51. PubMed PMID: 7971583.

124. Plopper CG. Comparative morphologic features of bronchiolar epithelial cells. The Clara cell. Am Rev Respir Dis. 1983;128(2 Pt 2):S37-41. doi: 10.1164/arrd.1983.128.2P2.S37. PubMed PMID: 6881705.

125. Redondo E, Gázquez A, García A, Vadillo S, Masot AJ. Dominant expression of interleukin-8 vs interleukin-1β and tumour necrosis factor alpha in lungs of lambs experimentally infected with Mannheimia haemolytica. N Z Vet J. 2011;59(5):225-32. doi: 10.1080/00480169.2011.596180. PubMed PMID: 21851299.

126. Ackermann MR, Gallup JM, Zabner J, Evans RB, Brockus CW, Meyerholz DK, et al. Differential expression of sheep beta-defensin-1 and -2 and interleukin 8 during acute Mannheimia haemolytica pneumonia. Microb Pathog. 2004;37(1):21-7. doi: 10.1016/j.micpath.2004.04.003. PubMed PMID: 15194156.

127. Olivier A, Gallup J, de Macedo MM, Varga SM, Ackermann M. Human respiratory syncytial virus A2 strain replicates and induces innate immune responses by respiratory epithelia of neonatal lambs. Int J Exp Pathol. 2009;90(4):431-8. doi: 10.1111/j.1365-2613.2009.00643.x. PubMed PMID: 19659901; PubMed Central PMCID: PMCPMC2741153.

128. Salathe M, Guldimann P, Conner GE, Wanner A. Hydrogen peroxide-scavenging properties of sheep airway mucus. Am J Respir Crit Care Med. 1995;151(5):1543-50. doi: 10.1164/ajrccm.151.5.7735613. PubMed PMID: 7735613.

129. Salathe M, Holderby M, Forteza R, Abraham WM, Wanner A, Conner GE. Isolation and characterization of a peroxidase from the airway. Am J Respir Cell Mol Biol. 1997;17(1):97-105. doi: 10.1165/ajrcmb.17.1.2719. PubMed PMID: 9224215.

130. Gerson C, Sabater J, Scuri M, Torbati A, Coffey R, Abraham JW, et al. The lactoperoxidase system functions in bacterial clearance of airways. Am J Respir Cell Mol Biol. 2000;22(6):665-71. doi: 10.1165/ajrcmb.22.6.3980. PubMed PMID: 10837362.

131. Derscheid RJ, van Geelen A, Gallup JM, Kienzle T, Shelly DA, Cihlar T, et al. Human respiratory syncytial virus memphis 37 causes acute respiratory disease in perinatal lamb lung. Biores Open Access. 2014;3(2):60-9. doi: 10.1089/biores.2013.0044. PubMed PMID: 24804166; PubMed Central PMCID: PMCPMC3994985.

132. Derscheid RJ, van Geelen A, McGill JL, Gallup JM, Cihlar T, Sacco RE, et al. Human respiratory syncytial virus Memphis 37 grown in HEp-2 cells causes more severe disease in lambs than virus grown in Vero cells. Viruses. 2013;5(11):2881-97. Epub 2013/11/22. doi: 10.3390/v5112881. PubMed PMID: 24284879; PubMed Central PMCID: PMCPMC3856420.

133. Johnson JE, Gonzales RA, Olson SJ, Wright PF, Graham BS. The histopathology of fatal untreated human respiratory syncytial virus infection. Mod Pathol. 2007;20(1):108-19. Epub 2006/11/24. doi: 10.1038/modpathol.3800725. PubMed PMID: 17143259.

134. Lehmkuhl HD, Gough PM, Reed DE. Characterization and identification of a bovine respiratory syncytial virus isolated from young calves. Am J Vet Res. 1979;40(1):124-6. PubMed PMID: 453673.

135. Lehmkuhl HD, Cutlip RC. Experimental respiratory syncytial virus infection in feeder-age lambs. Am J Vet Res. 1979;40(12):1729-30. PubMed PMID: 525890.

136. Derscheid RJ, Gallup JM, Knudson CJ, Varga SM, Grosz DD, van Geelen A, et al. Effects of formalin-inactivated respiratory syncytial virus (FI-RSV) in the perinatal lamb model of RSV. PLoS One. 2013;8(12):e81472. Epub 2013/12/06. doi: 10.1371/journal.pone.0081472. PubMed PMID: 24324695; PubMed Central PMCID: PMCPMC3855688.

137. Meehan JT, Cutlip RC, Lehmkuhl HD, Kluge JP, Ackermann MR. Infected cell types in ovine lung following exposure to bovine respiratory syncytial virus. Vet Pathol. 1994;31(2):229-36. doi: 10.1177/030098589403100210. PubMed PMID: 8203086.

138. Grubor B, Gallup JM, Meyerholz DK, Crouch EC, Evans RB, Brogden KA, et al. Enhanced surfactant protein and defensin mRNA levels and reduced viral replication during parainfluenza virus type 3 pneumonia in neonatal lambs. Clin Diagn Lab Immunol. 2004;11(3):599-607. doi: 10.1128/CDLI.11.3.599-607.2004. PubMed PMID: 15138188; PubMed Central PMCID: PMCPMC404576.

139. Kim HW, Canchola JG, Brandt CD, Pyles G, Chanock RM, Jensen K, et al. Respiratory syncytial virus disease in infants despite prior administration of antigenic inactivated vaccine. Am J Epidemiol. 1969;89(4):422-34. PubMed PMID: 4305198.

140. Murphy BR, Prince GA, Walsh EE, Kim HW, Parrott RH, Hemming VG, et al. Dissociation between serum neutralizing and glycoprotein antibody responses of infants and children who received inactivated respiratory syncytial virus vaccine. J Clin Microbiol. 1986;24(2):197-202. PubMed PMID: 3755730; PubMed Central PMCID: PMCPMC268874.

141. Murphy BR, Sotnikov AV, Lawrence LA, Banks SM, Prince GA. Enhanced pulmonary histopathology is observed in cotton rats immunized with formalin-inactivated respiratory syncytial virus (RSV) or purified F glycoprotein and challenged with RSV 3-6 months after immunization. Vaccine. 1990;8(5):497-502. PubMed PMID: 2251875.

142. Waris ME, Tsou C, Erdman DD, Zaki SR, Anderson LJ. Respiratory synctial virus infection in BALB/c mice previously immunized with formalin-inactivated virus induces enhanced pulmonary inflammatory response with a predominant Th2-like cytokine pattern. J Virol. 1996;70(5):2852-60. PubMed PMID: 8627759; PubMed Central PMCID: PMCPMC190142.

143. Connors M, Giese NA, Kulkarni AB, Firestone CY, Morse HC, Murphy BR. Enhanced pulmonary histopathology induced by respiratory syncytial virus (RSV) challenge of formalin-inactivated RSV-immunized BALB/c mice is abrogated by depletion of interleukin-4 (IL-4) and IL-10. J Virol. 1994;68(8):5321-5. PubMed PMID: 8035532; PubMed Central PMCID: PMCPMC236482.

144. van Diepen A, Brand HK, de Waal L, Bijl M, Jong VL, Kuiken T, et al. Host proteome correlates of vaccine-mediated enhanced disease in a mouse model of respiratory syncytial virus infection. J Virol. 2015;89(9):5022-31. Epub 2015/02/18. doi: 10.1128/JVI.03630-14. PubMed PMID: 25694607; PubMed Central PMCID: PMCPMC4403458.

145. Stott EJ, Ball LA, Young KK, Furze J, Wertz GW. Human respiratory syncytial virus glycoprotein G expressed from a recombinant vaccinia virus vector protects mice against live-virus challenge. J Virol. 1986;60(2):607-13. PubMed PMID: 3773052; PubMed Central PMCID: PMCPMC288932.

146. Culley FJ, Pollott J, Openshaw PJ. Age at first viral infection determines the pattern of T cell-mediated disease during reinfection in adulthood. J Exp Med. 2002;196(10):1381-6. PubMed PMID: 12438429; PubMed Central PMCID: PMCPMC2193991.

147. Plotnicky H, Siegrist CA, Aubry JP, Bonnefoy JY, Corvaïa N, Nguyen TN, et al. Enhanced pulmonary immunopathology following neonatal priming with formalin-inactivated respiratory syncytial virus but not with the BBG2NA vaccine candidate. Vaccine. 2003;21(19-20):2651-60. PubMed PMID: 12744902.

148. Hussell T, Georgiou A, Sparer TE, Matthews S, Pala P, Openshaw PJ. Host genetic determinants of vaccine-induced eosinophilia during respiratory syncytial virus infection. J Immunol. 1998;161(11):6215-22. PubMed PMID: 9834108.

149. Sparer TE, Matthews S, Hussell T, Rae AJ, Garcia-Barreno B, Melero JA, et al. Eliminating a region of respiratory syncytial virus attachment protein allows induction of protective immunity without vaccine-enhanced lung eosinophilia. J Exp Med. 1998;187(11):1921-6. PubMed PMID: 9607931; PubMed Central PMCID: PMCPMC2212312.

150. Corvaïa N, Tournier P, Nguyen TN, Haeuw JF, Power UF, Binz H, et al. Challenge of BALB/c mice with respiratory syncytial virus does not enhance the Th2 pathway induced after immunization with a recombinant G fusion protein, BBG2NA, in aluminum hydroxide. J Infect Dis. 1997;176(3):560-9. PubMed PMID: 9291300.

151. Power UF, Plotnicky-Gilquin H, Huss T, Robert A, Trudel M, Ståhl S, et al. Induction of protective immunity in rodents by vaccination with a prokaryotically expressed recombinant fusion protein containing a respiratory syncytial virus G protein fragment. Virology. 1997;230(2):155-66. doi: 10.1006/viro.1997.8465. PubMed PMID: 9143271.

152. Plotnicky-Gilquin H, Huss T, Aubry JP, Haeuw JF, Beck A, Bonnefoy JY, et al. Absence of lung immunopathology following respiratory syncytial virus (RSV) challenge in mice immunized with a recombinant RSV G protein fragment. Virology. 1999;258(1):128-40. doi: 10.1006/viro.1999.9702. PubMed PMID: 10329575.

153. Power UF, Plotnicky H, Blaecke A, Nguyen TN. The immunogenicity, protective efficacy and safety of BBG2Na, a subunit respiratory syncytial virus (RSV) vaccine candidate, against RSV-B. Vaccine. 2003;22(2):168-76. PubMed PMID: 14615143.

154. Belshe RB, Anderson EL, Walsh EE. Immunogenicity of purified F glycoprotein of respiratory syncytial virus: clinical and immune responses to subsequent natural infection in children. J Infect Dis. 1993;168(4):1024-9. PubMed PMID: 8376814.

155. Groothuis JR, King SJ, Hogerman DA, Paradiso PR, Simoes EA. Safety and immunogenicity of a purified F protein respiratory syncytial virus (PFP-2) vaccine in seropositive children with bronchopulmonary dysplasia. J Infect Dis. 1998;177(2):467-9. PubMed PMID: 9466539.

156. Tristram DA, Welliver RC, Mohar CK, Hogerman DA, Hildreth SW, Paradiso P. Immunogenicity and safety of respiratory syncytial virus subunit vaccine in seropositive children 18-36 months old. J Infect Dis. 1993;167(1):191-5. PubMed PMID: 8418166.

157. Paradiso PR, Hildreth SW, Hogerman DA, Speelman DJ, Lewin EB, Oren J, et al. Safety and immunogenicity of a subunit respiratory syncytial virus vaccine in children 24 to 48 months old. Pediatr Infect Dis J. 1994;13(9):792-8. PubMed PMID: 7808848.

158. Wathen MW, Kakuk TJ, Brideau RJ, Hausknecht EC, Cole SL, Zaya RM. Vaccination of cotton rats with a chimeric FG glycoprotein of human respiratory syncytial virus induces minimal pulmonary pathology on challenge. J Infect Dis. 1991;163(3):477-82. PubMed PMID: 1995720.

159. Connors M, Collins PL, Firestone CY, Sotnikov AV, Waitze A, Davis AR, et al. Cotton rats previously immunized with a chimeric RSV FG glycoprotein develop enhanced pulmonary pathology when infected with RSV, a phenomenon not encountered following immunization with vaccinia--RSV recombinants or RSV. Vaccine. 1992;10(7):475-84. PubMed PMID: 1609551.

160. Rigter A, Widjaja I, Versantvoort H, Coenjaerts FE, van Roosmalen M, Leenhouts K, et al. A protective and safe intranasal RSV vaccine based on a recombinant prefusion-like form of the F protein bound to bacterium-like particles. PLoS One. 2013;8(8):e71072. Epub 2013/08/12. doi: 10.1371/journal.pone.0071072. PubMed PMID: 23951084; PubMed Central PMCID: PMCPMC3741363.

161. McLellan JS, Chen M, Leung S, Graepel KW, Du X, Yang Y, et al. Structure of RSV fusion glycoprotein trimer bound to a prefusion-specific neutralizing antibody. Science. 2013;340(6136):1113-7. Epub 2013/04/25. doi: 10.1126/science.1234914. PubMed PMID: 23618766; PubMed Central PMCID: PMCPMC4459498.

162. Liljeroos L, Krzyzaniak MA, Helenius A, Butcher SJ. Architecture of respiratory syncytial virus revealed by electron cryotomography. Proc Natl Acad Sci U S A. 2013;110(27):11133-8. Epub 2013/06/17. doi: 10.1073/pnas.1309070110. PubMed PMID: 23776214; PubMed Central PMCID: PMCPMC3703984.

163. Mousa JJ, Kose N, Matta P, Gilchuk P, Crowe JE. A novel pre-fusion conformation-specific neutralizing epitope on the respiratory syncytial virus fusion protein. Nat Microbiol. 2017;2:16271. Epub 2017/01/30. doi: 10.1038/nmicrobiol.2016.271. PubMed PMID: 28134924; PubMed Central PMCID: PMCPMC5463187.

164. Karron RA, Buchholz UJ, Collins PL. Live-attenuated respiratory syncytial virus vaccines. Curr Top Microbiol Immunol. 2013;372:259-84. doi: 10.1007/978-3-642-38919-1_13. PubMed PMID: 24362694; PubMed Central PMCID: PMCPMC4794267.

165. Pringle CR, Filipiuk AH, Robinson BS, Watt PJ, Higgins P, Tyrrell DA. Immunogenicity and pathogenicity of a triple temperature-sensitive modified respiratory syncytial virus in adult volunteers. Vaccine. 1993;11(4):473-8. PubMed PMID: 8470433.

166. Wright PF, Karron RA, Belshe RB, Thompson J, Crowe JE, Boyce TG, et al. Evaluation of a live, cold-passaged, temperature-sensitive, respiratory syncytial virus vaccine candidate in infancy. J Infect Dis. 2000;182(5):1331-42. Epub 2000/09/22. doi: 10.1086/315859. PubMed PMID: 11010838.

167. Karron RA, Wright PF, Belshe RB, Thumar B, Casey R, Newman F, et al. Identification of a recombinant live attenuated respiratory syncytial virus vaccine candidate that is highly attenuated in infants. J Infect Dis. 2005;191(7):1093-104. Epub 2005/03/01. doi: 10.1086/427813. PubMed PMID: 15747245.

168. Karron RA, Thumar B, Schappell E, Buchholz UJ, Collins PL. Attenuation of live respiratory syncytial virus vaccines is associated with reductions in levels of nasal cytokines. J Infect Dis. 2013;207(11):1773-9. Epub 2013/03/12. doi: 10.1093/infdis/jit089. PubMed PMID: 23482643; PubMed Central PMCID: PMCPMC3693589.

169. Malkin E, Yogev R, Abughali N, Sliman J, Wang CK, Zuo F, et al. Safety and immunogenicity of a live attenuated RSV vaccine in healthy RSV-seronegative children 5 to 24 months of age. PLoS One. 2013;8(10):e77104. Epub 2013/10/29. doi: 10.1371/journal.pone.0077104. PubMed PMID: 24204744; PubMed Central PMCID: PMCPMC3812203.

170. McFarland EJ, Karron RA, Muresan P, Cunningham CK, Valentine ME, Perlowski C, et al. Live-Attenuated Respiratory Syncytial Virus Vaccine Candidate With Deletion of RNA Synthesis Regulatory Protein M2-2 is Highly Immunogenic in Children. The Journal of Infectious Diseases. 2018;217(9):1347-55.

171. Neuzil KM, Johnson JE, Tang YW, Prieels JP, Slaoui M, Gar N, et al. Adjuvants influence the quantitative and qualitative immune response in BALB/c mice immunized with respiratory syncytial virus FG subunit vaccine. Vaccine. 1997;15(5):525-32. PubMed PMID: 9160520.

172. Hancock GE, Heers KM, Smith JD. QS-21 synergizes with recombinant interleukin-12 to create a potent adjuvant formulation for the fusion protein of respiratory syncytial virus. Viral Immunol. 2000;13(4):503-9. doi: 10.1089/vim.2000.13.503. PubMed PMID: 11192297.

173. Hancock GE, Heers KM, Smith JD, Scheuer CA, Ibraghimov AR, Pryharski KS. CpG containing oligodeoxynucleotides are potent adjuvants for parenteral vaccination with the fusion (F) protein of respiratory syncytial virus (RSV). Vaccine. 2001;19(32):4874-82. PubMed PMID: 11535341.

174. Ma Y, Jiao YY, Yu YZ, Jiang N, Hua Y, Zhang XJ, et al. A Built-In CpG Adjuvant in RSV F Protein DNA Vaccine Drives a Th1 Polarized and Enhanced Protective Immune Response. Viruses. 2018;10(1). Epub 2018/01/15. doi: 10.3390/v10010038. PubMed PMID: 29342954; PubMed Central PMCID: PMCPMC5795451.

175. Yamaguchi Y, Harker JA, Wang B, Openshaw PJ, Tregoning JS, Culley FJ. Preexposure to CpG protects against the delayed effects of neonatal respiratory syncytial virus infection. J Virol. 2012;86(19):10456-61. Epub 2012/07/18. doi: 10.1128/JVI.01082-12. PubMed PMID: 22811525; PubMed Central PMCID: PMCPMC3457284.

176. Mapletoft JW, Oumouna M, Townsend HG, Gomis S, Babiuk LA, van Drunen Littel-van den Hurk S. Formulation with CpG oligodeoxynucleotides increases cellular immunity and protection induced by vaccination of calves with formalin-inactivated bovine respiratory syncytial virus. Virology. 2006;353(2):316-23. Epub 2006/07/07. doi: 10.1016/j.virol.2006.06.001. PubMed PMID: 16828832.

177. Regner M, Culley F, Fontannaz P, Hu K, Morein B, Lambert PH, et al. Safety and efficacy of immune-stimulating complex-based antigen delivery systems for neonatal immunisation against respiratory syncytial virus infection. Microbes Infect. 2004;6(7):666-75. doi: 10.1016/j.micinf.2004.03.005. PubMed PMID: 15158774.

178. Kamphuis T, Stegmann T, Meijerhof T, Wilschut J, de Haan A. A virosomal respiratory syncytial virus vaccine adjuvanted with monophosphoryl lipid A provides protection against viral challenge without priming for enhanced disease in cotton rats. Influenza Other Respir Viruses. 2013;7(6):1227-36. Epub 2013/04/10. doi: 10.1111/irv.12112. PubMed PMID: 23575113; PubMed Central PMCID: PMCPMC4634254.

179. Shafique M, Meijerhof T, Wilschut J, de Haan A. Evaluation of an intranasal virosomal vaccine against respiratory syncytial virus in mice: effect of TLR2 and NOD2 ligands on induction of systemic and mucosal immune responses. PLoS One. 2013;8(4):e61287. Epub 2013/04/08. doi: 10.1371/journal.pone.0061287. PubMed PMID: 23593453; PubMed Central PMCID: PMCPMC3620164.

180. Olszewska W, Suezer Y, Sutter G, Openshaw PJ. Protective and disease-enhancing immune responses induced by recombinant modified vaccinia Ankara (MVA) expressing respiratory syncytial virus proteins. Vaccine. 2004;23(2):215-21. doi: 10.1016/j.vaccine.2004.05.015. PubMed PMID: 15531040.

181. Wyatt LS, Whitehead SS, Venanzi KA, Murphy BR, Moss B. Priming and boosting immunity to respiratory syncytial virus by recombinant replication-defective vaccinia virus MVA. Vaccine. 1999;18(5-6):392-7. PubMed PMID: 10519927.

182. Kim E, Okada K, Beeler JA, Crim RL, Piedra PA, Gilbert BE, et al. Development of an adenovirus-based respiratory syncytial virus vaccine: preclinical evaluation of efficacy, immunogenicity, and enhanced disease in a cotton rat model. J Virol. 2014;88(9):5100-8. Epub 2014/02/26. doi: 10.1128/JVI.03194-13. PubMed PMID: 24574396; PubMed Central PMCID: PMCPMC3993798.

183. Lee YN, Hwang HS, Kim MC, Lee YT, Kim YJ, Lee FE, et al. Protection against respiratory syncytial virus by inactivated influenza virus carrying a fusion protein neutralizing epitope in a chimeric hemagglutinin. Nanomedicine. 2016;12(3):759-70. Epub 2015/12/02. doi: 10.1016/j.nano.2015.11.007. PubMed PMID: 26656630; PubMed Central PMCID: PMCPMC4811744.

184. Jones BG, Sealy RE, Rudraraju R, Traina-Dorge VL, Finneyfrock B, Cook A, et al. Sendai virus-based RSV vaccine protects African green monkeys from RSV infection. Vaccine. 2012;30(5):959-68. Epub 2011/11/23. doi: 10.1016/j.vaccine.2011.11.046. PubMed PMID: 22119594; PubMed Central PMCID: PMCPMC3256274.

185. Wiegand MA, Gori-Savellini G, Gandolfo C, Papa G, Kaufmann C, Felder E, et al. A Respiratory Syncytial Virus Vaccine Vectored by a Stable Chimeric and Replication-Deficient Sendai Virus Protects Mice without Inducing Enhanced Disease. J Virol. 2017;91(10). Epub 2017/04/28. doi: 10.1128/JVI.02298-16. PubMed PMID: 28250126; PubMed Central PMCID: PMCPMC5411584.

186. Martinez-Sobrido L, Gitiban N, Fernandez-Sesma A, Cros J, Mertz SE, Jewell NA, et al. Protection against respiratory syncytial virus by a recombinant Newcastle disease virus vector. J Virol. 2006;80(3):1130-9. doi: 10.1128/JVI.80.3.1130-1139.2006. PubMed PMID: 16414990; PubMed Central PMCID: PMCPMC1346968.

187. Cautivo KM, Bueno SM, Cortes CM, Wozniak A, Riedel CA, Kalergis AM. Efficient lung recruitment of respiratory syncytial virus-specific Th1 cells induced by recombinant bacillus Calmette-Guérin promotes virus clearance and protects from infection. J Immunol. 2010;185(12):7633-45. Epub 2010/11/17. doi: 10.4049/jimmunol.0903452. PubMed PMID: 21084664.

188. Quan FS, Kim Y, Lee S, Yi H, Kang SM, Bozja J, et al. Viruslike particle vaccine induces protection against respiratory syncytial virus infection in mice. J Infect Dis. 2011;204(7):987-95. doi: 10.1093/infdis/jir474. PubMed PMID: 21881112; PubMed Central PMCID: PMCPMC3164432.

189. Lee S, Quan FS, Kwon Y, Sakamoto K, Kang SM, Compans RW, et al. Additive protection induced by mixed virus-like particles presenting respiratory syncytial virus fusion or attachment glycoproteins. Antiviral Res. 2014;111:129-35. Epub 2014/09/18. doi: 10.1016/j.antiviral.2014.09.005. PubMed PMID: 25239522; PubMed Central PMCID: PMCPMC4252885.

190. Smith G, Raghunandan R, Wu Y, Liu Y, Massare M, Nathan M, et al. Respiratory syncytial virus fusion glycoprotein expressed in insect cells form protein nanoparticles that induce protective immunity in cotton rats. PLoS One. 2012;7(11):e50852. Epub 2012/11/30. doi: 10.1371/journal.pone.0050852. PubMed PMID: 23226404; PubMed Central PMCID: PMCPMC3511306.

191. Jorquera PA, Choi Y, Oakley KE, Powell TJ, Boyd JG, Palath N, et al. Nanoparticle vaccines encompassing the respiratory syncytial virus (RSV) G protein CX3C chemokine motif induce robust immunity protecting from challenge and disease. PLoS One. 2013;8(9):e74905. Epub 2013/09/10. doi: 10.1371/journal.pone.0074905. PubMed PMID: 24040360; PubMed Central PMCID: PMCPMC3769300.

192. Ko EJ, Kwon YM, Lee JS, Hwang HS, Yoo SE, Lee YN, et al. Virus-like nanoparticle and DNA vaccination confers protection against respiratory syncytial virus by modulating innate and adaptive immune cells. Nanomedicine. 2015;11(1):99-108. Epub 2014/08/08. doi: 10.1016/j.nano.2014.07.013. PubMed PMID: 25109662; PubMed Central PMCID: PMCPMC4280318.

193. Johnson S, Oliver C, Prince GA, Hemming VG, Pfarr DS, Wang SC, et al. Development of a humanized monoclonal antibody (MEDI-493) with potent in vitro and in vivo activity against respiratory syncytial virus. J Infect Dis. 1997;176(5):1215-24. PubMed PMID: 9359721.

194. Homaira N, Rawlinson W, Snelling TL, Jaffe A. Effectiveness of Palivizumab in Preventing RSV Hospitalization in High Risk Children: A Real-World Perspective. Int J Pediatr. 2014;2014:571609. Epub 2014/12/04. doi: 10.1155/2014/571609. PubMed PMID: 25548575; PubMed Central PMCID: PMCPMC4274815.

195. Santos RP, Chao J, Nepo AG, Butt S, Stellrecht KA, Pearce JM, et al. The use of intravenous palivizumab for treatment of persistent RSV infection in children with leukemia. Pediatrics. 2012;130(6):e1695-9. Epub 2012/11/12. doi: 10.1542/peds.2011-1768. PubMed PMID: 23147965.

196. Blake SM, Tanaka D, Bendz LM, Staebler S, Brandon D. Evaluation of the Financial and Health Burden of Infants at Risk for Respiratory Syncytial Virus. Adv Neonatal Care. 2017;17(4):292-8. doi: 10.1097/ANC.0000000000000367. PubMed PMID: 27926583.

197. Boukhvalova M, Blanco JC, Falsey AR, Mond J. Treatment with novel RSV Ig RI-002 controls viral replication and reduces pulmonary damage in immunocompromised Sigmodon hispidus. Bone Marrow Transplant. 2016;51(1):119-26. Epub 2015/09/14. doi: 10.1038/bmt.2015.212. PubMed PMID: 26367224.

198. Wasserman RL, Lumry W, Harris J, Levy R, Stein M, Forbes L, et al. Efficacy, Safety, and Pharmacokinetics of a New 10 % Liquid Intravenous Immunoglobulin Containing High Titer Neutralizing Antibody to RSV and Other Respiratory Viruses in Subjects with Primary Immunodeficiency Disease. J Clin Immunol. 2016;36(6):590-9. Epub 2016/06/20. doi: 10.1007/s10875-016-0308-z. PubMed PMID: 27324887; PubMed Central PMCID: PMCPMC4940435.

199. Wasserman RL, Greener BN, Mond J. RI-002, an intravenous immunoglobulin containing high titer neutralizing antibody to RSV and other respiratory viruses for use in primary immunodeficiency disease and other immune compromised populations. Expert Rev Clin Immunol. 2017;13(12):1107-19. Epub 2017/10/16. doi: 10.1080/1744666X.2017.1389647. PubMed PMID: 29035131.

200. Sivapalasingam S, Caballero-Perez D, Houghton M, Yang F, Davis J, Gao B, et al. Phase 1 study evaluating safety, tolerability, pharmacokinetics and immunogenicity of REGN2222 in healthy adults: a new human monoclonal RSV-F antibody for RSV prevention2015; Volume 2.

201. Griffin MP, Khan AA, Esser MT, Jensen K, Takas T, Kankam MK, et al. Safety, Tolerability, and Pharmacokinetics of MEDI8897, the Respiratory Syncytial Virus Prefusion F-Targeting Monoclonal Antibody with an Extended Half-Life, in Healthy Adults. Antimicrob Agents Chemother. 2017;61(3). Epub 2017/02/23. doi: 10.1128/AAC.01714-16. PubMed PMID: 27956428; PubMed Central PMCID: PMCPMC5328523.

202. Detalle L, Stohr T, Palomo C, Piedra PA, Gilbert BE, Mas V, et al. Generation and Characterization of ALX-0171, a Potent Novel Therapeutic Nanobody for the Treatment of Respiratory Syncytial Virus Infection. Antimicrob Agents Chemother. 2016;60(1):6-13. Epub 2015/10/05. doi: 10.1128/AAC.01802-15. PubMed PMID: 26438495; PubMed Central PMCID: PMCPMC4704182.

203. Van Heeke G, Allosery K, De Brabandere V, De Smedt T, Detalle L, de Fougerolles A. Nanobodies® as inhaled biotherapeutics for lung diseases. Pharmacol Ther. 2017;169:47-56. Epub 2016/06/29. doi: 10.1016/j.pharmthera.2016.06.012. PubMed PMID: 27373507.

204. Falsey AR, Koval C, DeVincenzo JP, Walsh EE. Compassionate use experience with high-titer respiratory syncytical virus (RSV) immunoglobulin in RSV-infected immunocompromised persons. Transpl Infect Dis. 2017;19(2). Epub 2017/03/06. doi: 10.1111/tid.12657. PubMed PMID: 28054734.

205. Krilov LR. Safety issues related to the administration of ribavirin. Pediatr Infect Dis J. 2002;21(5):479-81. PubMed PMID: 12150196.

206. Toovey S, Wu J, Wang V, Griffin P, Lau A, Elliott S. Safety And Pharmacokinetics In Healthy Volunteers Of The Anti-RSV Antiviral AK0529. 1st International Meeting on Respiratory Pathogens; Singapore2015.

207. Draffan AG, Bond S, Fenner J. Preclinical characterization of an orally bioavailable fusion inhibitor, BTA-C585, for the treatment of RSV infection. 4th Interscience Conference on Antimicrobial Agents and Chemotherapy (ICAAC) Meeting; Washington DC2014.

208. Stevens M, Rusch S, DeVincenzo J, Kim YI, Harrison L, Meals EA, et al. Antiviral Activity of Oral JNJ-53718678 in Healthy Adult Volunteers Challenged With Respiratory Syncytial Virus: A Placebo-Controlled Study. J Infect Dis. 2018;218(5):748-56. doi: 10.1093/infdis/jiy227. PubMed PMID: 29684148.

209. Huntjens DRH, Ouwerkerk-Mahadevan S, Brochot A, Rusch S, Stevens M, Verloes R. Population Pharmacokinetic Modeling of JNJ-53718678, a Novel Fusion Inhibitor for the Treatment of Respiratory Syncytial Virus: Results from a Phase I, Double-Blind, Randomized, Placebo-Controlled First-in-Human Study in Healthy Adult Subjects. Clin Pharmacokinet. 2017;56(11):1331-42. doi: 10.1007/s40262-017-0522-8. PubMed PMID: 28238203.

210. Mackman RL, Sangi M, Sperandio D, Parrish JP, Eisenberg E, Perron M, et al. Discovery of an oral respiratory syncytial virus (RSV) fusion inhibitor (GS-5806) and clinical proof of concept in a human RSV challenge study. J Med Chem. 2015;58(4):1630-43. Epub 2015/01/27. doi: 10.1021/jm5017768. PubMed PMID: 25574686.

211. Perron M, Stray K, Kinkade A, Theodore D, Lee G, Eisenberg E, et al. GS-5806 Inhibits a Broad Range of Respiratory Syncytial Virus Clinical Isolates by Blocking the Virus-Cell Fusion Process. Antimicrob Agents Chemother. 2015;60(3):1264-73. Epub 2015/12/14. doi: 10.1128/AAC.01497-15. PubMed PMID: 26666922; PubMed Central PMCID: PMCPMC4776015.

212. Samuel D, Xing W, Niedziela-Majka A, Wong JS, Hung M, Brendza KM, et al. GS-5806 inhibits pre- to postfusion conformational changes of the respiratory syncytial virus fusion protein. Antimicrob Agents Chemother. 2015;59(11):7109-12. Epub 2015/08/31. doi: 10.1128/AAC.00761-15. PubMed PMID: 26324264; PubMed Central PMCID: PMCPMC4604407.

213. DeVincenzo JP, Whitley RJ, Mackman RL, Scaglioni-Weinlich C, Harrison L, Farrell E, et al. Oral GS-5806 activity in a respiratory syncytial virus challenge study. N Engl J Med. 2014;371(8):711-22. doi: 10.1056/NEJMoa1401184. PubMed PMID: 25140957.

214. DeVincenzo JT, D., Oluwayi O, Mori J, Thomas E, Mathews N, Harland R, et al. Safety and Efficacy of Oral RV521 in a Human Respiratory Syncytial Virus (RSV) Phase 2a Challenge Study. American Thoracic Society 2018 International Conference; San Diego, California: American Journal of Respiratory and Critical Care Medicine; 2018.

215. Battles MB, Langedijk JP, Furmanova-Hollenstein P, Chaiwatpongsakorn S, Costello HM, Kwanten L, et al. Molecular mechanism of respiratory syncytial virus fusion inhibitors. Nat Chem Biol. 2016;12(2):87-93. Epub 2015/12/07. doi: 10.1038/nchembio.1982. PubMed PMID: 26641933; PubMed Central PMCID: PMCPMC4731865.

216. DeVincenzo JP, McClure MW, Symons JA, Fathi H, Westland C, Chanda S, et al. Activity of Oral ALS-008176 in a Respiratory Syncytial Virus Challenge Study. N Engl J Med. 2015;373(21):2048-58. doi: 10.1056/NEJMoa1413275. PubMed PMID: 26580997.

217. Wang G, Deval J, Hong J, Dyatkina N, Prhavc M, Taylor J, et al. Discovery of 4'-chloromethyl-2'-deoxy-3',5'-di-O-isobutyryl-2'-fluorocytidine (ALS-8176), a first-in-class RSV polymerase inhibitor for treatment of human respiratory syncytial virus infection. J Med Chem. 2015;58(4):1862-78. Epub 2015/02/10. doi: 10.1021/jm5017279. PubMed PMID: 25667954.

218. Chapman J, Abbott E, Alber DG, Baxter RC, Bithell SK, Henderson EA, et al. RSV604, a novel inhibitor of respiratory syncytial virus replication. Antimicrob Agents Chemother. 2007;51(9):3346-53. Epub 2007/06/18. doi: 10.1128/AAC.00211-07. PubMed PMID: 17576833; PubMed Central PMCID: PMCPMC2043207.

219. Challa S, Scott AD, Yuzhakov O, Zhou Y, Tiong-Yip CL, Gao N, et al. Mechanism of action for respiratory syncytial virus inhibitor RSV604. Antimicrob Agents Chemother. 2015;59(2):1080-7. Epub 2014/12/01. doi: 10.1128/AAC.04119-14. PubMed PMID: 25451060; PubMed Central PMCID: PMCPMC4335855.

220. Gottlieb J, Zamora MR, Hodges T, Musk AW, Sommerwerk U, Dilling D, et al. ALN-RSV01 for prevention of bronchiolitis obliterans syndrome after respiratory syncytial virus infection in lung transplant recipients. J Heart Lung Transplant. 2016;35(2):213-21. Epub 2015/09/03. doi: 10.1016/j.healun.2015.08.012. PubMed PMID: 26452996.

CHAPTER 2. THERAPEUTIC EFFICACY OF JNJ-53718678, A HUMAN RESPIRATORY SYNCYTIAL FUSION INHIBITOR, IN NEONATAL LAMBS

Modified from a manuscript published as part of an article entitled

"*Therapeutic efficacy of a respiratory syncytial virus fusion inhibitor,*

Nature Communications (2017)

Panchan Sitthicharoenchai[1], Sarhad S. Alnajjar[1], Alejandro Larios-Mora[1], Anil Koul[2], Dirk Roymans[2], Peter Rigaux[2], Jack M. Gallup[1] and Mark R. Ackermann[2]

[1]College of Veterinary Medicine, Iowa State University, Ames, IA.

[2]Janssen Infectious Diseases and Vaccines, Janssen Pharmaceutica NV, Beerse Belgium.

Abstract

Human respiratory syncytial virus (hRSV) is a leading cause of respiratory infection in infants and children worldwide. It is crucial to explore new and effective treatment methods for hRSV. This study assessed the therapeutic efficacy of hRSV fusion protein inhibitor (hRSV-FPI) in a lamb model of RSV infection that has close similarities to hRSV infection in infants. A total of twenty-two, 1-3 days old lambs were divided into 5 groups; hRSV infected with administration of daily intragastric 1 mg/kg (T1) (n=4), 5 mg/kg (T5) (n=4) and 25 mg/kg (T25) (n=4) dosage of RSV-FPI for 5 consecutive days, hRSV infected with no treatment (n=5), and negative control (n=5). Clinical signs were recorded daily and at day 6 post-infection, all lambs were euthanized and necropsied. In T5 and T25 treatment groups, lambs lacked clinical signs of RSV infection and hRSV lesions were not detected. Focus-forming unit (FFU) assay did not detect viable virus in the lung tissue samples and low amount of virus was detected in BALF samples with 25 mg/ml dosage. No significant reduction of viable virus

was observed with 1 mg/kg dosage of RSV-FPI. Viral FFU level paralleled the amount of viral mRNA detected by RT-qPCR. In summary, intragastric administration of hRSV-FPI at the appropriate dosage significantly reduced clinical signs, gross lung lesions and presence of hRSV in the lung tissue of lambs. This compound is a good candidate for future therapeutic usage for hRSV in infants and children.

Introduction

Human respiratory syncytial virus (hRSV) is a common cause of respiratory infection in infants and children worldwide. The virus causes respiratory symptoms including rhinitis, bronchiolitis, pneumonia and occasionally otitis media. The most common susceptible individuals are children younger than 5 years old and adults over the age of 65. Previous epidemiological data reported the disease causing hospitalization of approximately 160,000 to 180,000 children under the age of 5 and an average of 177,000 hospitalized and 14,000 deaths in adults over the age of 65 each year in the United States [1]. The disease outcome can be more severe and fatal in children younger than 1 year of age [2]. Many research investigations have been made to find or develop prevention and treatment methods for hRSV and these range from vaccination to therapeutic antibody treatments and antiviral drugs. To date, there is no licensed vaccine for hRSV. Earlier vaccine development and usage of hRSV-formalin inactivated vaccine resulted in vaccine-enhancement immunopathology and death [3]. At present, only two therapeutic compounds are approved specifically for hRSV treatment which includes palivizumab, a humanized monoclonal antibody against F protein, and ribavirin, an antiviral guanosine analog. Previous data indicated that the use of palivizumab resulted in the reduction of hRSV-associated hospitalization rates by 55% in premature infants, when comparing to placebo [4]. This compound is recommended as a prophylactic regimen for

patients with high risk of hRSV infection [5]. Few studies have reported the use of palivizumab as a hRSV treatment approach [6]. Ribavirin on the other hand is a broad-spectrum antiviral drug that inhibits inosine-5'-monophosphate dehydrogenase (IMPDH) resulting in reduced formation of mRNA and viral polymerase. The use of this aerosolized drug has been implicated for severe cases of hRSV infection, but the results still remain controversial due to the failure to have a significant therapeutic effect, its high cost and the direct and indirect side effects [7, 8]. Treatment in most cases for hRSV remains mostly supportive.

Attempts in finding alternative immunotherapy and antiviral compounds are crucial. Many candidates of anti-hRSV drugs are currently at different stages of development, preclinical tests and some in phases of clinical trials [9]. One of the most widely studied are hRSV small molecule fusion protein inhibitors (hRSV-FPI) that interact with the viral fusion protein and inhibits viral entry [10]. The process in development of the therapeutic compounds requires multiple efficacy and safety tests which involve laboratory experiments and trials in a hRSV-animal model such as cotton rats, ruminants, ferrets, non-human primates, and a recently established neonatal lamb model [11]. The hRSV-infected lamb model has similarities in lung anatomy, pulmonary immune response and pathology to human infants and represents an affective model for hRSV infection [12]. In this study, we evaluated the efficacy of an orally administered hRSV fusion protein inhibitor (hRSV-FPI) in a hRSV-lamb model.

Materials and Methods

Virus and Treatment Compound Preparations

Human respiratory syncytial virus Memphis 37 strain (hRSV M37) was grown on HEp-2 cell line and collected 48-72 hours after infection. The virus was extracted by freeze-thawing at -80°C followed by centrifugation (25,000 rpm, 10 min) to discard the cellular components.

The supernatant containing hRSV M37 was collected in 20% sucrose and stored at -80°C, by a procedure previously published by Grosz et al., 2014 [13]. The viral titer was evaluated using the standard focus-forming unit (FFU) assay.

Fusion protein inhibitor, JNJ-53718678, was diluted in 20% acidified hydroxypropryl-β- cyclodextrin (20 % HP-β-CD + HCl) at pH 2 (adjusted pH 7-7.4) to 6.25, 1.25 or 0.25 mg/ml prior to dosing and stored at room temperature. Administration of the compound was performed using gavage catheter with each dose washed down by 5 ml of 20 % HP-β-CD+HCl, pH 7-7.4.

Animal Model and Experimental Design

A total of 22, 1-3 day old colostrum-deprived lambs (Polypay, Suffolk and Dorsett crossbred) were randomly separated into 5 groups including hRSV infected lambs administered 3 different dosage of hRSV-FPI, JNJ-53718678, at 1) 25 mg/kg (T25) (n=4); 2) 5 mg/kg (T5) (n=4); 3) 1 mg/ml (T1) (n=4); 4) hRSV infected given placebo vehicle (hRSV) (n=5); and 5) uninfected lambs (control) (n=5). Delivery of hRSV M37 was performed by nebulization at the concentration of 3.05×10^7 FFU/lamb in 7 ml cell culture media containing 20% sucrose over a 30-minute period. Different concentrations of hRSV-FPI were given via intragastric administration each day for 5 consecutive days after hRSV infection. Intragastric administration using orogastric gavage of hRSV-FPI in 20% acidified hydroxypropyl-β-cyclodextrin (HP-β-CD+HCl) solution was given at three different dosages (25, 5 and 1 mg/kg) with a hRSV placebo group receiving vehicle containing 20% HP-β-CD+HCl once daily for 6 consecutive days.

Measurements of body weight, body temperature, respiratory rate, heart rate and antibiotic administration (ceftiofur sodium (Naxcel®)) were performed daily on all lambs. Plasma samples were collected at 24 hours prior to hRSV infection and 2, 24, 48, 72, 96, 120, 144 hours after the first treatment dose. All animals were euthanized by sodium pentobarbital overdose on day 6 post-hRSV infection. Animal use and experimental procedures were approved by the Iowa State University's IACUC committee (IACUC # 3-14-7748-0).

Sample Collections and Necropsy

Lung gross examination and scoring were performed by estimating the percentage affected and converted to a scoring scheme from 1 to 4 (0% = 0, 1-9% = 1, 10-39% = 2, 40-69% = 3, 70-100% = 4). Bronchoalveolar lavage fluid (BALF) was collected from the right caudal lobe and right middle lung lobe using 5 ml, cold double-modified Iscove's media (DMIM) (42.5% Iscove's modified Dulbecco's medium, 7.5% glycerol, 1% heat-inactivated fetal bovine serum, 49% Dulbecco's modified eagle medium (DMEM) and 5 μg/ml kanamycin sulfate). For viral detection and pharmacokinetic analysis, lung tissue samples were collected from right cranial, left cranial, left middle and left caudal, frozen in liquid nitrogen and stored at -80°C until further processing. In addition, two pieces of lung tissue samples from right cranial, left cranial, left middle and left caudal lobes were placed in tissue cassettes and fixed in 10% neutral-buffered formalin for histopathological and immunohistochemical staining.

Laboratory Analysis

Quantification of JNJ-53718678 in plasma, lung and BALF

The plasma, lung and BALF samples were analyzed for JNJ-53718678 level by liquid chromatography-tandem mass spectrometry (LC-MS/MS). The lower limit of quantifications were 2.5 ng/ml for plasma and BALF and 12.5 ng/g for lung samples.

Histopathology and immunohistochemistry (IHC)

Tissue cassettes containing lung samples were processed by the Histopathology Laboratory, Department of Veterinary Pathology, College of Veterinary Medicine, Iowa State University for hematoxylin and eosin (H&E) stained slides, and unstained slides for immunohistochemical detection of hRSV antigen. For immunohistochemistry, the slide sections were placed in a heated oven (58°C) and directly immersed in xylene for deparaffinization process. The slides were then rehydrated through a series of graded alcohols (100%, 95%, 70% methanol) with initial endogenous peroxidase blocking (3% hydrogen peroxide in methanol solution) then placed in double distilled water (ddH_2O). Antigen retrieval was performed by placing the slides in pH 9.0 10 mM TRIZMA Base, 1 mM EDTA buffer and 0.05% Tween 20 and heated to 125°C using a pressure-cooking device (Decloaking Chamber Plus, Biocare Medical, Concord, CA, USA). Subsequent steps of IHC staining were performed using a programmable automated IHC machine (BioGenex OptiMax i6000 staining system, USA). The protocol consisted of serum blocking with 3% bovine serum albumin (BSA) in TRIS-buffered saline with 0.05% Tween (TBST), followed by 20% normal swine serum (NSS) in TBST for 15 minutes each. The slides were then incubated with primary antibody for 90 minutes (1:500 polyclonal goat anti-RSV antibody (Millipore/Chemicon, Darmstadt, Germany) in 10% NSS, 3% BSA in TBST solution. Subsequently, the slides were washed

twice with PBST then incubated for 45 minutes with 1:300 dilution of biotinylated rabbit anti-goat IgG antibody in 10% NSS, 3% BSA in TBST solution. Secondary peroxidase blocking was performed by incubating the tissue sections in 3% H_2O_2 in TBST for 25 minutes followed by two TBST washes. Slides were then incubated in 1:200 streptavidin-horse radish peroxidase diluted in TBST for 30 minutes and washed 3 times with TBST. The slides were taken out of the machine and manually stained with chromogen substrate (Nova Red staining solution) for 60-90 seconds and the reactions were stopped with ddH_2O. After chromogenic development, the slides were counterstained with Shandon's hematoxylin and mounted under cover-slipped.

Lung histopathological scores were determined with H&E stained lung tissue sections. The scores ranged from 0 to 4 from lowest to highest pathological changes. Criteria for scoring include; lung consolidation, bronchitis, syncytial formation, bronchial and bronchiolar epithelial necrosis, bronchial and bronchiolar epithelial hyperplasia, presence of neutrophilic infiltration, perivascular and peribronchiolar lymphocytic infiltrates (Supplementary Table 1). Number of bronchioles and alveoli with hRSV signal were counted in a total of 20 fields at 200X magnification with 22mm objective field from IHC slides of right cranial, left cranial, left middle and left caudal lung lobes. Semi-quantitative scores from 0-4 were assigned based on the number of positive signals observed in the bronchioles or alveoli (e.g. score 1=1-10 positive counts, score 2=11-39 positive counts, score 3=40-99 positive counts and score 4=>100 positive counts).

Focus forming unit (FFU) on bronchioalveolar lavage fluid (BALF) and lung tissue

Bronchioalveolar lavage fluid (BALF) and lung tissue samples were processed immediately after sample collection to detect viable virus using an infectious focus-forming unit assay (FFU). Prior to performing the assay, BALF samples were centrifuged at 15,600 x g. The supernatants were collected and spun through a spin column filter (Coster SPIN-X filter, Fisher Scientific, Hanover Park, IL, USA). In addition, lung tissue samples from right cranial, accessory, left cranial, left middle and left caudal (0.1 g each lobe, total of 0.5 g) were pooled and homogenized in 5 ml DMIM. Homogenized lung tissues were then centrifuged at 15,600 x g to remove large debris and supernatants were collected. Each lung sample supernatant was centrifuged 2-3 times through a spin column filter. The filtrates of BALF and homogenized lungs were collected and used in the FFU assay.

HEp-2 cells were grown in 12-well cell culture plates to 70-80% confluency in culture media (DMEM, 10% FBS, 50 μg/ml kanamycin sulfate). The BALF samples were tested at full strength and 10^{-1}, 10^{-2}, 10^{-3}, 10^{-4} concentrations achieved by 10-fold dilution of the BALF samples in culture media. The media of the readily grown HEp-2 cells in 12-well cell culture plates was removed and 200 μl of each sample concentration was pipetted into duplicate wells and incubated at 37°C, 5% CO_2 incubating chamber for 90 minutes. After sample incubation, 1 ml of culture media was added to each well and the plates were allowed to further incubate for 48 hours at 37°C, 5% CO_2. To start the staining process, the media was removed, and the cells were fixed in 60% acetone/40% methanol solution for 1 minute. The fixing solution was removed, and the plates were air-dried for 2 minutes before rehydrating with 1 ml/well TBST for 1 minute. TBST was removed and 1 ml blocking solution (3% BSA in TBST) was added

to each well and incubated for 30 minutes at room temperature. The blocking solution was removed, and primary polyclonal goat anti-RSV diluted to 1:800 with 3% BSA in TBST was added (325 µl/well) and incubated at 4°C, overnight with gentle rocking. All wells were washed 3 times with TBST and 1:800-diluted secondary fluorescence-tagged rabbit anti-goat IgG secondary antibody in TBST with 3% BSA was added to each well (325 µl/well). After a 30 minutes incubation at room temperature, the plates were washed three times with TBST and 1 ml of TBST was left in each well to prevent from drying. Each plate was observed under a fluorescence light microscope to count the infectious viral focus-forming colonies by averaging the result from the duplicated wells and calculating the FFU per ml.

Real-time reverse transcription polymerase chain reaction (RT-qPCR)

Lung tissue samples for RNA extraction were pooled from right cranial, left cranial, left middle and left caudal lung lobes (0.3 g each lobe) and homogenizing each 1.2 g pooled tissue amount for approximately 1 minute in 12 ml TRIzol solution (Invitrogen/Life Technologies, Carlsbad, CA, USA). A volume of 1.1 ml of each sample homogenate was taken for RNA extraction by adding 120 µl of chloroform and centrifuging at 12,000 x g, 4°C. After centrifugation, 550 µl of the upper aqueous layer was collected from each sample and mixed with 500 µl of isopropanol and allowed to sit for 10 minutes. The precipitated RNA was pelleted by centrifuging the samples for 10 minutes at 12,000 x g, 4°C. The RNA pellets were washed with 75% nuclease-free ethanol, centrifuged for 5 minutes at 16,000 x g, 4°C, allowed to air-dry for 35 minutes, then resuspended in 170 µl nuclease-free water and heated for 90 seconds at 60°C. Subsequent to heating, 70 µl of each RNA extracted sample was treated with DNase (TURBO-DNase, Ambion, Austin, TX, USA) after which 80 µl of the samples were

diluted 1:10 with 710 µl of nuclease-free water and 10 µl of RNaseOUT (Invitrogen/Life Technologies, Carlsbad, CA, USA). RNA quantity and purity were assessed by spectrophotometry at wavelengths of 260 nm and 280 nm.

At necropsy, 100 µl of BALF samples were stored at -80°C in 1 ml TRIzol solution until RNA isolation. The process of RNA isolation for BALF samples was performed according to TRIzol procedure (Invitrogen/Life Technologies, Clarlsbad, CA, USA). The resulting RNA from each BALF sample was resuspended in 100 µl nuclease-free water resuspended in 100 µl of nuclease-free water (Invitrogen/Life Technologies, Carlsbad, CA, USA) and incubated at 60°C for 2 minutes. The final RNA isolates were then diluted 1:10 with 710 µl of nuclease-free water and 10 µl of RNaseOUT (Invitrogen/Life Technologies, Carlsbad, CA, USA).

To quantify the amount of RSV viral particles, RT-qPCR was performed by targeting the nucleoprotein (N) mRNA of M37 RSV in each of the lung tissue and BALF RNA sample isolates. The primers and probe for the RSV M37 nucleoprotein (N) mRNA sequence in this study were designed using ABI Primer Express 2.0 based on RSV accession number M74568 (Supplementary Table 2). Expression of cytokine and chemokine mRNAs were evaluated including IFN-λ, IL-13, CCL2 (MCP-1), CCL3 (MIP-1α), CCL5 (RANTES), CXCL10 (IP10), CD274 (PD-L1) and CC10 with primer and probe sequences of all targets listed in (Supplementary Table 2). RT-qPCR was performed using One-Step Fast qRT-PCR Kit master mix (Quantabio, Gaithersburg, MD, USA) in a Gene Amp 5700 Sequence Detection System (Applied Biosystems, Carlsbad, CA, USA). A serial dilution of a mixture of samples (Stock I) was used to create the standard curve for each mRNA target, and all sample, standard and reagent dilutions were calculated and managed using PREXCEL-Q software [14]. Each sample

was duplicated and placed in the thermocycler for one round of pre-treatment (3 minutes at 50°C, then 30 seconds at 95°C) followed by 45 cycles of 3 seconds, 95°C and 30 seconds at 60°C. The virus copy number was calculated based on the standard curves generated from plasmid constructs. The relative quantity (rQ) of cytokine/chemokine and CD274 and CC10 mRNA expression were calculated using the following equation: $rQ = 10^{[(Cq - b)/m]}$ where Cq represents the quantification cycle, *b* is the *y*-intercept and *m* is the slope of the standard curve generated for each target from serial dilutions of Stock I [8].

Results

Compound Level in Plasma, BALF and Lung Tissue

Plasma concentration of JNJ-53718678 was measured daily once the compound was given with additional evaluation in the BALF and lung tissue (day 6) (Fig 1). Results showed in the initial dosage of the compound collected at 26 hpi, the concentrations were highest in the T25 group (539.48 ng/ml), followed by T5 (229.67 ng/ml) and were the lowest in T1 (20.06 ng/ml). The C_{trough} plasma concentration of the drug increases and stabilized after the second dosage point evaluated at 48 hpi with levels of ≥ 3208.5, 105.0, and 6.13 ng/ml, respectively from high to low dosage group. The lung/BALF to plasma ratio was evaluated to determine the distribution of compound to the target organ. The ratio of lung/plasma (T25=8.76, T5=9.98, and T1=11.08) was higher than BALF/plasma ratio (T25=0.14, T5=0.08 and T1=0.57).

Lung Pathology and Immunohistochemical Detection of hRSV

Lambs administered the 25 mg/kg dose (T25) lacked macroscopic hRSV-associated lung lesions and the average percentages of hRSV affected lung involvement in the T5 and T1

groups were 1.43% and 35.95%, respectively (Fig 2). Bronchiolitis, syncytial cell formation and epithelial necrosis were undetectable in all treatment groups with none of other criteria detected for high treatment dose. Semi-quantitative evaluation of hRSV antigen localization with IHC staining scores were only detected in the low dose group (0.25±0.125 in the bronchioles and 0.33±0.31 in the alveoli). The average IHC scores of the hRSV infected group receiving no treatment were 1.83±0.26 in the bronchiolar and 2.46±0.44 in the alveoli (Fig 3, 4).

Clinical signs related to hRSV (e.g. wheezing and coughing) were not observed throughout the study. At day 3 pi, the body temperature increased slightly higher in the RSV inoculate groups. The respiratory rate and the heart rate were higher than normal range in all groups (normal respiratory rate in sheep = 20-40 breaths per minute, normal heart rate in sheep = 80-130 beats per minute) likely related to stress induced from restraining. All groups had similar trend of increasing body weight.

Viral Titer and Viral RNA detection

The viral titers and levels of viral RNA detected in each treatment groups were tabulated (Fig 5). Detection of viable virus in the lung and BALF at 6 dpi with FFU assay demonstrated a reduction of virus in a dose-dependent manner with the lowest average viral titers in the high dose group (T25) (BALF=2.50 FFU/ml, lung=0.00 FFU/g), moderate titers in the medium dose group (T5) (BALF=$3.34x10^2$ FFU/ml, lung=$1.28x10^2$ FFU/g) and the highest viral titers in the low dose group (T1) ($4.38x10^4$ FFU/ml, lung=$2.24x10^5$ FFU/g). Similar dose-dependent trend was observed with quantification of virions by RT-qPCR in the lung and BALF. The average level of virion copies in BALF and lung of the T25 were $5.99x10^6$

copies/ml and $7.75x10^3$ copies/g, T5 were $1.60x10^7$ copies/ml and $2.78x10^4$ copies/g, and T1 were $1.31x10^8$ copies/ml and $4.22x10^5$ copies/g. There was a significant reduction of BALF and lung viral titer ($p<0.001$) and viral RNA (BALF = $p<0.05$ and lung = $p<0.01$) at >16 fold with the T25. Significant reduction of BALF and lung viral titer ($p<0.01$) and lung viral RNA ($p<0.05$) were also detected in T5 group. No hRSV virus was detected with FFU and RT-qPCR in the negative control group.

Cytokine and Chemokines mRNA Expression

Evaluation of cytokine and chemokine mRNA expression demonstrated an increasing trend of CXCL10 (IP10), CCL3 (MCP-1α), CD274 (PD-L1) and IFN- λ corresponding with higher viral load. However, there were no significant differences in measured cytokine and chemokine levels between hRSV infected and treatment groups when compared to the non-infected group with a one-way ANOVA (Fig 6).

Discussion

Neonatal HRSV-Infected Lamb Model, a Model for Human Infants with HRSV Infection

Many animal models have been used to study the efficacy of vaccines, various therapeutics agents, and the pathogenesis of hRSV infection. Rodents represent the most widely used model of hRSV infection, with numerous studies using cotton rats [15, 16] and laboratory mice [17, 18]. These rodent models are useful for studying the pathogenesis and immunological response of hRSV infection. Some concerns with using rodent species as a human model are the differences in lung anatomical structure, lack of certain immunologic components such as interleukin-8 (IL-8) and variation of hRSV infection permissiveness compared to typical hRSV infection in human. Non-human primates (NHPs) have close

similarity with humans and are an ideal animal model for pathogenesis, vaccine testing and antiviral therapeutic studies [19-24]. The use of NHPs requires specialized facilities and some regulatory requirements. HRSV-infection in the neonatal lamb has many advantages for modeling hRSV infection in human infants because of the close similarities in pulmonary anatomy, immune response and viral induced lung pathology [12]. The tracheobronchial tree of sheep is characterized by irregular dichotomous branching similar to humans and large mammals. This feature can impact the deposition of aerosolized compound administration. The character of the immune response to hRSV infection is an important part of hRSV pathogenesis. The IL-8 gene is absent in rats and mice [25] and this cytokine plays a significant role in the recruitment of neutrophilic response to hRSV infection in humans [26, 27]. The expression of IL-8 gene is present in sheep and many other mammals [28]. The lung lesions of hRSV inoculation through nebulization are characterized by necrotizing and neutrophilic bronchiolitis, lymphoplasmacytic adventitial infiltrates and occasional syncytial cell formation with hRSV antigen localization in bronchiolar epithelium and occasionally in type II pneumocyte, with peak lesion development at 6 dpi [29]. In this study and others we have completed, we were able to replicate and establish similar hRSV lesions in infected lambs and also demonstrated differences in lesions and levels of virus at different dose of small molecule fusion protein inhibitor. Other studies of therapeutic compound testing with the hRSV-infected neonatal lamb model include administration of VEGF [30], CC10 [31], iodide administration [32] and immunotherapeutic compound, ALX-0171 [33]. Furthermore, vaccination studies with formalin-inactivated hRSV has been tested in this lamb model and demonstrated disease enhancement with subsequent hRSV infection [34]. Thus, the neonatal hRSV-infected lamb

model remains as a suitable option for preclinical therapeutic and vaccine testing of hRSV infection, especially for representing human infants.

Fusion Protein as Therapeutic Target for Small Molecule Inhibitor of HRSV

Entry of hRSV into host cells is facilitated by attachment of G and F protein to cellular receptors including annexin II [35], CX3CR1 [36], nucleolin [37] and heparan sulfate proteoglycans [38]. These viral proteins and receptors are potential targets for novel therapeutics for hRSV with the most studied therapeutic target being the viral F protein. The use of a high throughput screening assay for compounds that inhibit hRSV F protein has led to the identification of many small-molecule inhibitors targeting hRSV F protein. Blockage of F protein using specific inhibitors such as CL-309623 and RFI-641 has been shown to prevent entry and fusion of the virus *in vitro* [39, 40]. JNJ-53718678, a recently discovered hRSV-FPI, binds and stabilizes the metastable prefusion conformation of hRSV F protein at the central cavity of the F protein trimer, thus preventing viral entry and attachment [41]. A similar mechanism was reported in other small-molecule F protein inhibitors including GS-5806 [42-45]. Other mechanisms of F protein inhibitors involve blocking the binding of the F protein by creating a hydrophobic environment [40] and interacting with the HRA domain of the F protein (MDT-637, BMS-433771) [46, 47]. A recent study has suggested that there is a common binding site of these compounds at the pocket inside the trimeric ectodomain of the prefusion F protein [10]. The administration of these compounds has shown to inhibit hRSV replication *in vitro* and reduce viral titers in the lungs of hRSV infected mice [48].

Orally Administered Fusion Protein Inhibitor, JNJ-53718678, Reduced the Viral Load and Lung Lesions in a Dose-Dependent Manner in HRSV-Infected Lambs

Evaluation of effective small molecule inhibitors includes compound efficacy, inhibitor-resistance mutation of the F protein, tolerability and safety of the compound, appropriate delivery route, half-life of the compound in tissue and pharmacokinetic distribution. The oral regimen of JNJ-53718678 diluted in 20% HP-β-CD+HCl, pH 7-7.4 given to the neonatal lamb model at up to 25 mg/kg did not appear to cause any clinical side-effects in the 6-day period of administration. When administered at a level of 25 mg/kg given 1 day post infection, plasma levels appeared to increase and stabilize by the time of the second daily oral dose (48 hpi), which overlaps with the 24-72 day post-infection progressive period of increase viral load in the neonatal lamb model infected with hRSV M37 [29]. The compound concentration in the lung was higher than in BALF at day 6 with a high compound lung/plasma ratio indicating good distribution of the compound to the target organ. The pulmonary viral load and lung lesions were reduced in a dose-dependent manner with a significant reduction of the viral titer and viral RNA at 25 and 5 mg/kg dosage level (Fig 5). Viral mRNA was present in the lung at the high dosage level, but lack of viral focus forming units indicates a lack of replicating and/or viable virions. This can be due to the compound ability to bind and neutralize the infectious virions similar to previously tested *in vitro* experiments [10, 41]. However, we could not rule out the carry over-effect of the inhibitor compound in the viral plaque assay particularly in the high dose group.

Conclusions

The use of a neonatal lamb model of hRSV-infection is an appropriate option for preclinical testing of therapeutic compounds and vaccines for hRSV. Evaluation of the orally administered small molecule F protein inhibitor, JNJ-53718678, at the appropriate dosage in hRSV-infected lamb model demonstrated significantly reduced lung lesions, and a decreased amount of viable virus and viral particles. This potent antiviral compound is a suitable candidate for hRSV therapy with good potential for further clinical evaluation.

Acknowledgments

We would like to thank Janssen Infectious Diseases & Vaccines, Janssen Pharmaceutica NV, Beerse, Belgium for the funding in this study. We also would like to thank the Iowa State University, Veterinary Pathology Histology Laboratory technicians, Toni Christofferson, Deb Moore and Diane Gerjets, and Laboratory Animal Resources and Livestock Infectious Disease Isolation Facility staff, Diane McDonald, Kathleen Mullin, and Dale Hinderaker for their help and support.

Declaration of Conflicting Interests

This study was funded by Janssen Infectious Diseases & Vaccines, Janssen Pharmaceutica NV, Beerse, Belgium.

References

1. Thompson WW, Shay DK, Weintraub E, Brammer L, Cox N, Anderson LJ, et al. Mortality associated with influenza and respiratory syncytial virus in the United States. JAMA. 2003;289(2):179-86. PubMed PMID: 12517228.

2. Shay DK, Holman RC, Newman RD, Liu LL, Stout JW, Anderson LJ. Bronchiolitis-associated hospitalizations among US children, 1980-1996. Jama. 1999;282(15):1440-6. PubMed PMID: Medline:10535434.

3. Kim HW, Canchola JG, Brandt CD, Pyles G, Chanock RM, Jensen K, et al. Respiratory syncytial virus disease in infants despite prior administration of antigenic inactivated vaccine. Am J Epidemiol. 1969;89(4):422-34. PubMed PMID: 4305198.

4. Homaira N, Rawlinson W, Snelling TL, Jaffe A. Effectiveness of Palivizumab in Preventing RSV Hospitalization in High Risk Children: A Real-World Perspective. Int J Pediatr. 2014;2014:571609. Epub 2014/12/04. doi: 10.1155/2014/571609. PubMed PMID: 25548575; PubMed Central PMCID: PMCPMC4274815.

5. Johnson S, Oliver C, Prince GA, Hemming VG, Pfarr DS, Wang SC, et al. Development of a humanized monoclonal antibody (MEDI-493) with potent in vitro and in vivo activity against respiratory syncytial virus. J Infect Dis. 1997;176(5):1215-24. PubMed PMID: 9359721.

6. Santos RP, Chao J, Nepo AG, Butt S, Stellrecht KA, Pearce JM, et al. The use of intravenous palivizumab for treatment of persistent RSV infection in children with leukemia. Pediatrics. 2012;130(6):e1695-9. Epub 2012/11/12. doi: 10.1542/peds.2011-1768. PubMed PMID: 23147965.

7. Krilov LR. Palivizumab in the prevention of respiratory syncytial virus disease. Expert Opin Biol Ther. 2002;2(7):763-9. doi: 10.1517/14712598.2.7.763. PubMed PMID: 12387675.

8. Krilov LR. Safety issues related to the administration of ribavirin. Pediatr Infect Dis J. 2002;21(5):479-81. PubMed PMID: 12150196.

9. Heylen E, Neyts J, Jochmans D. Drug candidates and model systems in respiratory syncytial virus antiviral drug discovery. Biochem Pharmacol. 2017;127:1-12. Epub 2016/09/19. doi: 10.1016/j.bcp.2016.09.014. PubMed PMID: 27659812.

10. Battles MB, Langedijk JP, Furmanova-Hollenstein P, Chaiwatpongsakorn S, Costello HM, Kwanten L, et al. Molecular mechanism of respiratory syncytial virus fusion inhibitors. Nat Chem Biol. 2016;12(2):87-93. Epub 2015/12/07. doi: 10.1038/nchembio.1982. PubMed PMID: 26641933; PubMed Central PMCID: PMCPMC4731865.

11. Taylor G. Animal models of respiratory syncytial virus infection. Vaccine. 2017;35(3):469-80. Epub 2016/11/29. doi: 10.1016/j.vaccine.2016.11.054. PubMed PMID: 27908639; PubMed Central PMCID: PMCPMC5244256.

12. Derscheid RJ, Ackermann MR. Perinatal lamb model of respiratory syncytial virus (RSV) infection. Viruses. 2012;4(10):2359-78. Epub 2012/10/23. doi: 10.3390/v4102359. PubMed PMID: 23202468; PubMed Central PMCID: PMCPMC3497056.

13. Grosz DD, van Geelen A, Gallup JM, Hostetter SJ, Derscheid RJ, Ackermann MR. Sucrose stabilization of Respiratory Syncytial Virus (RSV) during nebulization and experimental infection. BMC Res Notes. 2014;7:158. doi: 10.1186/1756-0500-7-158. PubMed PMID: 24642084; PubMed Central PMCID: PMC3995326.

14. Gallup JM, Ackermann MR. The 'PREXCEL-Q Method' for qPCR. Int J Biomed Sci. 2008;4(4):273-93. PubMed PMID: 19759920; PubMed Central PMCID: PMC2744046.

15. Boukhvalova MS, Blanco JC. The cotton rat Sigmodon hispidus model of respiratory syncytial virus infection. Curr Top Microbiol Immunol. 2013;372:347-58. doi: 10.1007/978-3-642-38919-1_17. PubMed PMID: 24362698.

16. Boukhvalova M, Blanco JC, Falsey AR, Mond J. Treatment with novel RSV Ig RI-002 controls viral replication and reduces pulmonary damage in immunocompromised Sigmodon hispidus. Bone Marrow Transplant. 2016;51(1):119-26. Epub 2015/09/14. doi: 10.1038/bmt.2015.212. PubMed PMID: 26367224.

17. Openshaw PJ. The mouse model of respiratory syncytial virus disease. Curr Top Microbiol Immunol. 2013;372:359-69. doi: 10.1007/978-3-642-38919-1_18. PubMed PMID: 24362699.

18. Prince GA, Horswood RL, Berndt J, Suffin SC, Chanock RM. Respiratory syncytial virus infection in inbred mice. Infect Immun. 1979;26(2):764-6. PubMed PMID: 546793; PubMed Central PMCID: PMCPMC414679.

19. Papin JF, Wolf RF, Kosanke SD, Jenkins JD, Moore SN, Anderson MP, et al. Infant baboons infected with respiratory syncytial virus develop clinical and pathological changes that parallel those of human infants. Am J Physiol Lung Cell Mol Physiol. 2013;304(8):L530-9. Epub 2013/02/15. doi: 10.1152/ajplung.00173.2012. PubMed PMID: 23418091; PubMed Central PMCID: PMCPMC3625990.

20. Prince GA, Suffin SC, Prevar DA, Camargo E, Sly DL, London WT, et al. Respiratory syncytial virus infection in owl monkeys: viral shedding, immunological response, and associated illness caused by wild-type virus and two temperature-sensitive mutants. Infect Immun. 1979;26(3):1009-13. PubMed PMID: 118925; PubMed Central PMCID: PMCPMC414720.

21. Hemming VG, Prince GA, Horswood RL, London WJ, Murphy BR, Walsh EE, et al. Studies of passive immunotherapy for infections of respiratory syncytial virus in the respiratory tract of a primate model. J Infect Dis. 1985;152(5):1083-7. PubMed PMID: 4045247.

22. Belshe RB, Richardson LS, London WT, Sly DL, Lorfeld JH, Camargo E, et al. Experimental respiratory syncytial virus infection of four species of primates. J Med Virol. 1977;1(3):157-62. PubMed PMID: 416176.

23. Richardson LS, Belshe RB, London WT, Sly DL, Prevar DA, Camargo E, et al. Evaluation of five temperature-sensitive mutants of respiratory syncytial virus in primates: I. Viral shedding, immunologic response, and associated illness. J Med Virol. 1978;3(2):91-100. PubMed PMID: 104004.

24. Richardson LS, Belshe RB, Sly DL, London WT, Prevar DA, Camargo E, et al. Experimental respiratory syncytial virus pneumonia in cebus monkeys. J Med Virol. 1978;2(1):45-59. PubMed PMID: 210254.

25. Modi WS, Yoshimura T. Isolation of novel GRO genes and a phylogenetic analysis of the CXC chemokine subfamily in mammals. Mol Biol Evol. 1999;16(2):180-93. doi: 10.1093/oxfordjournals.molbev.a026101. PubMed PMID: 10028286.

26. Abu-Harb M, Bell F, Finn A, Rao WH, Nixon L, Shale D, et al. IL-8 and neutrophil elastase levels in the respiratory tract of infants with RSV bronchiolitis. Eur Respir J. 1999;14(1):139-43. PubMed PMID: 10489841.

27. Zhou Y, Yang J, Deng H, Xu H, Zhang J, Jin W, et al. Respiratory syncytial virus infection modulates interleukin‐8 production in respiratory epithelial cells through a transcription factor‐activator protein‐1 signaling pathway. Mol Med Rep. 2014;10(3):1443-7. Epub 2014/06/26. doi: 10.3892/mmr.2014.2357. PubMed PMID: 24968899.

28. Redondo E, Gázquez A, García A, Vadillo S, Masot AJ. Dominant expression of interleukin-8 vs interleukin-1β and tumour necrosis factor alpha in lungs of lambs experimentally infected with Mannheimia haemolytica. N Z Vet J. 2011;59(5):225-32. doi: 10.1080/00480169.2011.596180. PubMed PMID: 21851299.

29. Larios Mora A, Detalle L, Van Geelen A, Davis MS, Stohr T, Gallup JM, et al. Kinetics of Respiratory Syncytial Virus (RSV) Memphis Strain 37 (M37) Infection in the Respiratory Tract of Newborn Lambs as an RSV Infection Model for Human Infants. PLoS One. 2015;10(12):e0143580. Epub 2015/12/07. doi: 10.1371/journal.pone.0143580. PubMed PMID: 26641081; PubMed Central PMCID: PMCPMC4671688.

30. Meyerholz DK, Gallup JM, Lazic T, de Macedo MM, Lehmkuhl HD, Ackermann MR. Pretreatment with recombinant human vascular endothelial growth factor reduces virus replication and inflammation in a perinatal lamb model of respiratory syncytial virus infection. Viral Immunol. 2007;20(1):188-96. doi: 10.1089/vim.2006.0089. PubMed PMID: 17425433; PubMed Central PMCID: PMCPMC2791062.

31. Ackermann MR. Lamb model of respiratory syncytial virus-associated lung disease: insights to pathogenesis and novel treatments. ILAR J. 2014;55(1):4-15. doi: 10.1093/ilar/ilu003. PubMed PMID: 24936027; PubMed Central PMCID: PMCPMC4158344.

32. Derscheid RJ, van Geelen A, Berkebile AR, Gallup JM, Hostetter SJ, Banfi B, et al. Increased concentration of iodide in airway secretions is associated with reduced respiratory syncytial virus disease severity. Am J Respir Cell Mol Biol. 2014;50(2):389-97. doi: 10.1165/rcmb.2012-0529OC. PubMed PMID: 24053146; PubMed Central PMCID: PMCPMC3930944.

33. Larios Mora A, Detalle L, Gallup JM, Van Geelen A, Stohr T, Duprez L, et al. Delivery of ALX-0171 by inhalation greatly reduces respiratory syncytial virus disease in newborn lambs. MAbs. 2018;10(5):778-95. doi: 10.1080/19420862.2018.1470727. PubMed PMID: 29733750.

34. Derscheid RJ, Gallup JM, Knudson CJ, Varga SM, Grosz DD, van Geelen A, et al. Effects of formalin-inactivated respiratory syncytial virus (FI-RSV) in the perinatal lamb model of RSV. PLoS One. 2013;8(12):e81472. Epub 2013/12/06. doi: 10.1371/journal.pone.0081472. PubMed PMID: 24324695; PubMed Central PMCID: PMCPMC3855688.

35. Malhotra R, Ward M, Bright H, Priest R, Foster MR, Hurle M, et al. Isolation and characterisation of potential respiratory syncytial virus receptor(s) on epithelial cells. Microbes Infect. 2003;5(2):123-33. PubMed PMID: 12650770.

36. Johnson SM, McNally BA, Ioannidis I, Flano E, Teng MN, Oomens AG, et al. Respiratory Syncytial Virus Uses CX3CR1 as a Receptor on Primary Human Airway Epithelial Cultures. PLoS Pathog. 2015;11(12):e1005318. Epub 2015/12/11. doi: 10.1371/journal.ppat.1005318. PubMed PMID: 26658574; PubMed Central PMCID: PMCPMC4676609.

37. Tayyari F, Marchant D, Moraes TJ, Duan W, Mastrangelo P, Hegele RG. Identification of nucleolin as a cellular receptor for human respiratory syncytial virus. Nat Med. 2011;17(9):1132-5. Epub 2011/08/14. doi: 10.1038/nm.2444. PubMed PMID: 21841784.

38. Donalisio M, Rusnati M, Cagno V, Civra A, Bugatti A, Giuliani A, et al. Inhibition of human respiratory syncytial virus infectivity by a dendrimeric heparan sulfate-binding peptide. Antimicrob Agents Chemother. 2012;56(10):5278-88. Epub 2012/07/30. doi: 10.1128/AAC.00771-12. PubMed PMID: 22850525; PubMed Central PMCID: PMCPMC3457392.

39. Razinkov V, Gazumyan A, Nikitenko A, Ellestad G, Krishnamurthy G. RFI-641 inhibits entry of respiratory syncytial virus via interactions with fusion protein. Chem Biol. 2001;8(7):645-59. PubMed PMID: 11451666.

40. Razinkov V, Huntley C, Ellestad G, Krishnamurthy G. RSV entry inhibitors block F-protein mediated fusion with model membranes. Antiviral Res. 2002;55(1):189-200. PubMed PMID: 12076763.

41. Roymans D, Alnajjar SS, Battles MB, Sitthicharoenchai P, Furmanova-Hollenstein P, Rigaux P, et al. Therapeutic efficacy of a respiratory syncytial virus fusion inhibitor. Nat Commun. 2017;8(1):167. Epub 2017/08/01. doi: 10.1038/s41467-017-00170-x. PubMed PMID: 28761099.

42. DeVincenzo JP, Whitley RJ, Mackman RL, Scaglioni-Weinlich C, Harrison L, Farrell E, et al. Oral GS-5806 activity in a respiratory syncytial virus challenge study. N Engl J Med. 2014;371(8):711-22. doi: 10.1056/NEJMoa1401184. PubMed PMID: 25140957.

43. Mackman RL, Sangi M, Sperandio D, Parrish JP, Eisenberg E, Perron M, et al. Discovery of an oral respiratory syncytial virus (RSV) fusion inhibitor (GS-5806) and clinical proof of concept in a human RSV challenge study. J Med Chem. 2015;58(4):1630-43. Epub 2015/01/27. doi: 10.1021/jm5017768. PubMed PMID: 25574686.

44. Perron M, Stray K, Kinkade A, Theodore D, Lee G, Eisenberg E, et al. GS-5806 Inhibits a Broad Range of Respiratory Syncytial Virus Clinical Isolates by Blocking the Virus-Cell Fusion Process. Antimicrob Agents Chemother. 2015;60(3):1264-73. Epub 2015/12/14. doi: 10.1128/AAC.01497-15. PubMed PMID: 26666922; PubMed Central PMCID: PMCPMC4776015.

45. Samuel D, Xing W, Niedziela-Majka A, Wong JS, Hung M, Brendza KM, et al. GS-5806 inhibits pre- to postfusion conformational changes of the respiratory syncytial virus fusion protein. Antimicrob Agents Chemother. 2015;59(11):7109-12. Epub 2015/08/31. doi: 10.1128/AAC.00761-15. PubMed PMID: 26324264; PubMed Central PMCID: PMCPMC4604407.

46. Kim YI, Pareek R, Murphy R, Harrison L, Farrell E, Cook R, et al. The antiviral effects of RSV fusion inhibitor, MDT-637, on clinical isolates, vs its achievable concentrations in the human respiratory tract and comparison to ribavirin. Influenza Other Respir Viruses. 2017;11(6):525-30. Epub 2017/10/30. doi: 10.1111/irv.12503. PubMed PMID: 28990339; PubMed Central PMCID: PMCPMC5705693.

47. Cianci C, Meanwell N, Krystal M. Antiviral activity and molecular mechanism of an orally active respiratory syncytial virus fusion inhibitor. J Antimicrob Chemother. 2005;55(3):289-92. Epub 2005/01/28. doi: 10.1093/jac/dkh558. PubMed PMID: 15681582.

48. Cianci C, Yu KL, Combrink K, Sin N, Pearce B, Wang A, et al. Orally active fusion inhibitor of respiratory syncytial virus. Antimicrob Agents Chemother. 2004;48(2):413-22. PubMed PMID: 14742189; PubMed Central PMCID: PMC321540.

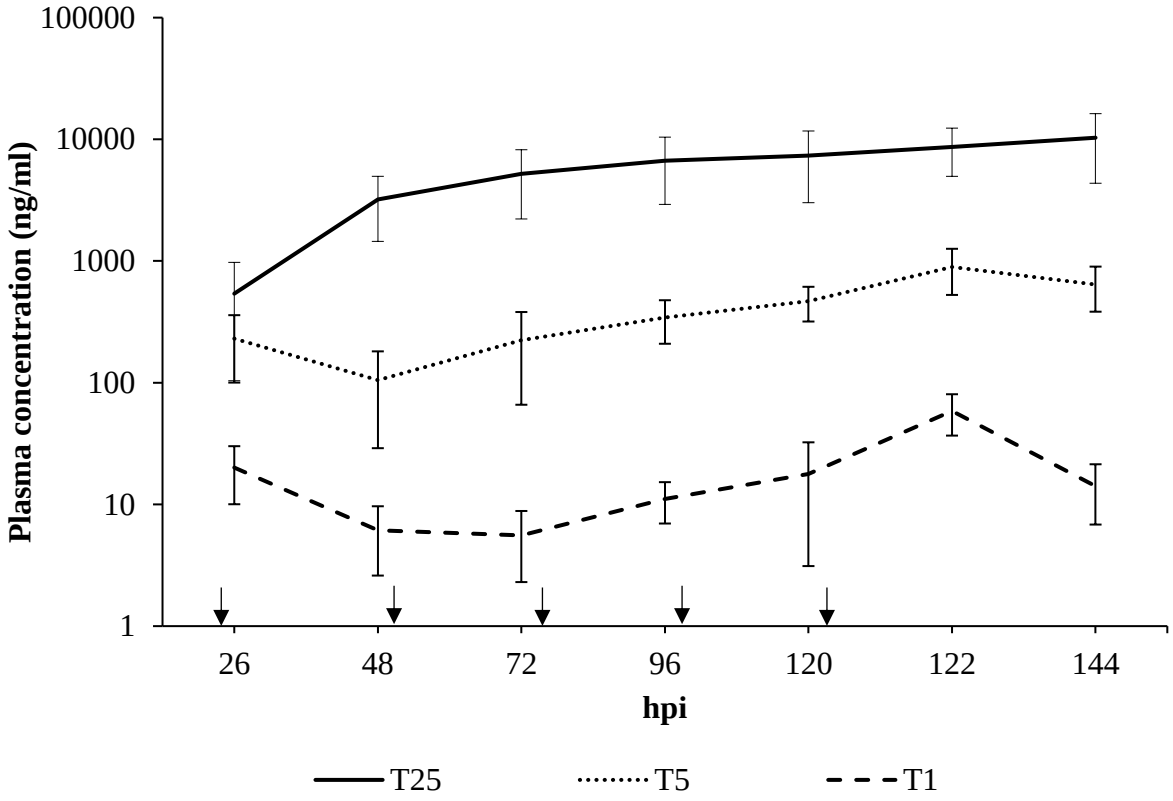

Figure 1: Plasma compound levels of JNJ-53718678

The level of compound in plasma of 25 mg/kg (T25), 5 mg/kg (T5) and 1 mg/kg (T1) treatment groups evaluated at different time points. The time of treatment administration is indicated by the arrows.

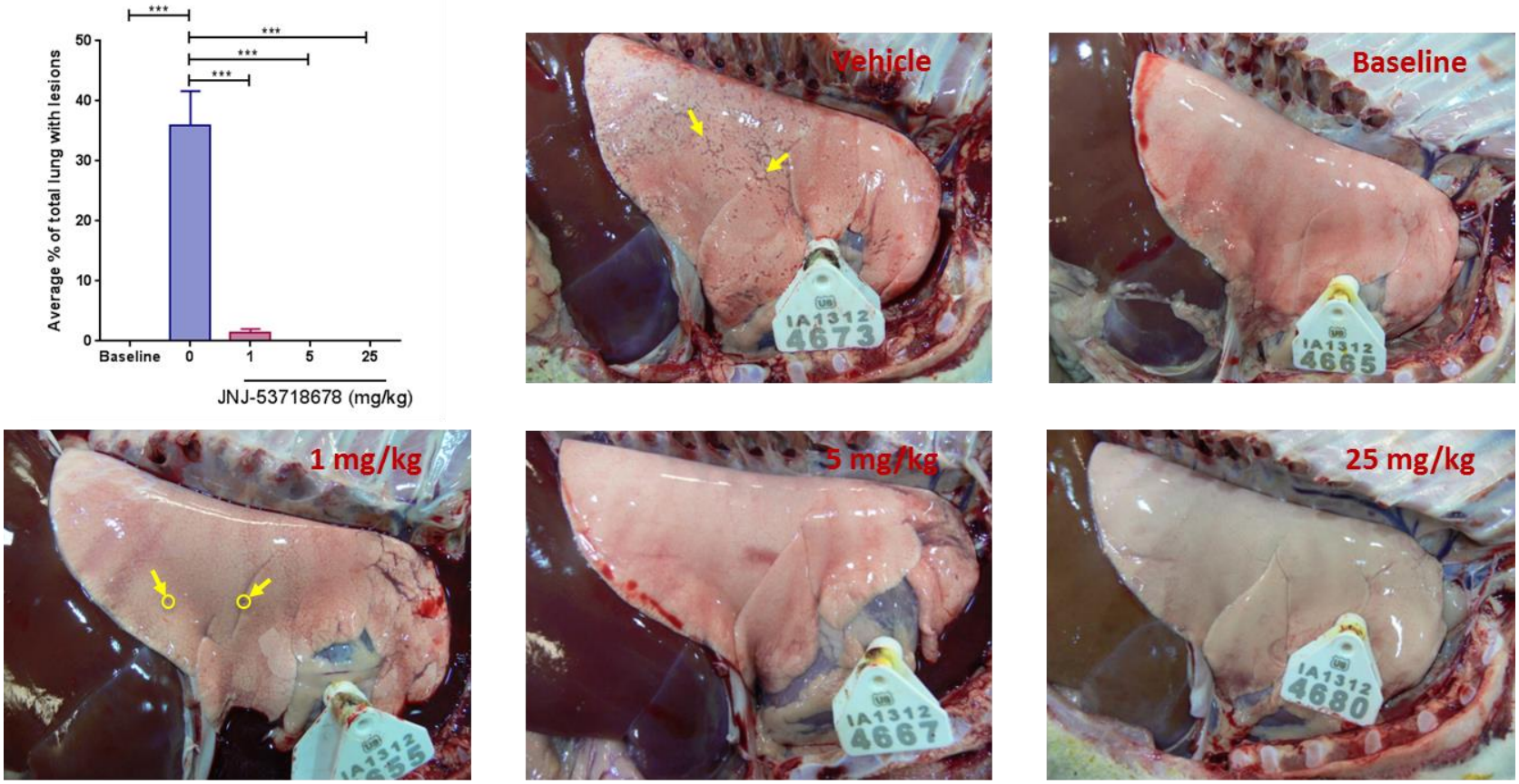

Figure 2: Morphological changes of lungs and average gross hRSV-associated lung lesion

The figures represent the gross changes in the non-treated vehicle group, treatment groups administered 25, 5, 1 mg/kg of JNJ-537118678 and negative control group. Average percentage of total lung lesion is compared in the graph (top left).

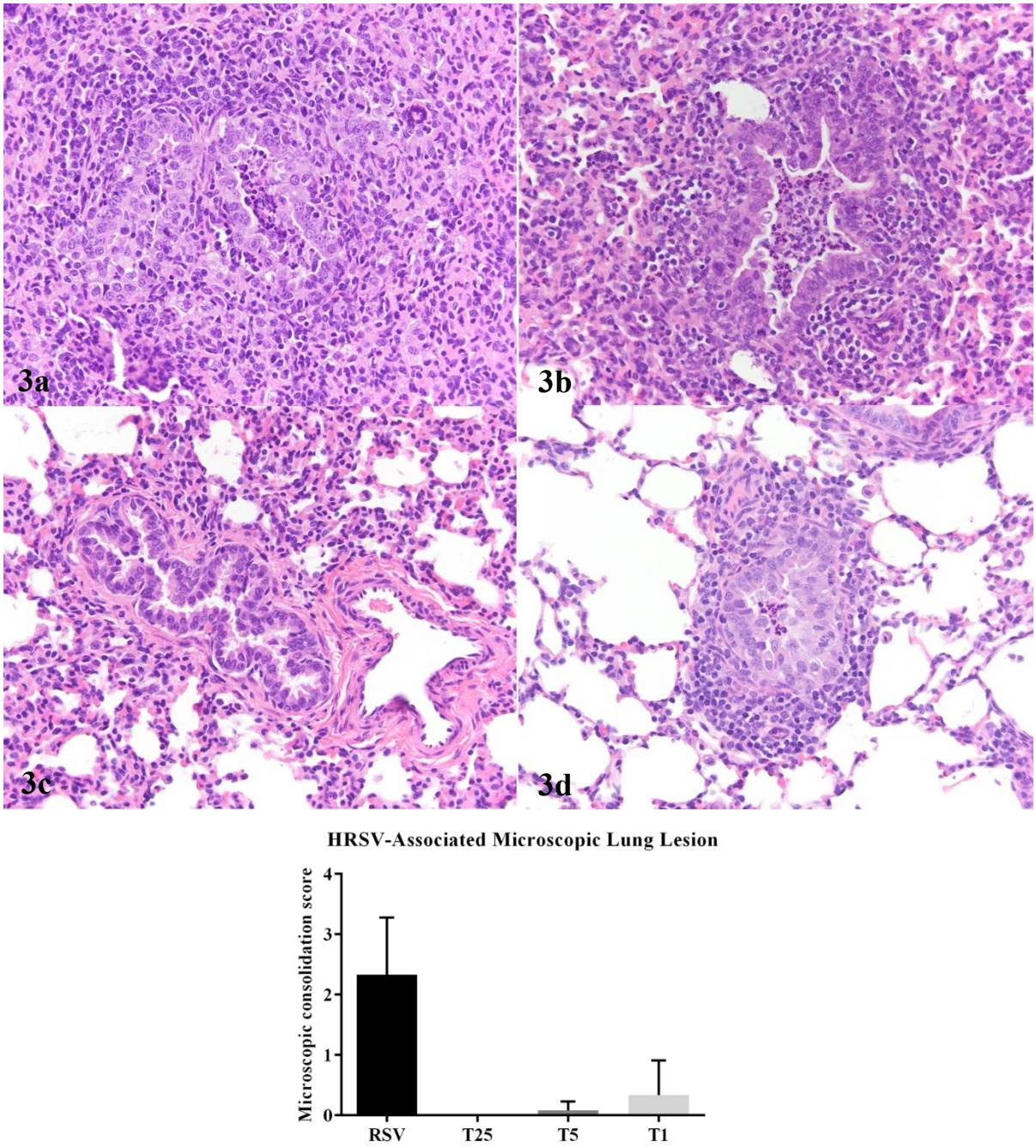

Figure 3: Microscopic lung lesions in hRSV-infected lambs and average microscopic consolidation score

Marked to moderate neutrophilic and necrotizing bronchiolitis with syncytial cell formation and lymphoplasmacytic peribronchiolar cuffs were presented in the non-treated hRSV-infected lambs (3a, 3b). There is lack of inflammatory changes in the bronchioles of 25 mg/kg treatment of fusion inhibitor (T25) (3c). Mild neutrophilic inflammation and lymphoplamacytic perivascular cuffs were present in the 5 mg/kg (T5) and 1 mg/kg treatment group (T1) (3d).

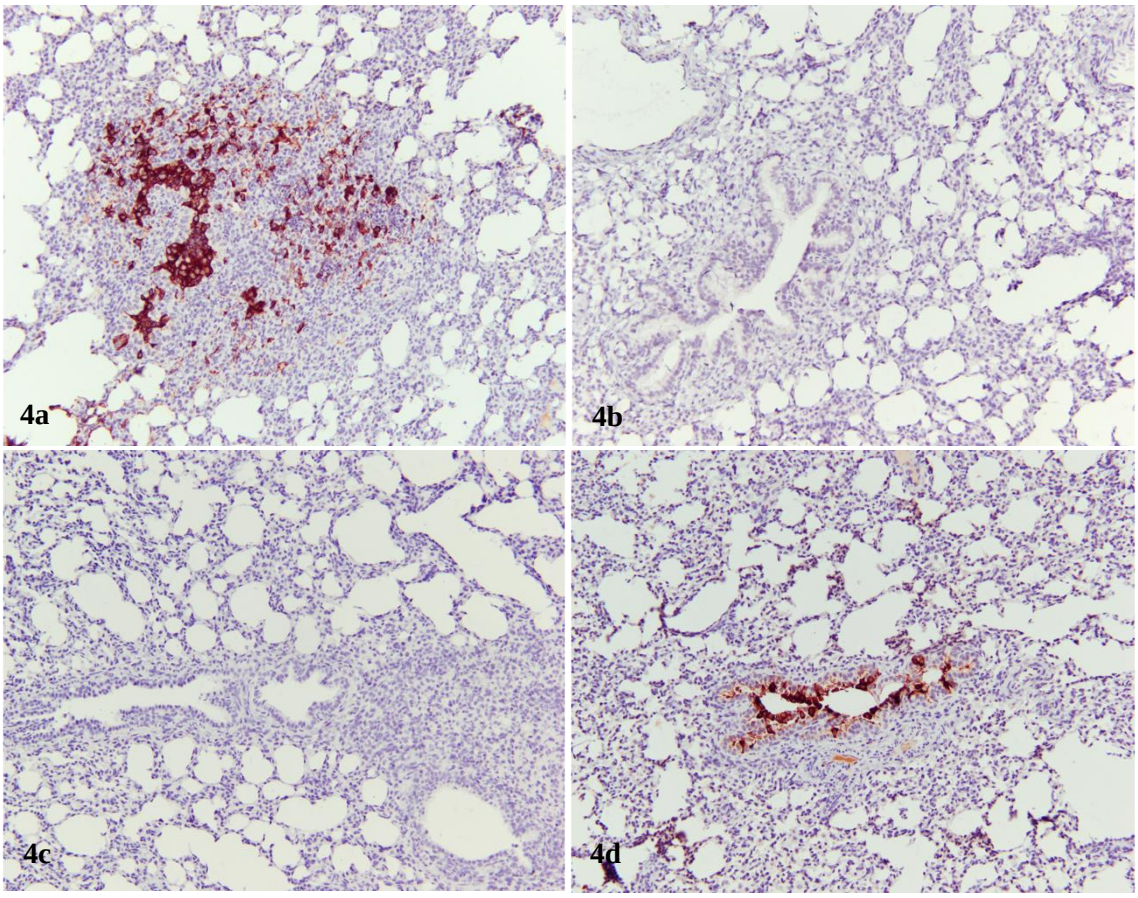

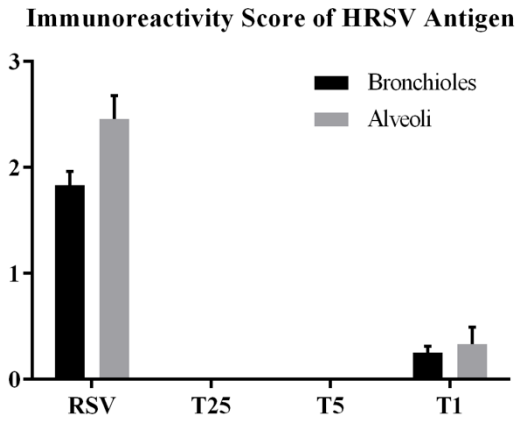

Figure 4: Immunohistochemical detection of hRSV antigen and immunoreactivity score

Immunohistochemical staining of hRSV antigen was detected in sloughed/intact bronchiolar epithelial cells, pulmonary alveolar macrophages and type II pneumocytes in hRSV-infected vehicle group (4a). Lack of antigen detection were presented in 25 mg/kg (T25) (4b) and 5 mg/kg treatment groups (T5) (4c) and hRSV antigen were detected at less amount in 1 mg/kg (T1) (4d). Nova red stain, 200X.

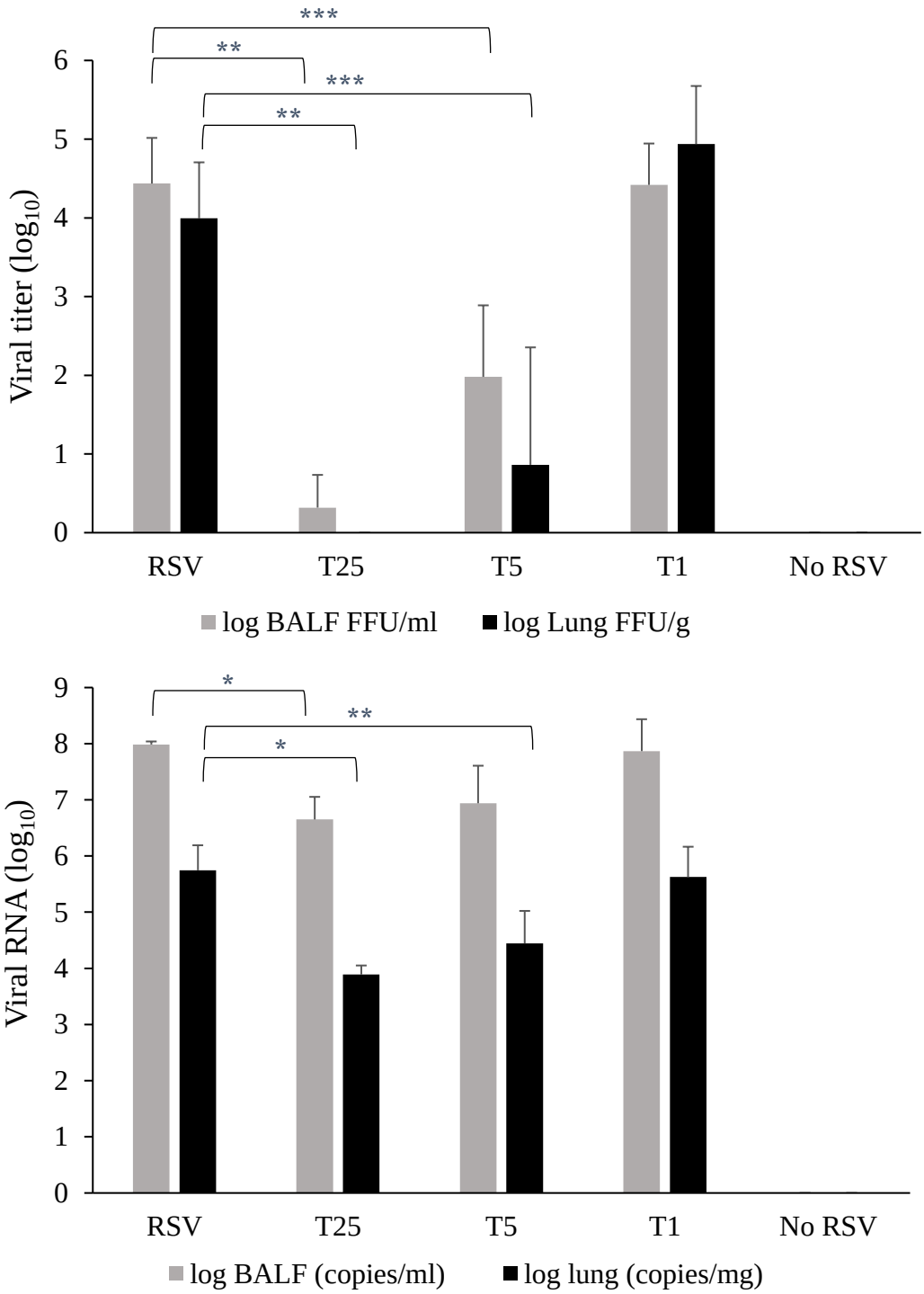

Figure 5: Viral titer detected in focus forming unit and RT-qPCR

Level of viral titer detected by FFU (top) and viral RNA detected by RT-qPCR (bottom) in different treatment groups. Statistical analysis was performed by one-way ANOVA followed by Dunnett's post hoc test (*$p<0.05$, **$p<0.01$, ***$p<0.001$).

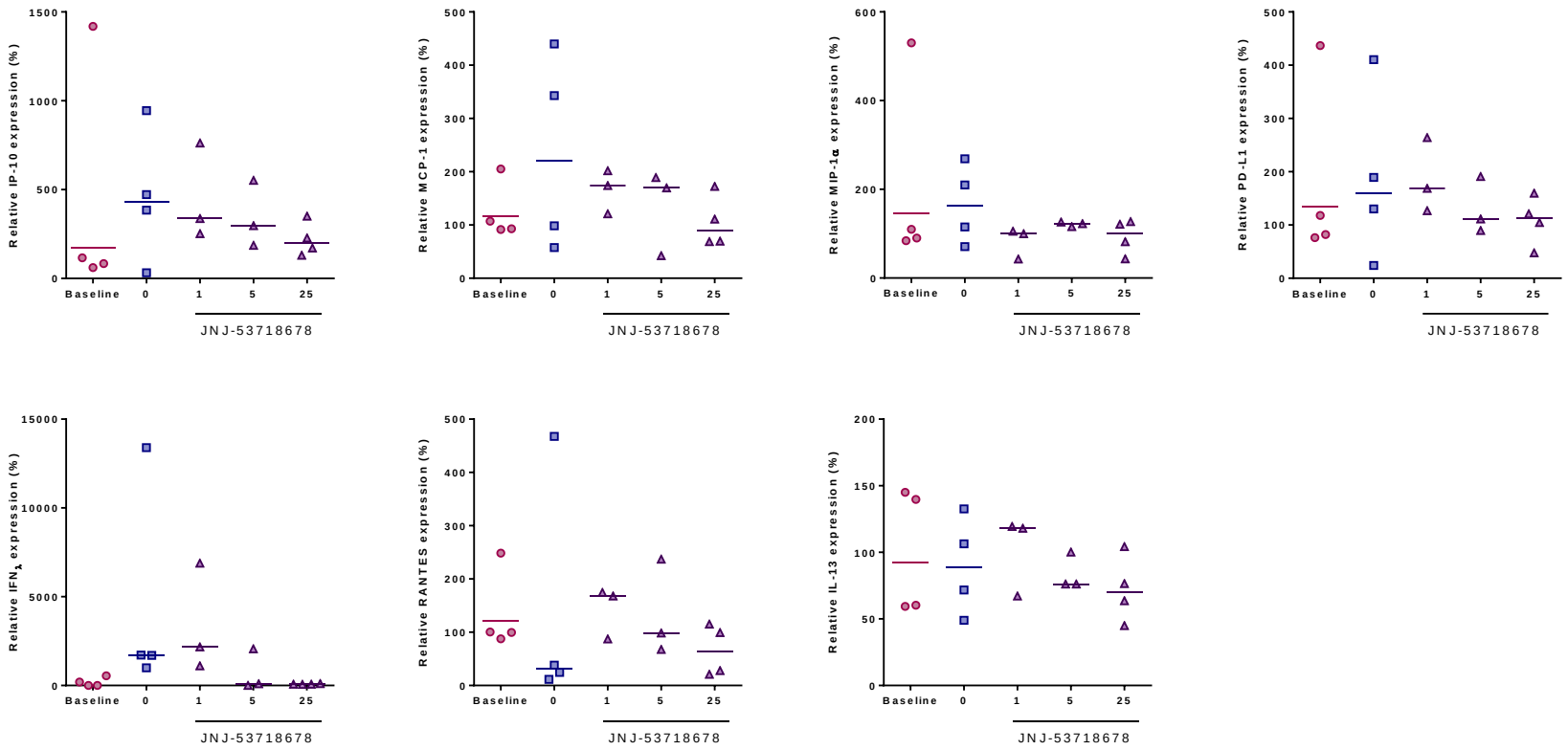

Figure 6: Cytokines and chemokines mRNA expression (IP-10, MCP-1, MIP-1α, PD-L1, IFNλ, RANTES and IL-13)

Graphs represent individual data points and geometric mean values (horizontal bar) of each treatment and the non-treatment group.

CHAPTER 3. EFFICACY OF THE HUMAN RESPIRATORY SYNCYTIAL VIRUS (HRSV) REPLICATION INHIBITOR JNJ-64166037 IN HRSV INFECTED LAMBS

Modified from an abstract manuscript presented at

11th International Respiratory Syncytial Virus Symposium

Oct 31 – Nov 4, 2018, Asheville, NC USA

Panchan Sitthicharoenchai[1], Sarhad S. Alnajjar[1,6], David Lançois[4], Dirk Roymans[3], Peter Rigaux[3], Alejandro Larios-Mora[2], Jack M. Gallup[7] and Mark R. Ackermann[5,6]

[1] Department of Veterinary Pathology, College of Veterinary Medicine, Iowa State University, Ames, IA. [2]Department of Veterinary Diagnostic and Production Animal Medicine, College of Veterinary Medicine, Iowa State University, Ames, IA. [3]Janssen Infectious Diseases and Vaccines, Janssen Pharmaceutica NV, Beerse Belgium. [4]Janssen Research & Development, Division of Janssen-Cilag S.A., Val de Reuil, France. [5]Department of Biomedical Sciences, Carlson College of Veterinary Medicine, Oregon State University, Corvallis, Oregon. [6]LambCure LLC, Corvallis, Oregon. [7]Boehringer Ingelheim, Ames, Iowa

Abstract

Background: The purpose of this study was to evaluate the therapeutic efficacy of a non-fusion replication inhibitor (JNJ-64166037) against human respiratory syncytial virus (hRSV) in a lamb model of human respiratory syncytial virus (hRSV) infection that mimics hRSV in newborn infants. In contrast to semi-permissive models, hRSV replicates to a high extent in lambs and causes lung pathology that is similar to lesions that develop in human pediatric populations.

Methods: Neonatal lambs (1-3 days of age) were infected with the clinical isolate hRSV Memphis 37 via nebulization. Infected lambs were treated orally with JNJ-64166037 1 hour after virus inoculation then once daily 24 hours after the first treatment with three different doses (2, 10 and 50 mg/kg). Clinical signs were recorded daily, and lambs were euthanized

day 6 post-infection. Virus titers in the lung and bronchoalveolar lavages were measured by a focus forming unit (FFU) assay and viral mRNA in lung and BALF were measured by RT-qPCR. Macroscopic and microscopic lung lesions were scored, and viral distributions were determined by immunohistochemistry and RNA *in situ* hybridization.

Results: JNJ-64166037 plasma levels remained above the protein-adjusted EC_{90} at the highest tested dose (50 mg/kg) with a lung-to-plasma ratio of 0.7 indicating that the compound was distributed to the infected lung. A dose-dependent antiviral effect was associated with a potent reduction (>100 fold) of detectable lung infectious virions at 50 mg/kg. In addition, the amount of hRSV RNA correlated the pronounced decrease in infectious virions. Similar observations were seen in bronchioalveolar lavages. Consistently, the amount of virus detected in the lung of the lambs treated with 50 mg/kg was significantly lower than with lower dose treatments. Lungs of lambs receiving the 50 mg/kg dose lacked macroscopic and microscopic lesions.

Conclusion: Oral administration of the non-fusion replication inhibitor JNJ-64166037 at appropriate dose has potent antiviral effects in the lamb model of RSV infection in a dose-dependent manner. This mode of therapeutic intervention eliminated the hRSV-induced lung lesions assessed in the model. JNJ-64166037 might offer new opportunities for RSV bronchiolitis treatment in infants and children.

Introduction

Human respiratory syncytial virus (hRSV) is a leading cause of viral respiratory tract infection in infants and children worldwide manifesting in bronchiolitis and pneumonia. Severe hRSV infection have been reported in preterm infants and children younger than 1 year

of age resulting in hospitalization and death in certain cases [1]. The virus can also cause detrimental disease in older individuals of more than 65 years of age [2].

Development of effective vaccines and therapeutic compounds is essential for prevention and treatment of hRSV infection. A formalin-inactivated hRSV vaccine used in human infants was unsatisfactory, resulting in vaccine-induced disease enhancement with subsequent hRSV infection [3]. Alternatively, therapeutic and prophylactic compounds that inhibit viral entry and interfere with viral replication by targeting viral fusion (F) protein and machinery required for viral replication, such as viral RNA polymerase, nucleocapsid mRNA, hRSV nucleoprotein and viral G protein, have been studied and developed for precise, mechanistic, molecular therapies [4]. Such compounds require extensive laboratory testing, animal trials in the preclinical stage, and multiple phases of clinical trials in humans. An animal model for hRSV infection in infants has been established in newborn lambs in order to study the pathogenesis and response to many types of prophylaxis and treatments [5]. In contrast to semi-permissive hRSV replication in some animal models, hRSV replicates to a high extent in lambs and causes lung pathology that is similar to lesions observed in human pediatric populations [6]. The objective of this study was to evaluate the efficacy of hRSV replication inhibitor (JNJ-64166037), for the therapeutic treatment of hRSV by experimental trial on hRSV infected neonatal lamb model of hRSV infection in infants.

Materials and Methods

Animal Model and Experimental Design

Colostrum-deprived lambs, 1-3 days of age, were infected with clinical isolate of hRSV Memphis 37 via nebulization of 6 ml viral solution to achieve the final viral inoculant amount of 3.5×10^7 FFU/lamb. Infected lambs were treated orally 1 hour after virus inoculation then

once daily 24 hours after the first treatment with different doses of antiviral replication inhibitor compound JNJ-64166037 (i.e., 2 mg/kg (T2, n=5), 10 mg/kg (T10, n=5), and 50 mg/kg (T50, n=5)). Positive hRSV infected control lambs (RSV, n=6) were given 20% acidified hydroxypropryl-β- cyclodextrin (20 % HP-β-CD + HCl) treatment vehicle. Mock infection with pure culture media was administered in the negative control group (control, n=5).

Measurements of body weight, body temperature, respiratory rate, and heart rate were performed daily on all lambs. Each animal received daily prophylactic antibiotic treatment (ceftiofur sodium, Naxcel®). Plasma samples were collected sequentially to determine the kinetics of compound in circulation at pre-dose, 2h after the first and last dose, and at 24h following each dose up to 144h. The animals were later euthanized with sodium pentobarbital at day 6 post-infection to collect bronchoalveolar lavage fluid (BALF) and lung samples for further virus quantification and tissue analysis. BALFs were collected from the right caudal lobe and right middle lung lobe of each lamb using 5 ml, cold double-modified Iscove's media (DMIM) (42.5% Iscove's modified Dulbecco's medium, 7.5% glycerol, 1% heat-inactivated fetal bovine serum, 49% Dulbecco's modified eagle medium (DMEM) and 5 μg/ml kanamycin sulfate). For viral detection and pharmacokinetic analysis, lung tissue samples were collected from right cranial, left cranial, left middle and left caudal lobes, frozen in liquid nitrogen and stored at -80°C until further processing. In addition, lung tissue samples from right cranial, left cranial, left middle and left caudal lobes were placed in tissue cassettes and fixed in 10% neutral-buffered formalin for histopathological, immunohistochemical staining and RNA *in situ* hybridization. Animal use and experimental procedures were approved by IACUC and IBC at Iowa State University (IACUC# 3-14-7748-0, IBC# 01-D/I-0008-A/H).

Viral Stock Preparation and Nebulization

Human respiratory syncytial virus Memphis 37 strain (hRSV M37) was grown on HEp-2 cell line with Dulbecco's Modified Eagle Medium (DMEM) containing 10% fetal bovine serum (FBS) and 50 μg/ml kanamycin sulfate. Once the viral growth achieved more than 90% cytopathic effect, the virus was extracted by freeze-thawing process of viral infected cells. Clarification process was performed by centrifugation at 5,000 x g for 10 mins. The supernatant was diluted with 20% sucrose then stored at -80°C [7]. A small sample of the stock virus were collected to determine the viral titer through a viral plaques assay. The virus stock was then diluted into 6 ml of culture media to the concentration of 2.5×10^7 FFU/ml needed to achieve appropriate final dose administration of 3.5×10^7 FFU/lamb. PARI LC Sprint™ nebulizers were used to administer 6 ml of the diluted virus to T50, T10, T2 and RSV groups, and delivered pure culture media to the mock-infected negative control group.

Replication Inhibitor Formulation, Administration and Quantification

The hRSV replication inhibitor, JNJ-64166037, was dissolved in 20% acidified hydroxypropryl-β- cyclodextrin (20 % HP-β-CD + HCl) at pH 7.4 to 12.5, 2.5, or 0.5 mg/ml concentrations and stored at 4°C prior to compound delivery. An appropriate amount of the compound for each treatment group (2, 10 and 50 mg/kg) was orally administered to the lambs through gavage catheter then followed by 5 ml of 20 % HP-β-CD+HCl, pH 7-7.4 to wash down any compound residues. The plasma, lung and BALF samples were analyzed for JNJ-64166037 levels by liquid chromatography-tandem mass spectrometry (LC-MS/MS). The lower limit of quantifications was 2.5 ng/ml for plasma and BALF and 12.5 ng/g for lung samples.

Focus Forming Unit (FFU) on BALF and lung tissue

The focus forming unit (FFU) assay was conducted on the BALF and lung tissue samples to evaluate the hRSV viral titers. Prior to performing the FFU assay, BALF samples were clarified by centrifugation at 15,600 x g. The supernatants were collected and spun through spin column filters (Coster SPIN-X filter, Fisher Scientific, Hanover Park, IL, USA). A similar clarification process was performed with lung tissue samples by pooling and homogenizing the right cranial, accessory, left cranial, left middle and left caudals (0.1 g each lobe, total of 0.5 g) in 5 ml DMEM. Homogenized lung tissues were then centrifuged at 15,600 x g to remove cellular debris and the supernatants were collected. Each lung supernatant was centrifuged 2-3 times through spin column filters. The filtrates of BALF and homogenized lung were collected for further evaluation with the FFU assay.

HEp-2 cells were grown in 12-well cell culture plates to 70-80% confluency with DMEM culture media containing 10% FBS and 50 μg/ml kanamycin sulfate prior to adding the samples. The BALF and lung samples were tested at full strength and 10^{-1}, 10^{-2}, 10^{-3}, 10^{-4} concentrations achieved by 10-fold dilution of the samples with culture media. The media was removed from the HEp-2 12-well cell culture plates and 200 μl of each BALF concentration was placed in duplicate wells then incubated at 37°C, 5% CO_2 incubating chamber for 90 minutes. After this initial sample incubation, 1 ml of culture media was added to each well and the plates were further incubation for 48 hours at 37°C, 5% CO_2.

Fluorescent staining of the viral infected cells was performed by adding 60% acetone/40% methanol fixative solution for 1 minute. The fixing solution was removed, and the plates were air-dried then rehydrated with 1 ml Tris buffer saline with 0.05% Tween (TBST)/well. TBST was removed and 1 ml blocking solution (3% BSA (Fisher Scientific,

Hanover Park, IL, USA) in TBST) was added to each well and incubated for 30 minutes at room temperature. The blocking solution was removed, and primary polyclonal goat anti-RSV (EMD Millipore, Billerica, MA) diluted to 1:800 with 3% BSA in TBST was added (325 µl/well) and incubated at 4°C, overnight on a rotator. All wells were washed 3 times with TBST and then 1:800 diluted secondary fluorescence tagged rabbit anti-goat IgG (Alexa Fluor® 488 F(ab')2 fragment of rabbit anti-goat IgG (H+L), Molecular Probes/Life Technologies) with 3% BSA in TBST was added in to each well (325 µl/well). After 30 minutes of incubation at room temperature, the plates were washed three times with TBST and 1 ml of TBST was added in each well to prevent drying. Fluorescent plaques were counted under an inverted fluorescence light microscope and viral titers (FFU/ml) were calculated by averaging the number of plaques in the duplicate wells.

Real-Time Reverse Transcription Polymerase Chain Reaction (RT-qPCR)

Lung tissue samples from the right cranial, left cranial, left middle and left caudal lung lobes (~0.3 g/lobe) of each lamb was pooled and homogenized in 12 ml TRIzol solution (Invitrogen/Life Technologies, Carlsbad, CA, USA) for RNA extraction. A total volume of 1.1 ml of the lung homogenate in TRIzol solution from each sample was mixed with 120 µl of chloroform then centrifuged at 12,000 x g, 4°C. After centrifugation, 550 µl of the upper aqueous layer was collected from each sample and mixed with 500 µl of isopropanol for 10 minutes. The precipitated RNA was collected by centrifuging the samples for 10 minutes at 12,000 x g, 4°C. The final RNA pellets were resuspended in 170 µl nuclease-free water and heated for 90 seconds at 60°C. Subsequently, 70 µl of each RNA extracted sample was treated with DNase (TURBO-DNase, Ambion, Austin, TX, USA) then 80 µl of the samples were

diluted 1:10 with nuclease-free water (710 µl) and RNaseOUT (10 µl) (Invitrogen/Life Technologies, Carlsbad, CA, USA). The amount of RNA was measured using spectrophotometry at wavelength of 260/280 nm.

At necropsy, 100 µl of each BALF sample was store at -80°C in 1 ml TRIzol solution until RNA isolation. The process of RNA isolation for BALF samples was performed according to TRIzol procedure (Invitrogen/Life Technologies, Clarlsbad, CA, USA) to obtain sample RNA pellets. Each pellet was collected and resuspended in 100 µl of nuclease-free water (Invitrogen/Life Technologies, Carlsbad, CA, USA) and incubated at 60°C for 2 minutes. The final RNA insolated BALF samples were diluted 1:10 with nuclease-free water (710 µl) and RNaseOUT (10 µl) (Invitrogen/Life Technologies, Carlsbad, CA, USA).

Quantification of hRSV viral particles with RT-qPCR was performed on RNA isolated of lung and BALF samples by targeting the nucleoprotein (N) mRNA of M37 RSV. The primers and probe for the RSV M37 nucleoprotein (N) mRNA sequence in this study were designed using ABI Primer Express 2.0 based on RSV GenBank accession number M74568 (Supplementary Table 2). Cytokines/chemokines (IFN-λ, IL-13, MCP-1 (CCL2), MIP-1α (CCL3), RANTES (CCL5), IP10 (CXCL10)), PD-L1 (CD274), and CC10 mRNA expressions were evaluated in the lung samples with primer and probe sequences of all targets listed in Supplementary Table 2. RT-qPCR was conducted using One-Step Fast RT-qPCR Kit master mix (Quanta, Bioscience, Gaithersburg, MD, USA) in a Gene Amp 5700 Sequence Detection System (Applied Biosystmes, Carlsbad, CA, USA). The amount of PCR reagents were calculated and managed using PREXCEL-Q software [8]. Each sample was duplicated and placed in the thermocycler for one round of pre-treatment (3 minutes at 50°C, then 30 seconds at 95°C) followed by 45 cycles of 3 seconds, 95°C and 30 seconds at 60°C. The virus copy

number was calculated based on the standard curve generated from a plasmid construct. The relative quantity (rQ) of cytokine/chemokine and CD274 and CC10 mRNA expression was calculated from sample mixture (Stock I) with the following equation: $rQ=10^{[(Cq-b)/m]}$ where Cq represents the cycle time value, *b* is the *y*-intercept and *m* is the slope from the standard curve of Stock I [8].

Immunohistochemistry (IHC) Detection of HRSV Antigen

Tissue cassettes containing lung samples were processed by the Histopathology Laboratory, Department of Veterinary Pathology, College of Veterinary Medicine, Iowa State University for hematoxylin and eosin (H&E) stained slides and unstained slides for immunohistochemical detection of hRSV antigen. For immunohistochemistry, the slide sections were placed in heated oven (58°C) and directly immersed in xylene for deparaffinization process. The slides were then rehydrated through gradient alcohol (100%, 95%, 70% methanol) with initial endogenous peroxidase blocking (3% hydrogen peroxide in methanol solution) then placed in double distilled water (ddH_2O). Antigen retrieval process was performed by placing the slides in pH 9.0 19 mM TRIZMA Base, 1 mM EDTA buffer and 0.05% Tween 20 and heated at 125°C using pressure-cooking device (Decloaking Chamber Plus, Biocare Medical, Concord, CA, USA). Subsequent steps of IHC staining were performed using programmed IHC automated machine (BioGenex OptiMax i6000 staining system, USA). The protocol consisted of serum blocking with 3% bovine serum albumin (BSA) in Tris buffer saline with 0.05% Tween (TBST), then with 20% normal swine serum (NSS) in TBST for 15 minutes each. The slides were then incubated with primary antibody for 90 minutes (1:500 polyclonal goat anti-RSV antibody (Millipore/Chemicon, Darmstadt, Germany) in 10% NSS,

3% BSA in TBST solution. Subsequently, the slides were washed twice with PBST then incubated for 45 minutes with 1:300 dilution of biotinylated rabbit anti-goat IgG antibody in 10% NSS, 3% BSA in TBST solution. Secondary peroxidase blocking was performed by incubating the tissue section in 3% H_2O_2 in TBST for 25 minutes followed by two TBST washes. Next, the slides were incubated in 1:200 streptavidin-horseradish peroxidase diluted in TBST for 30 minutes and washed 3 times with TBST. The slides were manually stained with chromogen substrate (Nova Red staining solution) for 60-90 seconds and immediately placed in tap water to stop the reaction. Shandon's hematoxylin was used as nuclear counterstain.

Lung HRSV Lesion Evaluation

The macroscopic and microscopic lung associated hRSV lesions were examined and scored with a semi-quantitative system in order to evaluate and compare the extent of virus associated lung pathology. The macroscopic lung scores were based on the average percentage of dark-red consolidated areas distributed in each lung lobe and converted to scoring scale from 0 to 4 (e.g. 0% = 0, 1-9% = 1, 10-39% = 2, 40-69% = 3, 70-100% = 4). Lung histopathological scores were determined with H&E staining of two representative lung tissue sections taken from each right cranial, left cranial, left middle and left caudal lung lobes of each lamb. Criteria for scoring (0 to 4 from lowest to highest pathological changes) include; microscopic lung consolidation, bronchitis, syncytial formation, bronchial and bronchiolar epithelial necrosis, bronchial and bronchiolar epithelial hyperplasia, presence of neutrophilic infiltration, perivascular and peribronchiolar lymphocytic infiltrates (Table 1). The degree of hRSV antigen detected with IHC was evaluated by counting the number of bronchioles and alveoli

with positive hRSV antigen signal in 20 fields at 100X (field number 22) per slide each containing sections from right cranial, left cranial, left middle and left caudal lung lobes from each lamb (e.g. score 1=1-10 positive counts, score 2=11-39 positive counts, score 3=40-99 positive counts and score 4=>100 positive counts).

In Situ Hybridization (RNAscope®)

Viral RNA was detected in formalin-fixed paraffin embedded (FFPE) lung tissue by RNA *in situ* hybridization (RNAscope®, ACD Bio) assay [9] with probe sequence targeting the nucleoprotein (N) of hRSV Memphis 37 (Cat No. 439861). Briefly, the FF E lung tissue blocks were sectioned at 5 μm thickness and deparaffinized with 100% ethanol solution. Next, endogenous peroxidase activity was blocked with hydrogen peroxide for 10 mins at room temperature, and then slides were heat treated by boiling with Target Retrieval Reagent® for 15 mins and enzymatic treatment with Protease Plus® at 40°C for 30 mins. Subsequently, probe hybridization (2h at 40°C) and amplification of the viral RNA target were conducted in HybEZ™ Hybridization System and RNAscope® 2.5 Assay platform. Positive control probe (PPIB) and negative control probe (DapB) were concurrently tested. The amplified viral target was stained with 3,4'-diaminobenzidine (DAB) chromogenic substrate (RNAscope® 2.5 HD Detection Reagent-Brown) and counterstained with hematoxylin.

The positive signal from RNA *in situ* hybridization was evaluated using manual light microscopic evaluation and image analysis software (HALO™). The bronchioles and alveoli with positive signal were manually counted then calculated based on 400 mm^2 of the pulmonary section. A total of twenty histological images taken at (200X) of the lung representing each lamb were analyzed through image analysis software. Cell-by-cell

expression profiles were quantified into different bin (Bin 0; <1 copy/cell, Bin 1; 1-3 copies/cell, Bin 2; 4-9 copies/cell, Bin 3; 10-15 copies/cell, Bin 4; (>15 copies/cell). Histo score (H score) of each image were calculated from the sum of the bin number were multiplied by the percentage of cells per bin [9, 10]. The averaged H score from the analyzed images represented the level of viral RNA detected by RNA *in situ* hybridization in each lamb.

Statistical Analysis

The quantitative data were evaluated on GraphPad Prism 6 statistical software with Kruskal-Wallis non-parametric test or with Dunn's multiple comparisons test to calculate significant statistical differences ($p<0.05$) between each experimental group. The results from viral titer, viral mRNA, and chemokines/cytokines mRNA expression were statistically analyzed. Due to unexpected death loss of the positive control RSV group, viral titer and mRNA data from previous experiments with similar conditions (e.g. age, dose of infection, duration after viral inoculation) were included to calculate the statistical analysis. Correlation of multiple variables (Spearman r) were performed on the viral FFU titer, quantification of virion by RT-qPCR, IHC score and H score obtained from RNA *in situ* hybridization.

Results

Clinical signs and symptoms associated with hRSV infection

Clinical parameters including body temperature, body weight, heart rate and respiratory rate were within the normal range in all lambs. Increased respiratory effort were detected at 6 dpi in 1/3 lambs of RSV, 0/5 lambs in T50, 1/3 lambs in T10, and 1/4 lambs in T2. Wheezing or coughing were not observed in any treatment group throughout the course of study.

Pharmacokinetic of Replicator Inhibitor JNJ-64166037

The replicator inhibitor (JNJ-64166037) plasma concentration levels increased in a dose dependent manner with C_{trough} levels maintained at more than or equal to 1400, 277, 120 ng/ml under high dose (T50), medium dose (T10) and low dose treatments (T2), respectively (Fig 1). Exposure of JNJ-64166037 was on average higher in lavaged-lung tissue as compared to the epithelial lining fluid (ELF). The lung to plasma ratio was 0.72 and ELF to plasma ratio was 0.10 in the T50 group indicating moderate distribution of the compound into the lung.

Viral Titer and Viral RNA detection

Both the average virus titers determined by FFU and viral mRNA level determined by RT-qPCR in BALFs were higher than in the lung homogenates. Viral titer and mRNA levels in the treatment groups from both BALF and lung samples were reduced compared to the untreated group in a dose-dependent manner. The hRSV FFU viral titers were below the detection level in all lung samples and in 1 of 5 BALF samples from the high dose group (T50). The geometric means of the viral titer in BALF samples were $1.23x10^2$, $2.54x10^4$, $7.85x10^4$, $3.60x10^4$ FFU/ml, and in the lung samples were 0, $9.20x10^2$, $1.36x10^4$, $1.51x10^4$ FFU/g in T50, T10, T2, and RSV respectively. The viral titer in BALF and lung in the high dose group (T50) were significantly lower ($p<0.05$) compared to the low dose group (T2). In addition, the viral titer in the lung of T50 was significantly reduced compared to the non-treated group (RSV) (Fig 2a, 2b). No viable virus was detected by FFU in both BALF and lung samples of the negative control group.

A similar trend of dose-dependent reduction in RSV was demonstrated with the level of viral mRNA detected by RT-qPCR. The geometric means of the viral mRNA level in BALF

samples were $1.67x10^5$, $2.41x10^7$, $8.08x10^7$, $9.66x10^7$ virion/ml, and in the lung samples were $2.66x10^6$, $1.07x10^9$, $3.76x10^9$, $4.71x10^8$ virion/g in T50, T10, T2, and RSV group, respectively. The level of hRSV virion in the high dose group (T50) was significant lower compared to the number of virions detected in the BALF ($p<0.05$) and lung ($p<0.01$) of the low dose group (T2), and the virion level in the non-treated group (RSV) only in the BALF sample ($p<0.01$) (Fig 2c, 2d). No hRSV mRNA was detected in either BALF or lung samples of the negative control group.

Lung Pathology and Detection of HRSV in Pulmonary Histological Tissue

The macroscopic lung lesions related to hRSV infection at 6 dpi appeared as multifocal 3-5 mm, dark-red consolidated areas involving the cranial and accessory lobes, and in more severe cases, extended into the caudal lobes (Fig 3). Total percentage involvement of hRSV lung lesions grossly was calculated by averaging the value assessed in each lung lobe. A higher percentage of lung lesions were present in low dose treatment group (T2) (51.6%) followed by intermediate dose (T10) (26.7%) and no macroscopic lesions were seen in the high dose group (T50) (0.00%) (Fig 4). Microscopic lung lesions of hRSV-infected neonatal lambs were characterized by necrotizing and neutrophilic bronchiolitis with lymphoplasmacytic adventitial infiltrates and syncytial cell formation with the average microscopic lung consolidation score of 2.08/4 (Fig 3). The average microscopic lung consolidation scores were higher in the low dose group (T2) (2.25/4), followed by intermediate dose (T10) (0.83/4) and were the lowest (score of 0/4) in the high dose group (T50) (Fig 4). In addition, the scores of bronchiolitis, syncytial formation, epithelial necrosis, epithelial hyperplasia, neutrophilic infiltrates,

peribronchiolar and perivascular lymphoplasmacytic infiltrates, had a similar trend between the treatment groups (Fig 4).

The hRSV antigen was identified by immunohistochemical staining of lung and was present in intact and sloughed bronchiolar epithelial cells, syncytial cells and type II pneumocytes (Fig 5). Occasionally, hRSV antigen was detected in pulmonary alveolar macrophages. Immunohistochemical staining of hRSV antigen in lung were scored based on the number of immunoreactive cells evident in the bronchioles and alveoli. Viral antigen was not detected in 2/5 lungs sampled from the high dose group (T50). The average immunoreactivity scores in the bronchioles and alveoli were significantly lower in high dose group (T50) (bronchioles = 0.08±0.11, alveoli = 0.05±0.11) compared to placebo group (RSV) (bronchioles = 1.71±0.39, alveoli = 2.96±0.82) and low dose group (T2) (bronchioles = 1.81±0.30, alveoli = 3.00±1.29) (Fig 6).

The viral hRSV RNA was detected within bronchiolar epithelial cells, type II pneumocytes and pulmonary alveolar macrophages via RNA *in situ* hybridization (RNAscope®). The virion detection appeared as brown DAB chromogenic staining characterized as dots where a single dot representing a single probe binding equivalent to a single copy of virion. With software image analysis, the density of the dots within each cell were calculated and graded in 4 tier bin; Bin 0; <1 copy/cell, Bin 1; 1-3 copies/cell, Bin 2; 4-9 copies/cell, Bin 3; 10-15 copies/cell, Bin 4; (>15 copies/cell) and further calculated into a quantitative H-score representing the degree of hRSV RNA virion expression in the lung. All infected lung samples had positive staining for hRSV virions. The overall percentage of positive cells were highest in low dose treatment group (T2, 11.52%) followed by intermediate-dose treatment (T10, 5.27%) and lowest in the high-dose treatment (T50, 0.26%). Similarly,

the mean H-score of the lungs were lowest in the high-dose treatment group (T50) (0.45±0.64) with increasing scores in the intermediate-dose group (T10) (13.61±3.56) and the highest scores in the low-dose treatment group (T2) (31.45±14.50). The hRSV infected group with no treatment had an average H-score of 19.52±20.65. There was a statistically significant differences of H-score was presented between the high dose group (T50) and the low dose group (T2) ($p<0.001$) (Fig 6). There was a strong correlation ($p<0.001$) between H score and IHC bronchiole lung score ($r=0.908$), lung viral FFU titer ($r=0.837$), FFU viral level ($r=0.784$), lung RT-qPCR viral level ($r=0.801$), BALF RT-qPCR ($r=0.757$) and IHC alveolar score ($r=0.768$).

Cytokine and Chemokines mRNA Expression

Evaluation of cytokine and chemokine mRNA expression demonstrated an increasing trend of CXCL10 (IP10), CCL2 (MCP-1), CCL3 (MIP-1α), CD274 (PD-L1) and IFN-λ in RSV-infected with no treatment (RSV) and low dose groups (T2) corresponding with higher viral load of these groups. Significant differences were observed in CCL2 (MIP-1α) levels between T50 and T2 and IFN-λ level of negative control group and T2. No significant differences or decreasing/increasing trend were observed in the level of RANTES and IL-3 mRNA expression (Fig 6).

Discussion

Infection of hRSV in immunocompetent adults often results in mild bronchiolitis, but can manifest as acute respiratory tract infection (ARTI) or severe acute respiratory infection (SARI) in infants and elderly individuals resulting in hospitalization and fatalities. There is

currently a need to develop effective methods of prevention and treatment of hRSV. Extensive laboratory and preclinical animal studies and testing are necessary on pharmaceutical compounds and vaccines prior to clinical phases of evaluation. Parameters accessed during `the preclinical development of these compounds include their intrinsic antiviral activity, safety/tolerability, developability, pharmacokinetics/pharmacodynamics, and the characterization of antiviral resistances. Antiviral activity tests require the use of experimental models for hRSV infection. An *in vitro* model of well-differentiated primary pediatric bronchial epithelial cells (WD-PBECs) has been developed and ascertained to be beneficial for hRSV pathogenesis research though there are limitation of this model for therapeutic and vaccination studies [10, 11]. Alternatively, reconstitution of 3D human airway epithelium cells (HuAECs) have been demonstrated to be a relevant *ex vivo* model for studying the efficacy of antiviral compounds [12]. However, animal models and assessment *in vivo* still remain indispensable for validating the antiviral compounds penetrating ability into the target organ at the appropriate level and time of exposure.

Several animal models of *in vivo* hRSV infection have been established and these include cotton rats [13, 14], laboratory mice [15, 16], ferrets [17], non-human primates (NHPs) [18, 19], and neonatal lambs [5, 6] which were used in this study. As a representative model for human infant lungs [5], the neonatal lambs infected with hRSV Memphis 37 virus developed pulmonary lesion characterized by necrotizing and neutrophilic bronchiolitis, with lymphoplasmacytic adventitial infiltrates and occasional syncytial cell formation with hRSV localizing in bronchiolar epithelium and occasionally in type II pneumocyte with peak lesion development at 6 dpi [20]. All the hRSV infected, positive control lambs (RSV) in this study had effective viral inoculation with similar pulmonary lesions as previously described. Studies

of therapeutic efficacy of compounds have been tested in neonatal lamb model of hRSV infection in infants and some have advanced into the clinical phase. The aerosolized compound, ALX-0171 in neonatal lambs had robust antiviral effect in reducing the pulmonary lung lesion even with late term dosing [21]. In addition, oral administration of fusion inhibitor compound, JNJ-53718678, had a potent effect in reducing the lung viral load and pulmonary lesion in hRSV-infected lambs [22].

Various hRSV antiviral compounds have been developed including fusion protein inhibitors [22-25], and non-fusion protein inhibitors that target G protein [26], viral RNA polymerase [27, 28], viral mRNA guanylylation [29] and viral nucleoprotein (N) [30]. The mechanism of fusion protein inhibitors is through the binding to the fusion protein in the pocket of the trimeric ectodomain of the metastable prefusion F protein, thus stabilizing the prefusion conformation and inhibiting viral entry [31]. Even with the structural differences of the fusion protein inhibitor compound, possible cross-resistance mutation of the virus has been identified in experimental settings [32] and with fusion inhibitors for other viruses [33]. Moreover, the effective treatment window reported *in vitro* with fusion inhibitors is limited in time with a potential loss of the antiviral effect once the virus has entered the cells, but the faculty of blocking the entry of the virus in neighboring cells. Also, considering the threat associated to the emergence of antiviral resistance (all fusion inhibitors published so far share the same binding pocket), an alternative mode of action is desirable. HRSV replication inhibitors that inhibit post-entry pathway of viral replication have shown a wider effective treatment window up to 3 days post infection when tested in the HuAEC model [12]. Efficacy of JNJ-64166037 replication inhibitor in neonatal lambs infected with hRSV was evaluated for antiviral efficacy but also for its impact on the hRSV-induced pathology: changes in clinical parameters and

degree of pulmonary lesion. No significant differences of general clinical parameters (RR, BW, BT and HR) were detected upon infection or modulated by the antiviral treatments. Increased respiratory efforts were seen in animals in the intermediate dose (T10), low dose (T2) and non-treatment group (RSV), but none in the high dose treatment group. The reduction of hRSV viral titer and RNA in the lung and BALF of treated lambs were dose-dependent. Oral administration of the hRSV replicator inhibitor in a single dose per day (q.d.) regimen with the first dose given at 1h post-inoculation for a duration of 6 days at 50 mg/kg dosage was most effective by significantly reducing hRSV infective viral titer at more than 2 log FFU/ml(g) in BALF and/or lung compared to the non-treated hRSV infected group. There were marked significant decreases of hRSV virions in the lung samples of lambs given 50 mg/kg regime at more than 2 log virion/g compared to the non-treated group.

Localization of hRSV antigen in lung tissue was determined with immunohistochemistry and *in situ* hybridization of viral RNA. The sensitivity of the *in situ* hybridization detection of viral RNA was higher (100%) than immunohistochemical detection of antigen (87.50%). With semi-quantitative scoring of immunoreactive cells in the bronchioles and alveoli, there was a significant decrease in the number of immunoreactive cells in the high dose treatment group (T50) when compared to the non-treatment group (RSV). Quantitative evaluation via image analysis software and calculation of modified H-score quantification method identified a similar dose-dependent trend of decreasing viral levels with significant differences between the high dose group compared to the low dose group. Overall positive signal in the high dose treatment group was very low (0.26%) with low expression of viral mRNA in the cells. The higher level of H score and presence of multiple clusters in lower

dose treatment groups and non-treated group would suggest a more active replication of the virus and cell to cell spread from hRSV infection.

With image analysis software, cell-by-cell expression profiles were grouped in 4-bins and percentages of expression level between treatment groups compared. This method can be utilized in interpreting the level of viral mRNA replication within the infected cells and effectiveness of the antiviral replicator inhibitor as well as effectively localizing the viral RNA. Interestingly, the H score level had significant correlation with the amount of hRSV viral antigen measured by FFU and RT-qPCR indicating effective predictive value of the viral level. This correlation indicate that the computer analysis and modification of scoring generated can represent the viral load in the lung tissue. Similar profiling of virions with RNA *in situ* hybridization have recently been performed in a few studies of other viral infection and pathogenesis [34]. An increasing number of studies have utilized this non-antibody based novel technique to localize virus antigen including Zika virus in ocular tissue of mice [35] and detection of Seneca virus-induced vesicular lesion in swine [36].

Conclusions

Oral administration of the non-fusion replication inhibitor JNJ-64166037 at the appropriate dose has potent antiviral effects in the lamb model of RSV infection by decreasing the level of hRSV in a dose-dependent manner. This mode of therapeutic intervention eliminated the hRSV-induced lung lesions assessed in the model. This study provides promising evidence that JNJ-64166037 might prove to be an effective treatment for RSV bronchiolitis in infants and children.

Acknowledgments

We would like to thank Janssen Infectious Diseases & Vaccines, Janssen Pharmaceutica NV, Beerse, Belgium for the funding in this study. We also would like to thank the Iowa State University, Veterinary Pathology Histology Laboratory technicians, Toni Christofferson, Deborah Moore and Diane Gerjets, and Laboratory Animal Resources and Livestock Infectious Disease Isolation Facility staff, Diane McDonald, Kathleen Mullin, and Dale Hinderaker for their help and support.

Declaration of Conflicting Interests

This study was funded by Janssen Infectious Diseases & Vaccines, Janssen Pharmaceutica NV, Beerse, Belgium.

References

1. Shay DK, Holman RC, Newman RD, Liu LL, Stout JW, Anderson LJ. Bronchiolitis-associated hospitalizations among US children, 1980-1996. JAMA. 1999;282(15):1440-6. PubMed PMID: 10535434.

2. Thompson WW, Shay DK, Weintraub E, Brammer L, Cox N, Anderson LJ, et al. Mortality associated with influenza and respiratory syncytial virus in the United States. JAMA. 2003;289(2):179-86. PubMed PMID: 12517228.

3. Kim HW, Canchola JG, Brandt CD, Pyles G, Chanock RM, Jensen K, et al. Respiratory syncytial virus disease in infants despite prior administration of antigenic inactivated vaccine. Am J Epidemiol. 1969;89(4):422-34. PubMed PMID: 4305198.

4. Heylen E, Neyts J, Jochmans D. Drug candidates and model systems in respiratory syncytial virus antiviral drug discovery. Biochem Pharmacol. 2017;127:1-12. Epub 2016/09/19. doi: 10.1016/j.bcp.2016.09.014. PubMed PMID: 27659812.

5. Derscheid RJ, Ackermann MR. Perinatal lamb model of respiratory syncytial virus (RSV) infection. Viruses. 2012;4(10):2359-78. Epub 2012/10/23. doi: 10.3390/v4102359. PubMed PMID: 23202468; PubMed Central PMCID: PMCPMC3497056.

6. Ackermann MR. Lamb model of respiratory syncytial virus-associated lung disease: insights to pathogenesis and novel treatments. ILAR J. 2014;55(1):4-15. doi: 10.1093/ilar/ilu003. PubMed PMID: 24936027; PubMed Central PMCID: PMCPMC4158344.

7. Grosz DD, van Geelen A, Gallup JM, Hostetter SJ, Derscheid RJ, Ackermann MR. Sucrose stabilization of Respiratory Syncytial Virus (RSV) during nebulization and experimental infection. BMC Res Notes. 2014;7:158. doi: 10.1186/1756-0500-7-158. PubMed PMID: 24642084; PubMed Central PMCID: PMC3995326.

8. Gallup JM, Ackermann MR. The 'PREXCEL-Q Method' for qPCR. Int J Biomed Sci. 2008;4(4):273-93. PubMed PMID: 19759920; PubMed Central PMCID: PMCPMC2744046.

9. Wang F, Flanagan J, Su N, Wang LC, Bui S, Nielson A, et al. RNAscope: a novel in situ RNA analysis platform for formalin-fixed, paraffin-embedded tissues. J Mol Diagn. 2012;14(1):22-9. doi: 10.1016/j.jmoldx.2011.08.002. PubMed PMID: 22166544; PubMed Central PMCID: PMCPMC3338343.

10. Henderson F, Myers A. RNAscope ® image analysis using HALO ® brightfield and fluorescent ISH modules. Indica Labs; 2018.

11. Henderson F, Myers A. RNAscope ® image analysis using HALO ® brightfieqld and fluorescent ISH modules. Indica Labs; 2018.

12. Villenave R, Thavagnanam S, Sarlang S, Parker J, Douglas I, Skibinski G, et al. In vitro modeling of respiratory syncytial virus infection of pediatric bronchial epithelium, the primary target of infection in vivo. Proc Natl Acad Sci U S A. 2012;109(13):5040-5. Epub 2012/03/12. doi: 10.1073/pnas.1110203109. PubMed PMID: 22411804; PubMed Central PMCID: PMCPMC3323997.

13. Tripp RA. Modeling respiratory syncytial virus cytopathogenesis in the human airway. Am J Respir Crit Care Med. 2013;188(7):766-7. doi: 10.1164/rccm.201308-1491ED. PubMed PMID: 24083857.

14. Mirabelli C, Jaspers M, Boon M, Jorissen M, Koukni M, Bardiot D, et al. Differential antiviral activities of respiratory syncytial virus (RSV) inhibitors in human airway epithelium. J Antimicrob Chemother. 2018. Epub 2018/03/27. doi: 10.1093/jac/dky089. PubMed PMID: 29596680; PubMed Central PMCID: PMCPMC6005027.

15. Boukhvalova MS, Blanco JC. The cotton rat Sigmodon hispidus model of respiratory syncytial virus infection. Curr Top Microbiol Immunol. 2013;372:347-58. doi: 10.1007/978-3-642-38919-1_17. PubMed PMID: 24362698.

16. Boukhvalova MS, Yim KC, Blanco J. Cotton rat model for testing vaccines and antivirals against respiratory syncytial virus. Antivir Chem Chemother. 2018;26:2040206618770518. doi: 10.1177/2040206618770518. PubMed PMID: 29768937; PubMed Central PMCID: PMCPMC5987903.

17. Cianci C, Genovesi EV, Lamb L, Medina I, Yang Z, Zadjura L, et al. Oral efficacy of a respiratory syncytial virus inhibitor in rodent models of infection. Antimicrob Agents Chemother. 2004;48(7):2448-54. doi: 10.1128/AAC.48.7.2448-2454.2004. PubMed PMID: 15215093; PubMed Central PMCID: PMCPMC434195.

18. Corvaïa N, Tournier P, Nguyen TN, Haeuw JF, Power UF, Binz H, et al. Challenge of BALB/c mice with respiratory syncytial virus does not enhance the Th2 pathway induced after immunization with a recombinant G fusion protein, BBG2NA, in aluminum hydroxide. J Infect Dis. 1997;176(3):560-9. PubMed PMID: 9291300.

19. Stittelaar KJ, de Waal L, van Amerongen G, Veldhuis Kroeze EJ, Fraaij PL, van Baalen CA, et al. Ferrets as a Novel Animal Model for Studying Human Respiratory Syncytial Virus Infections in Immunocompetent and Immunocompromised Hosts. Viruses. 2016;8(6). Epub 2016/06/14. doi: 10.3390/v8060168. PubMed PMID: 27314379; PubMed Central PMCID: PMCPMC4926188.

20. Babu PG, Selvan A, Christuraj S, David J, John TJ, Simoes EA. A primate model of respiratory syncytial virus infection. Indian J Exp Biol. 1998;36(8):758-62. PubMed PMID: 9838875.

21. Simoes EA, Hayward AR, Ponnuraj EM, Straumanis JP, Stenmark KR, Wilson HL, et al. Respiratory syncytial virus infects the Bonnet monkey, Macaca radiata. Pediatr Dev Pathol. 1999;2(4):316-26. PubMed PMID: 10347274.

22. Larios Mora A, Detalle L, Van Geelen A, Davis MS, Stohr T, Gallup JM, et al. Kinetics of Respiratory Syncytial Virus (RSV) Memphis Strain 37 (M37) Infection in the Respiratory Tract of Newborn Lambs as an RSV Infection Model for Human Infants. PLoS One. 2015;10(12):e0143580. Epub 2015/12/07. doi: 10.1371/journal.pone.0143580. PubMed PMID: 26641081; PubMed Central PMCID: PMCPMC4671688.

23. Larios Mora A, Detalle L, Gallup JM, Van Geelen A, Stohr T, Duprez L, et al. Delivery of ALX-0171 by inhalation greatly reduces respiratory syncytial virus disease in newborn lambs. MAbs. 2018;10(5):778-95. doi: 10.1080/19420862.2018.1470727. PubMed PMID: 29733750.

24. Roymans D, Alnajjar SS, Battles MB, Sitthicharoenchai P, Furmanova-Hollenstein P, Rigaux P, et al. Therapeutic efficacy of a respiratory syncytial virus fusion inhibitor. Nat Commun. 2017;8(1):167. Epub 2017/08/01. doi: 10.1038/s41467-017-00170-x. PubMed PMID: 28761099.

25. Mackman RL, Sangi M, Sperandio D, Parrish JP, Eisenberg E, Perron M, et al. Discovery of an oral respiratory syncytial virus (RSV) fusion inhibitor (GS-5806) and clinical proof of concept in a human RSV challenge study. J Med Chem. 2015;58(4):1630-43. Epub 2015/01/27. doi: 10.1021/jm5017768. PubMed PMID: 25574686.

26. Kim YI, Pareek R, Murphy R, Harrison L, Farrell E, Cook R, et al. The antiviral effects of RSV fusion inhibitor, MDT-637, on clinical isolates, vs its achievable concentrations in the human respiratory tract and comparison to ribavirin. Influenza Other Respir Viruses. 2017;11(6):525-30. Epub 2017/10/30. doi: 10.1111/irv.12503. PubMed PMID: 28990339; PubMed Central PMCID: PMCPMC5705693.

27. DeVincenzo JT, D., Oluwayi O, Mori J, Thomas E, Mathews N, Harland R, et al. Safety and Efficacy of Oral RV521 in a Human Respiratory Syncytial Virus (RSV) Phase 2a Challenge Study. American Thoracic Society 2018 International Conference; San Diego, California: American Journal of Respiratory and Critical Care Medicine; 2018.

28. Evans CW, Atkins C, Pathak A, Gilbert BE, Noah JW. Benzimidazole analogs inhibit respiratory syncytial virus G protein function. Antiviral Res. 2015;121:31-8. Epub 2015/06/24. doi: 10.1016/j.antiviral.2015.06.016. PubMed PMID: 26116756.

29. Tiong-Yip CL, Aschenbrenner L, Johnson KD, McLaughlin RE, Fan J, Challa S, et al. Characterization of a respiratory syncytial virus L protein inhibitor. Antimicrob Agents Chemother. 2014;58(7):3867-73. Epub 2014/04/28. doi: 10.1128/AAC.02540-14. PubMed PMID: 24777090; PubMed Central PMCID: PMCPMC4068518.

30. DeVincenzo JP, McClure MW, Symons JA, Fathi H, Westland C, Chanda S, et al. Activity of Oral ALS-008176 in a Respiratory Syncytial Virus Challenge Study. N Engl J Med. 2015;373(21):2048-58. doi: 10.1056/NEJMoa1413275. PubMed PMID: 26580997.

31. Liuzzi M, Mason SW, Cartier M, Lawetz C, McCollum RS, Dansereau N, et al. Inhibitors of respiratory syncytial virus replication target cotranscriptional mRNA guanylylation by viral RNA-dependent RNA polymerase. J Virol. 2005;79(20):13105-15. doi: 10.1128/JVI.79.20.13105-13115.2005. PubMed PMID: 16189012; PubMed Central PMCID: PMCPMC1235819.

32. Chapman J, Abbott E, Alber DG, Baxter RC, Bithell SK, Henderson EA, et al. RSV604, a novel inhibitor of respiratory syncytial virus replication. Antimicrob Agents Chemother. 2007;51(9):3346-53. Epub 2007/06/18. doi: 10.1128/AAC.00211-07. PubMed PMID: 17576833; PubMed Central PMCID: PMCPMC2043207.

33. Battles MB, Langedijk JP, Furmanova-Hollenstein P, Chaiwatpongsakorn S, Costello HM, Kwanten L, et al. Molecular mechanism of respiratory syncytial virus fusion inhibitors. Nat Chem Biol. 2016;12(2):87-93. Epub 2015/12/07. doi: 10.1038/nchembio.1982. PubMed PMID: 26641933; PubMed Central PMCID: PMCPMC4731865.

34. Yan D, Lee S, Thakkar VD, Luo M, Moore ML, Plemper RK. Cross-resistance mechanism of respiratory syncytial virus against structurally diverse entry inhibitors. Proc Natl Acad Sci U S A. 2014;111(33):E3441-9. Epub 2014/08/04. doi: 10.1073/pnas.1405198111. PubMed PMID: 25092342; PubMed Central PMCID: PMCPMC4143008.

35. Reeves JD, Lee FH, Miamidian JL, Jabara CB, Juntilla MM, Doms RW. Enfuvirtide resistance mutations: impact on human immunodeficiency virus envelope function, entry inhibitor sensitivity, and virus neutralization. J Virol. 2005;79(8):4991-9. doi: 10.1128/JVI.79.8.4991-4999.2005. PubMed PMID: 15795284; PubMed Central PMCID: PMCPMC1069568.

36. Schache AG, Liloglou T, Risk JM, Jones TM, Ma XJ, Wang H, et al. Validation of a novel diagnostic standard in HPV-positive oropharyngeal squamous cell carcinoma. Br J Cancer. 2013;108(6):1332-9. Epub 2013/02/14. doi: 10.1038/bjc.2013.63. PubMed PMID: 23412100; PubMed Central PMCID: PMCPMC3619267.

37. Miner JJ, Sene A, Richner JM, Smith AM, Santeford A, Ban N, et al. Zika Virus Infection in Mice Causes Panuveitis with Shedding of Virus in Tears. Cell Rep. 2016;16(12):3208-18. Epub 2016/09/06. doi: 10.1016/j.celrep.2016.08.079. PubMed PMID: 27612415; PubMed Central PMCID: PMCPMC5040391.

38. Resende TP, Marthaler DG, Vannucci FA. A novel RNA-based in situ hybridization to detect Seneca Valley virus in neonatal piglets and sows affected with vesicular disease. PLoS One. 2017;12(4):e0173190. Epub 2017/04/10. doi: 10.1371/journal.pone.0173190. PubMed PMID: 28394893; PubMed Central PMCID: PMCPMC5386259.

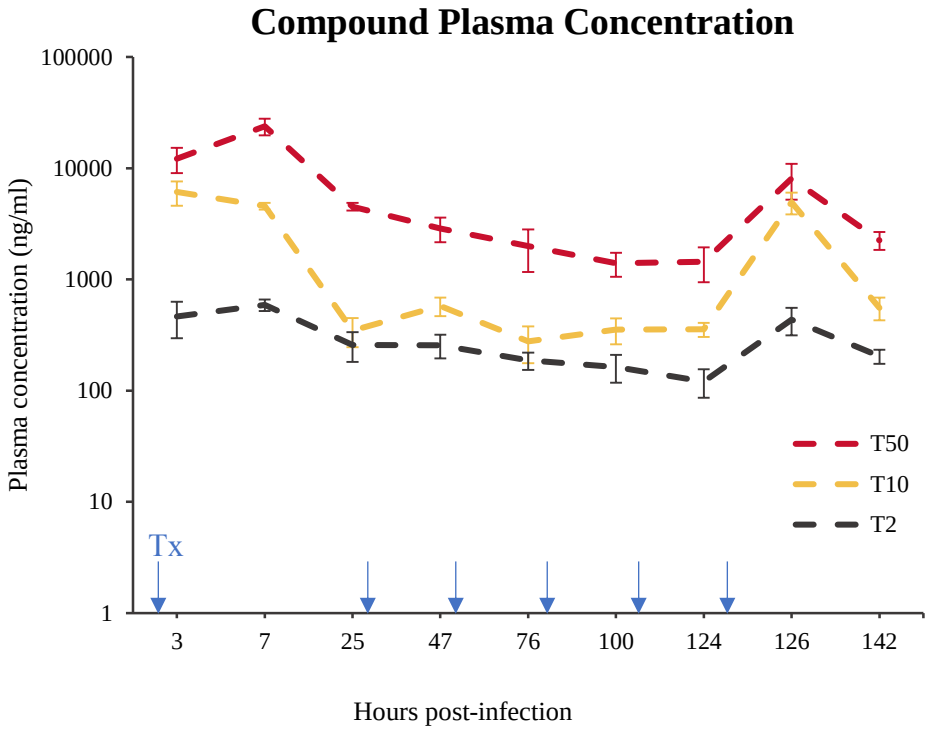

Figure 1: Plasma compound level of JNJ-64166037

The level of JNJ-64166037 in plasma of 50 mg/kg (T50), 10 mg/kg (T10) and 2 mg/kg (T2) treatment groups evaluated at different time points. The time of treatment compound administration is indicated by the blue arrows.

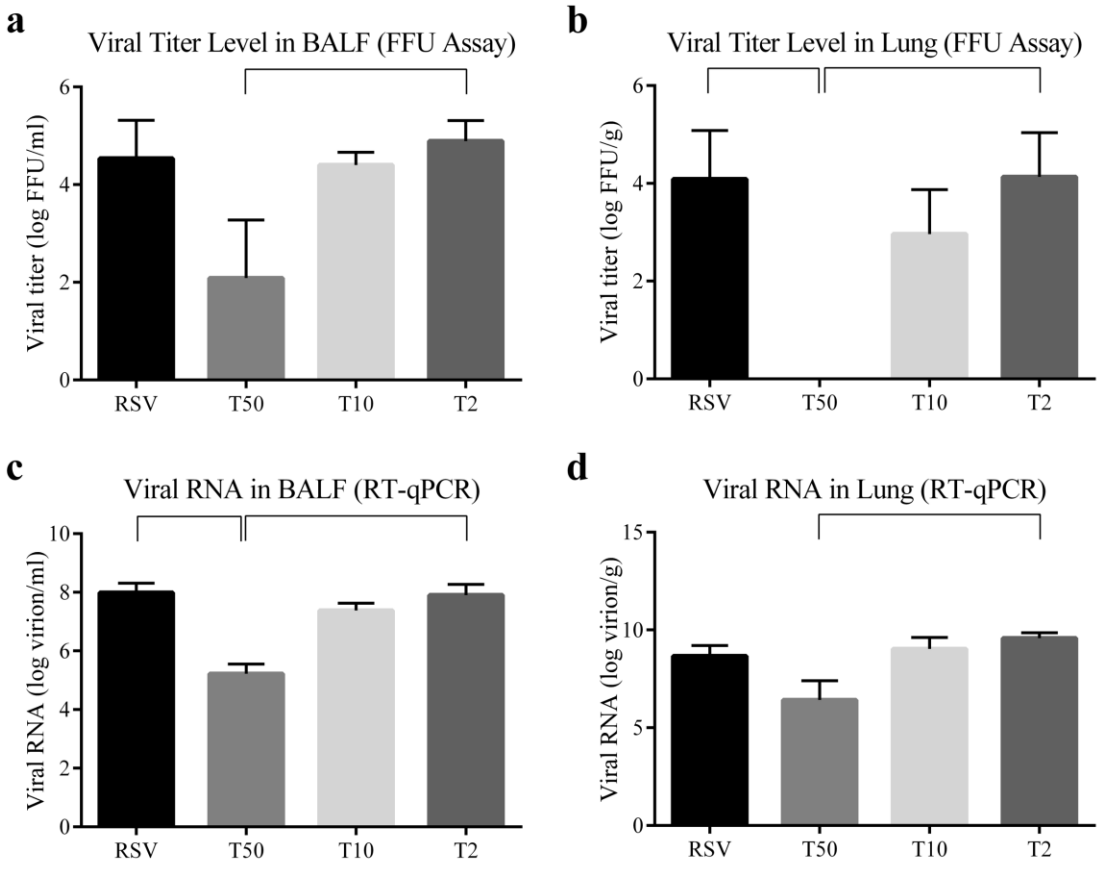

Figure 2: Viral titer level in BALF and lung detected with focus forming unit assay (FFU) and RT-qPCR

Levels of viral titer in BALF (a) and lung (b) detected by FFU and viral RNA detected in BALF (c) and lung (d) by RT-qPCR in different treatment groups (hRSV-infected non-treated lambs (RSV, n=6), 50 mg/kg treatment (T50, n=5), 10 mg/kg treatment (T10, n=3) and 2 mg/kg treatment (T2, n=4)).

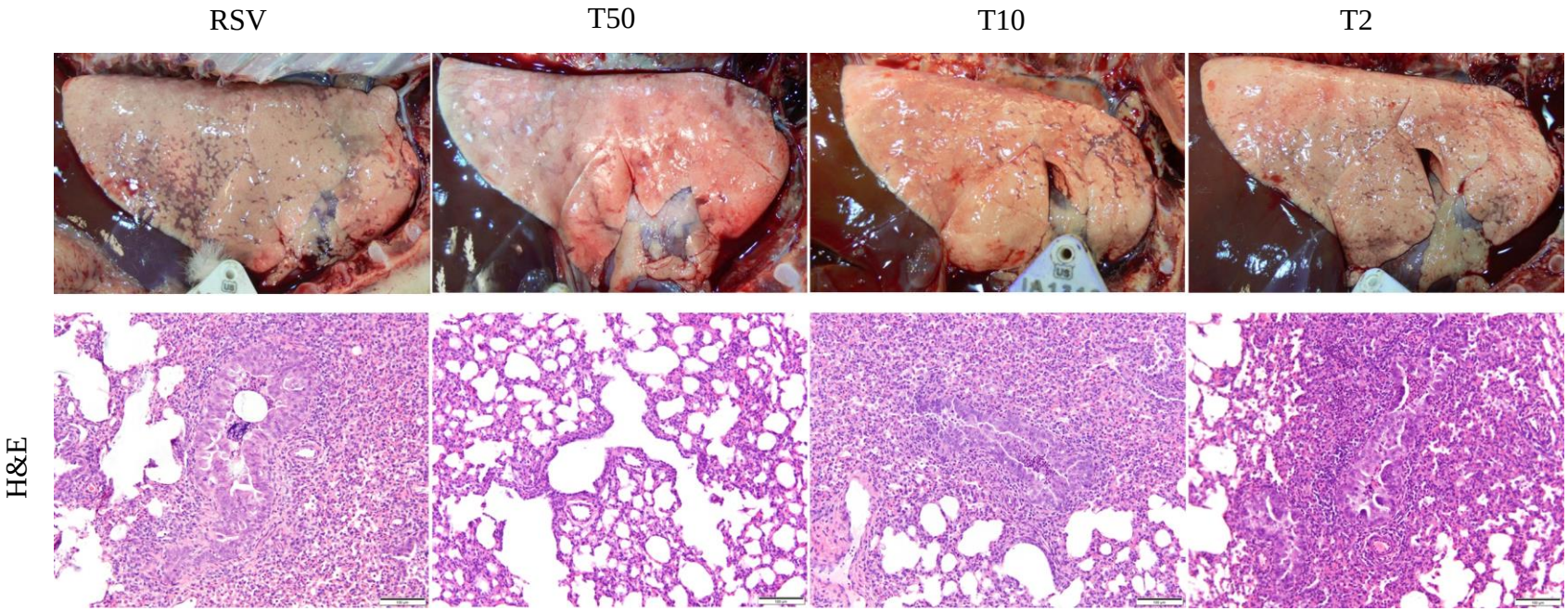

Figure 3: Gross and microscopic lesions in lung in vehicle and replication inhibitor treatment groups

Gross and microscopic lesions in lung in hRSV-infected non-treated lambs (RSV), 50 mg/kg treatment (T50), 10 mg/kg treatment (T10) and 2 mg/kg treatment (T2).

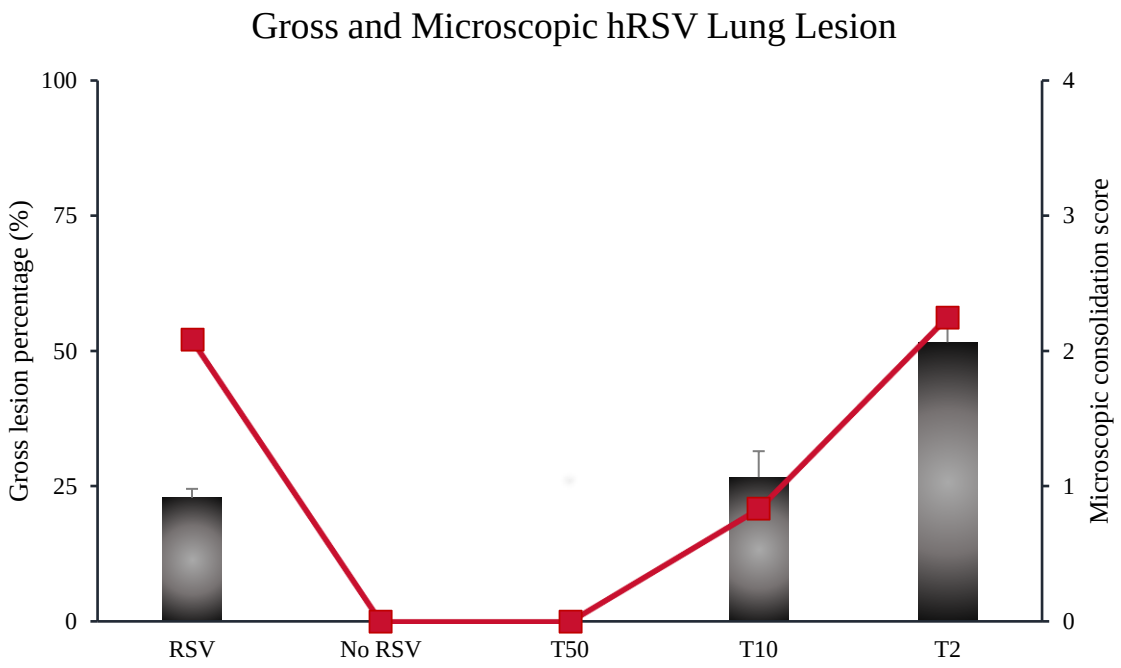

	CS	BR	SYN	EN	EH	NEU	BN	VN
RSV	2.08±1.28	1.75±0.87	0.50±0.50	1.17±0.52	1.83±0.80	1.75±0.90	1.67±1.18	1.50±0.75
T50	0	0	0	0	0	0	0	0
T10	0.83±0.52	0.92±0.58	0.67±0.52	0.67±0.58	0.67±0.58	0.83±0.52	0.83±0.52	0.83±0.52
T2	2.25±0.35	1.63±0.43	0.88±0.48	1.31±0.38	1.31±0.38	1.56±0.38	1.50±0.35	1.50±0.35
Neg	0	0	0	0	0	0	0	0

CS; microscopic consolidation, BR; bronchiolitis, SYN; syncytial formation, EN; epithelial necrosis, EH; epithelial hyperplasia, NEU; neutrophilic infiltrates in airways, BN; peribronchiolar lymphoplasmacytic infiltrates, VN; perivascular lymphoplasmacytic infiltrates

Figure 4: Percentage of HRSV-associated lung lesion and HRSV-associated microscopic lung score

Scoring of the macroscopic (bar) and microscopic (line) lung lesions were based on percentages of grossly affected lung parenchyma and microscopic score of consolidation in neonatal lamb of different experimental groups; RSV-infected with no treatment (RSV), 50 mg/kg treatment (T50), 10 mg/kg treatment (T10) and 2 mg/kg treatment (T2) and negative control group (Neg).

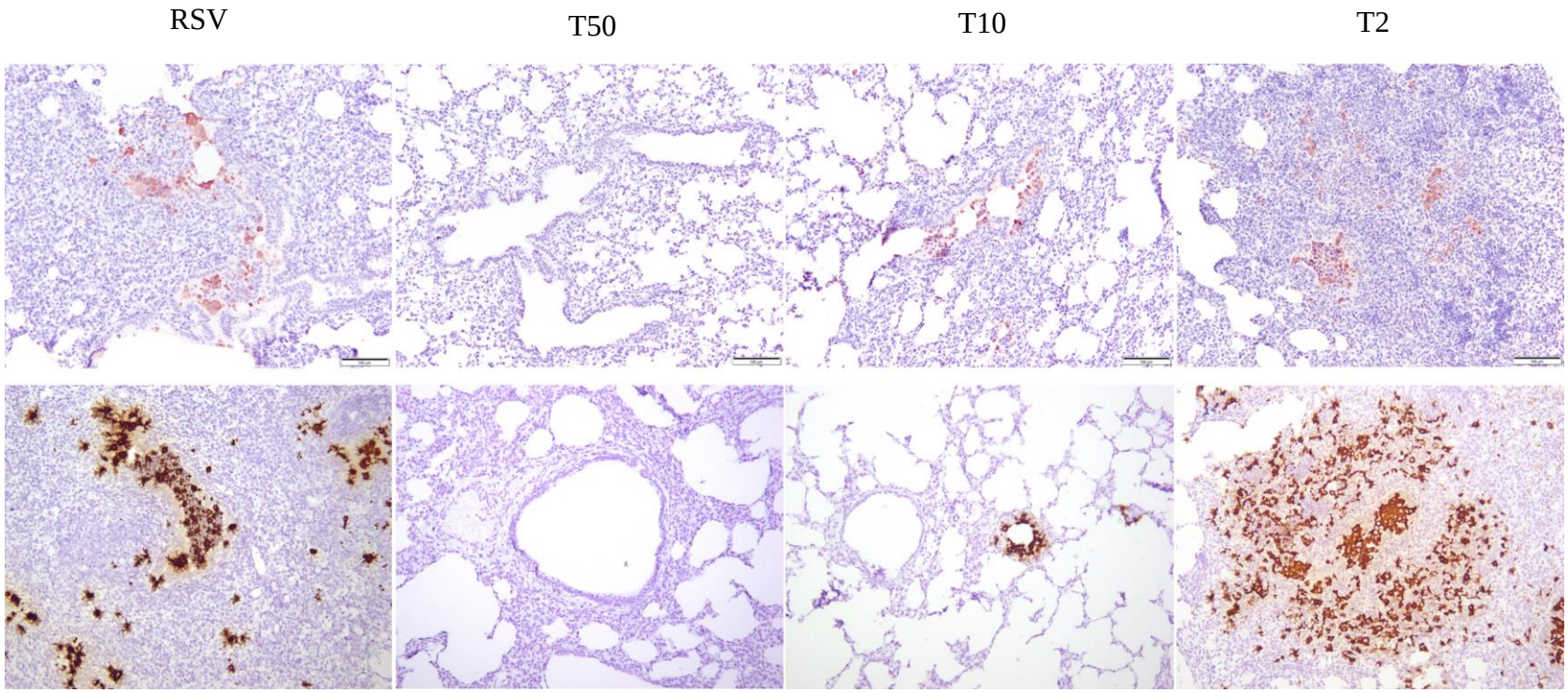

Figure 5: Immunohistochemical detection of hRSV antigen and RNA *in situ* hybridization

Immunohistochemical detection (top row) of RSV antigen (Nova red stain, 200X) and RNA *in situ* hybridization (bottom row) (DAB, 200X) in 50 mg/kg treatment (T50), 10 mg/kg treatment (T10) and 2 mg/kg treatment (T2) compared to hRSV-infected non-treated group (RSV).

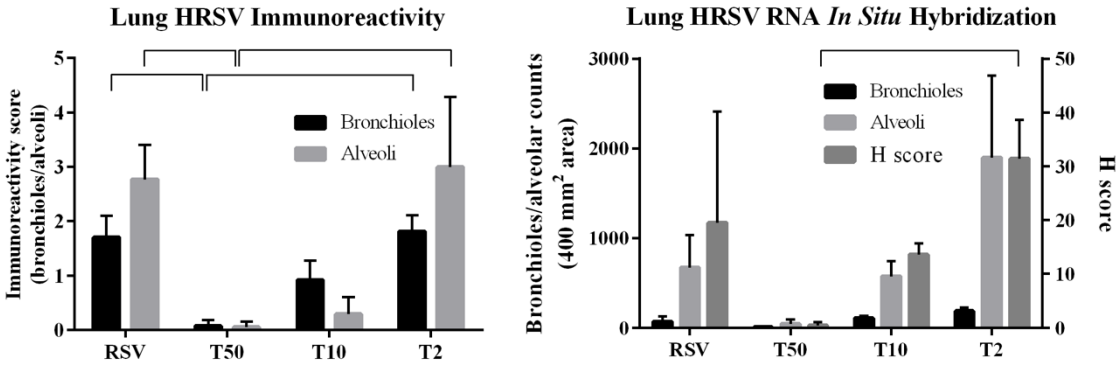

Figure 6: Immunoreactivity score and RNA *in situ* hybridization H score of hRSV

Immunohistochemical scores (left) of hRSV antigen detected in the lung section of each treatment group. Significant differences were observed between the level of virus in the 50 mg/kg treatment (T50) compared to non-treatment group (RSV) and 2 mg/kg treatment (T2). The level of H score of hRSV detected with RNA *in situ* hybridization (right) increased in a dose-dependent manner. Significant reduction of H score was observed when administered 50 mg/kg of JNJ-64166037 replication inhibitor to hRSV-infected lambs.

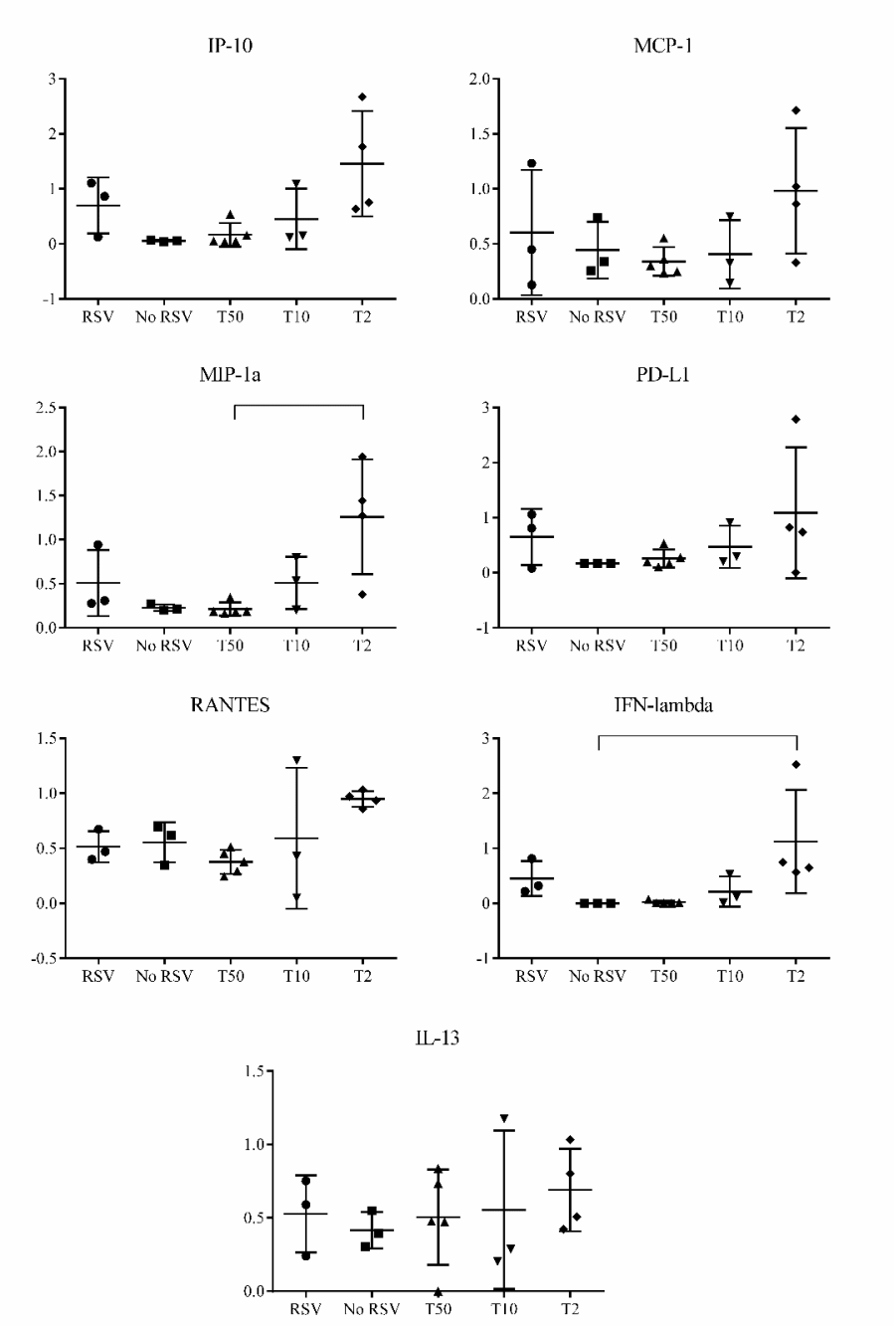

Figure 7: Cytokine and chemokine mRNA expression (IP-10, MCP-1, MIP-1α, PD-L1, RANTES, IFN-λ, and IL-13)

Cytokine and chemokine mRNA expression (IP-10, MCP-1, MIP-1α, PD-L1, RANTES, IFN-λ, and IL-13) displaying individual data points and geometric mean values (horizontal bar) of each treatment (50 mg/kg (T50), 10 mg/kg (T10) and 2 mg/kg (T2)) and non-treated group (RSV).

CHAPTER 4. EFFICACY AND TIME WINDOW FOR TREATMENT WITH COMBINATION THERAPY OF THE HUMAN RESPIRATORY SYNCYTIAL VIRUS (HRSV) FUSION INHIBITOR AND NON-FUSION PROTEIN INHIBITOR IN HRSV INFECTED LAMBS

Panchan Sitthicharoenchai[1], Sarhad S. Alnajjar[1,4], Dirk Roymans[2],

Peter Rigaux[2], Jack M. Gallup[5] and Mark R. Ackermann[3,4]

[1] Department of Veterinary Pathology, College of Veterinary Medicine, Iowa State University, Ames, IA. [2]Janssen Infectious Diseases and Vaccines, Janssen Pharmaceutica NV, Beerse Belgium. [3]Department of Biomedical Sciences, Carlson College of Veterinary Medicine, Oregon State University, Corvallis, Oregon. [4]LambCure LLC, Corvallis, Oregon. [5]Boehringer Ingelheim, Ames, Iowa

Abstract

Background: The purpose of this study was to determine the antiviral efficacy when administering a combination of inhibitors with distinctly different modes of action (fusion protein and non-fusion protein inhibitors) and investigate the time window in which monotherapy or combination therapy may be efficacious. This preclinical drug trial was performed in hRSV-infected neonatal lambs which are a model for hRSV infection of human infants that develop similar severe lung pathology.

Methods: The experiment was divided in two phases; a Phase I combination efficacy study and a Phase II treatment time window study. In both phases, 1-3 day(s) old lambs were infected with hRSV Memphis 37 by viral nebulization. In the Phase I combination efficacy study, combination treatment of hRSV fusion inhibitor and replication inhibitor was administered orally once daily starting at 24 hours after infection, and was compared with monotherapy of the fusion inhibitor or the replication inhibitor given in the same manner. The doses of the antiviral compounds were based on the ED_{50} dose response curve from previous *in vitro* studies. For the Phase II treatment time window study, administration of combination treatment was delayed to day 3 and 4 post-infection and was compared to similarly delayed

monotherapy treatment with the fusion inhibitor or replication inhibitor. All animals in both phases were euthanized at day 6 post-infection. Bronchoalveolar lavage fluid (BALF) and lung tissue samples were collected for quantification of viral load (focus forming unit assay (FFU) and real-time reverse transcriptase polymerase chain reaction (RT-qPCR)), and localization of viral antigen in lung tissue (immunohistochemistry (IHC) and RNA *in situ* hybridization (RNAscope®)). In addition, disease severity was assessed by clinical parameters, macroscopic, microscopic lung examination and expression of cytokines. Evaluation of cytokine mRNA expression (IFN-λ, IL-13, MCP-1 (CCL2), MIP-1α (CCL3), RANTES (CCL5), IP10 (CXCL10)) and expression of immune-related molecules against hRSV (PD-L1 (CD274) and CC10) were performed on lung tissue samples.

Results: The viral titer levels with combination therapy in BALF were reduced up to 28-fold with high dose (4 mg/kg fusion inhibitor and 0.75 mg/kg replication inhibitor) and 11-fold with low dose (2 mg/kg fusion inhibitor with 0.4 mg/kg replication) when compared to the non-treated group. Administration of the combination treatment had lower level of viral titer levels, compared to monotherapy with fusion (1.7=fold) or non-fusion inhibitors (2.46-fold) given at identical doses. At the high dose level of combination therapy (4 mg/kg fusion inhibitor and 0.75 mg/kg replication inhibitor), there was prominent reduction of viral titer. Monotherapy treatment of replication inhibitor alone at 0.4 mg/kg did not significantly reduced the amount of virus compared to non-treated lambs ($7.67x10^8$ virions/ml BALF), although the average level of the viral titer appeared lower ($6.80x10^7$ virion/ml BALF). The viral loads paralleled the observed degree of lung pathology.

The delayed administration of combination therapy at day 3 and day 4 post-infection as well as monotherapy with the replication inhibitor (4 mg/kg) at day 3 post-infection resulted

in significant reductions in viral load compared to fusion inhibitor monotherapy and non-treated lambs. Lung lesions had a slightly different pattern at this timepoint in which the combination treatment had a similar degree of lung lesion severity as the fusion inhibitor monotherapy while the replication inhibitor had increased lesion severity.

Conclusion: Administration of combination drug therapy against hRSV holds promising potential as a future treatment option in clinical settings when administered both early and late following detection of infection. This combined treatment had potent antiviral effects in the hRSV-infected lamb model and demonstrated a prolonged treatment window up to 4 days after infection. Furthermore, the neonatal lamb model of hRSV infection appeared suitable for antiviral therapeutic testing and pathogenesis studies of hRSV infection.

Introduction

Human respiratory syncytial virus (hRSV) is a common cause of acute respiratory tract infection (ALRI) in young children worldwide with infection resulting in bronchiolitis and pneumonia [1, 2]. Lower respiratory tract infection by hRSV can also be detrimental in elderly individuals and contributes to morbidity and mortality of people over the age of 65 in the United States [3-5]. Approaches to hRSV prevention, control and treatment relies on successful development of vaccines, immunoprophylaxis and antiviral compounds. Despite tremendous research and advancements in vaccine and therapeutic development, no vaccine has been approved for hRSV in humans. An approved immunotherapeutic compound, palivizumab (Synagis®), can be used for prophylactic treatment of hRSV, but due to short duration of half-life, variability of effectiveness and high price, it is not recommended for routine treatment [6-8]. Ribavirin, an antiviral nucleoside analog that blocks RNA synthesis, is another compound

that has been approved for treatment of hRSV, although with limited effectiveness and reports of multiple adverse effects [9-12]. A limited number of the pharmaceutical products are currently in phases of clinical trials including immunomodulatory compounds [13], small molecule inhibitors that target viral fusion protein which is associated with viral entry [14, 15], or other small molecules that inhibit the machinery necessary for viral replication such as viral RNA polymerase, and nucleoprotein [16, 17].

The mechanism of action of current molecule fusion protein inhibitors is through binding and stabilizing the metastable prefusion F protein which prevents viral entry and fusion with host cells [18, 19]. Cross-resistance mutation of the virus and the early effective treatment time window are concerns with using fusion protein inhibitors [18]. Viral replication inhibitors target the post-entry pathway of virus infection and have demonstrated a wider effective treatment window in laboratory settings [20]. To our knowledge, combination treatment with both fusion and replication inhibitors for hRSV has not been tested in any experimental animal model.

Validating the efficacy of therapeutic compound requires the use an appropriate animal model in the preclinical phase. The neonatal lamb model of hRSV infection has similarities to human infants that include similarity of lung size, airway structures, immunological response and lung lesions [21, 22]. In this study, we applied the lamb model for hRSV to test the efficacy of oral administration of a combination of a fusion protein inhibitor and non-fusion protein inhibitor. Furthermore, we explored the effective therapeutic time window of these compounds for the treatment of hRSV.

Materials and Methods

Animal Model and Experimental Design

This project was divided into two phases; a study assessing the efficacy of administering combination of a fusion protein inhibitor with a non-fusion protein inhibitor (Phase I) and a study to evaluate the time window for effective treatment with the combination therapy (Phase II). In both phases, 1-3 day(s) old, colostrum-deprived, neonatal lambs were infected with a clinical isolate of hRSV Memphis 37 via nebulization with the final amount of virus given equivalent to 3.5×10^7 FFU/lamb. A prophylactic antibiotic (ceftiofur sodium, Naxcel®) were administered to all animals participating in both phases of the study.

The treatment groups in the Phase I combination efficacy study included a high dose combination group (TxH, n=5) given 4 mg/kg fusion inhibitor with 0.75 mg/kg replication inhibitor, a low dose combination group (TxL, n=7) given 2 mg/kg fusion inhibitor with 0.4 mg/kg replication inhibitor, a low dose group receiving 2 mg/kg fusion inhibitor (TxF, n=7), and a treatment of low dose 0.4 mg/kg replication inhibitor (TxNF, n=7). The selected doses for both antiviral compounds in TxL, TxF and TxNF groups were at the level of ED_{50} based on previous analysis of dose responses. All compound(s) were administered once daily starting 24 hours after viral inoculation for a total of 5 consecutive days.

The Phase II combination treatment window study consisted of four treatment groups including a combination treatment of 10 mg/kg fusion inhibitor and 4 mg/kg replication inhibitor first given at 3 dpi (TxL3, n=5), a combination treatment of 15.5 mg/kg fusion inhibitor and 8 mg/kg replication inhibitor first given at 4 dpi (TxH4, n=5), monotherapy of fusion inhibitor (10 mg/kg) first given at 3 dpi (TxF3, n=5) and monotherapy of replication inhibitor (4 mg/kg) first given at 3 dpi (TxNF3, n=5). For both phases of the study, five hRSV infected lambs were used as positive controls by administering vehicle solution (20% acidified

hydroxypropryl-β- cyclodextrin) and three lambs mock infected with pure culture media were used as uninfected control.

Clinical parameters, including body weight, body temperature, respiratory rate, and heart rate, were measured daily. Blood collection was performed at different time points to evaluate the pharmacokinetics of the compounds in plasma. All lambs were sacrificed at 6 dpi with an over-dose of sodium pentobarbital. Necropsy was performed to evaluate the macroscopic lung lesion, collect lung samples and bronchoalveolar lavage fluid (BALF). Lung tissues were placed in 10% neutral buffered formalin for microscopic examination. Samples from right cranial, left cranial, left middle and left caudal lung lobes (0.5 g/each lobe) were pooled in 5 ml double-modified Iscove's media (DMIM) (42.5% Iscove's modified Dulbecco's medium, 7.5% glycerol, 1% heat-inactivated fetal bovine serum, 49% Dulbecco's modified eagle medium (DMEM) and 5 μg/ml kanamycin sulfate) and stored at 4°C for further processing for a viral plaque assay. Separate samples from each lobe were snap-frozen in liquid nitrogen and stored at -80°C. The BALF samples were collected from the right caudal lobes in 5 ml DMIM and stored at 4°C. Animal use and experimental procedure were approved by IACUC and IBC at Iowa State University (IACUC# 6-16-8293-O, IBC# 16-I-0028-A/H).

Viral Stock Preparation and Nebulization

The hRSV virus nebulization was performed as previously described [23, 24]. Briefly, human respiratory syncytial virus Memphis 37 strain (hRSV M37) was grown on HEp-2 cell line with Dulbecco's Modified Eagle Medium (DMEM) containing 10% fetal bovine serum (FBS) and 50 μg/ml kanamycin sulfate. The extracted virus was diluted with 20% sucrose then stored at -80°C until further use. A small sample of the stock virus was collected to determine

the amount of virus through viral plaques assay (FFU). In preparation for nebulization, the virus stock was thawed and diluted in culture media to obtain 2.5 x 10^7 FFU/ml. A total of 6 ml was nebulized to each lamb with PARI LC Sprint™ nebulizer to achieve a dose of 3.5 x 10^7 FFU/lamb. Pure culture media was nebulized to the negative control group.

Small Molecule Inhibitor Formulation, Administration and Quantification

Both the fusion protein inhibitor and replication inhibitor were dissolved in 20% acidified hydroxypropryl-β- cyclodextrin (20% HP-β-CD + HCl) at pH 7.4 to 0.5 mg/ml and 0.1875 mg/ml concentrations, respectively. The appropriate dose for each treatment group was administered through gavage catheter then followed by 5 ml of 20% HP-β-CD+HCl, pH 7.4 to wash down any compound residues. The collected plasma, lung and BALF samples were analyzed for treatment compound level by liquid chromatography-tandem mass spectrometry (LC-MS/MS).

Focus Forming Unit (FFU)

Quantification of viral titer was determined by the focus forming unit (FFU) plaque assay described previously [25]. Briefly, both BALFs and lung homogenate samples were clarified by spin column filter centrifugation. The collected filtrates were stored at 4°C and plated within 6 hours after collection. Plating of the samples was performed on previously prepared 12-well cell culture plate containing 70-80% confluency of HEp-2 cells at undiluted and 10^{-1}, 10^{-2}, 10^{-3}, 10^{-4} concentrations. The plates were incubated in 37°C, 5% CO_2 incubation chamber for 48h then inactivated and fixed with 60% acetone/40% methanol solution. Indirect immunofluorescence staining was performed using 1:800 primary polyclonal goat anti-RSV

(EMD Millipore, Billerica, MA) diluted with 3% bovine serum albumin (BSA) in Tris buffer saline with 0.05% Tween (TBST), overnight incubation at 4°C, and 1:800 secondary fluorescence tagged rabbit anti-goat IgG (Alexa Fluor® 488 F(ab')2 fragment of rabbit anti-goat IgG (H+L), Molecular Probes/Life Technologies) in 3% BSA in TBST, incubated for 30 min at room temperature. Fluorescent plaques were counted under inverted fluorescence light microscope and the FFU/ml calculated from the average number of plaques in the duplicated wells.

Real-Time Reverse Transcription Polymerase Chain Reaction (RT-qPCR)

Quantification of hRSV virions in BALF and lung samples and cytokine/chemokine mRNA expression level were assessed by RT-qPCR. In preparation of lung samples, the right cranial, left cranial, left middle and left caudal lung lobes (0.3 g each lobe) were pooled from each animal and homogenized in 12 ml of TRIzol solution (Invitrogen/Life Technologies, Carlsbad, CA, USA). A total amount of 100 ml from each BALF samples were directly placed in TRIzol solution. RNA isolation on the prepared lung and BALF samples in TRIzol was as previously described [25, 26]. The isolated RNA pellets were resuspended in 170 ul nuclease-free water. Additional DNase treatment (TURBO-DNase, Ambion, Austin, TX, USA) was performed in the isolated lung RNA samples. Both DNase treated lung RNA and BALF RNA isolates were diluted at 1:10 in nuclease-free water containing RNaseOUT (Invitrogen/Life Technologies, Carlsbad, CA, USA). The amount of RNA from each sample was quantified using spectrophotometry (Beckmann DU® 640B, Beckmann Coulter Inc., Brea, CA, USA) at OD 260/280 nm values. The samples were diluted to the final concentration of 0.7844 ng/μl.

The primers and probes for RT-qPCR quantification of hRSV and mRNA expression of IFN-λ, IL-13, CCL2 (MCP-1), CCL3 (MIP-1α), CCL5 (RANTES), CXCL10 (IP10), CD274 (PD-L1) and CC10 are listed in Supplementary Table 2. All primers and probes were generated using ABI Primer Express 2.0 software. RT-qPCR was performed using One-Step Fast qRT-PCR Kit master mix (Quanta, Bioscience, Gaithersburg, MD, USA) in a Gene Amp 5700 Sequence Detection System (Applied Biosystmes, Carlsbad, CA, USA). Prior to running the real-time thermocycler, the PCR reagents were calculated and managed using PREXCEL-Q software [27]. Each sample was duplicated and placed in the thermocycler for one round of pre-treatment (3 min at 50°C, then 30 sec at 95°C) followed by 45 cycles of 30 sec, 95°C and 30 sec at 60°C. The virus copy number per milligram was estimated based on the standard curve generated from amplified plasmid constructs. Standard curve for evaluating cytokine/chemokine mRNA level was generated from sample mixture (Stock I). The cycle time (Ct) values obtained from each sample were converted to relative quantity level (rQ) with the following equation: $rQ=10^{[(Cq-b)/m]}$ where *b* and *m* are the *y*-intercept and slope from the standard curve of Stock I [27].

Immunohistochemistry (IHC) Detection of HRSV Antigen

Immunohistochemical staining of hRSV antigen in lamb lung tissue was completed as described previously [25]. Briefly, 5 μm thick, formalin fixed paraffin-embedded lung tissue sections were processed for hRSV antigen localization by indirect immunohistochemical staining. After heat-induced antigen retrieval process (19 mM TRIZMA Base pH 9.0, 1 mM EDTA buffer and 0.05% Tween 20 at 125°C for 20 mins), the slides were blocked from non-specific background binding of antibody with 3% BSA and 20% normal swine serum. The

slides then were incubated for 90 min at room temperature with polyclonal goat anti-RSV antibody (Millipore/Chemicon, Darmstadt, Germany) diluted 1:500 in 10% NSS, 3% BSA in TBST solution and subsequently incubated for 45 min with 1:300 dilution of biotinylated rabbit anti-goat IgG antibody in 10% NSS, 3% BSA in TBST solution. Endogenous peroxidase blocking was performed with 3% H_2O_2 in TBST. Streptavidin-horse radish peroxidase at 1:200 dilution in TBST was incubated on the slides then Nova Red chromogenic substrate was use for detection and counterstained with Shandon's hematoxylin.

Lung HRSV Lesion Evaluation

The macroscopic and microscopic lung lesions were semi-quantitatively scored to evaluate and compare the extent of virus associated lung pathology and completed as described previously [25]. The macroscopic lung score was based on the average percentage of dark-red consolidated areas distributed in each the lung lobe and converted to the scoring scale from 0 to 4 (e.g. 0% = 0, 1-9% = 1, 10-39% = 2, 40-69% = 3, 70-100% = 4). Lung histopathological scores were determined with H&E stained lung tissue sections taken from each right cranial, left cranial, left middle and left caudal lung lobes of each lamb. Criteria for scoring (0 to 4 from lowest to highest pathological changes) include; microscopic lung consolidation, bronchitis, syncytial formation, bronchial and bronchiolar epithelial necrosis, bronchial and bronchiolar epithelial hyperplasia, presence of neutrophilic infiltration, perivascular and peribronchiolar lymphocytic infiltrates (Supplementary Table 1). The degree of hRSV antigen detection with IHC was semi-quantatively scored from a range of 0 to 4 by counting the number of bronchioles and alveoli with positive hRSV antigen signal in 20 fields at 100X (FOV 2.2 mm) per slide each containing sections from right cranial, left cranial, left middle and left

caudal lung lobes from each lamb (e.g. score 1=1-10 positive counts, score 2=11-39 positive counts, score 3=40-99 positive counts and score 4=>100 positive counts).

In Situ Hybridization (RNAscope®)

Viral RNA detection was performed in formalin-fixed paraffin embedded (FFPE) lung tissue by RNA *in situ* hybridization (RNAscope®, ACD Bio) assay [28] with probe sequence targeting the nucleoprotein (N) of hRSV Memphis 37 (Cat No. 439861). Briefly, the FFPE lung tissue blocks were sectioned at 5 μm thickness and deparaffinized with 100% ethanol solution. Endogenous peroxidase activity was blocked with hydrogen peroxide for 10 mins at room temperature. Antigen retrieval consisted of heat treatment by boiling with Target Retrieval Reagent® for 15 mins and enzymatic treatment with Protease Plus® at 40°C for 30 mins. Subsequently, probe hybridization (2h at 40°C) and amplification of the viral RNA target were conducted in HybEZ™ Hybridization System and RNAscope® 2.5 Assay platform. Positive control probe (PPIB) and negative control probe (DapB) were concurrently tested. The amplified viral target was stained with 3,4'-diaminobenzidine (DAB) chromogenic substrate (RNAscope® 2.5 HD Detection Reagent-Brown) and counterstained with hematoxylin.

The percentage of stained cells was determined by a semiquantitative method of scoring and a quantitative method with image analysis software (HALO™). The semi-quantitative method was performed by separate assessment of the number of bronchioles and alveoli containing positive signal and calculated based on a 400 μm^2 lung tissue area. In addition, image analyzer software was used to quantify cell-by cell the viral RNA expression profile and categorize the cells in different bins based on the expression level (Bin 0; <1

copy/cell, Bin 1; 1-3 copies/cell, Bin 2; 4-9 copies/cell, Bin 3; 10-15 copies/cell, Bin 4; (>15 copies/cell). Furthermore, H score of each image was calculated by the sum of the bin number multiplied by the percentage of cells per bin. The percentages of hRSV mRNA expression were calculated with the image analyzer from 20 histological images taken from the stained slides (200X, field number 22).

Statistical Analysis

The quantitative data were evaluated with GraphPad Prism 6 statistical software using a Kruskal-Wallis non-parametric test and Dunn's multiple comparisons test to calculate significant statistical differences ($p<0.05$) between each experimental group. The results from viral titer, viral mRNA, and chemokines/cytokines mRNA expression were statistically analyzed. Due to the low number and high variations on mRNA expression, the positive (n=25) and negative control RSV group (n=21) from previous experiments under similar conditions (e.g. age, dose of infection, duration after viral inoculation) were included to calculate the statistical analysis. Correlation of multiple variables (Spearman r) were performed on the viral FFU titer, quantification of virion by RT-qPCR, IHC score and H score obtained from RNA *in situ* hybridization.

Results

Pharmacokinetic of Fusion Protein Inhibitor and Replication Inhibitor

Both of the trough plasma concentration (C_{trough}) of small molecule inhibitors in all treatment groups maintained a stable increasing trend throughout the treatment period in the Phase I study (Fig 1). Slight difference in C_{trough} levels of fusion inhibitor was detected between the combination treatment (TxL) compared to the fusion inhibitor monotherapy administered

at the same dose (TxF). Likewise, the level of replication inhibitor plasma concentration detected in the combination treatment (TxL) was lower than replication inhibitor monotherapy (TxNF).

The fusion inhibitor compound was above detection level in all lung and ELF samples. The average concentration of fusion inhibitor distribution in TxL, TxH and TxF treatment groups were 949.4 ng/g, 4496 ng/g and 1816 ng/g in the lungs, and 253.1 ng/ml, 1,127 ng/ml and 788.3 ng/ml in ELFs. The average lung replication inhibitor concentration levels were 917.3 ng/g in the TxL, 1,861 ng/g in the TxH and 1,523 ng/g in the TxNF. The replication inhibitor compound in ELFs was below detection level in 3/7 lambs from the TxL and 3/7 lambs from the TxNF. The average concentration levels of the replication compound in the lungs were 111.3 ng/ml in the TxL, 316.8 ng/ml in the TxH and 123.4 ng/ml in the TxNF (Fig 1).

The average lung to plasma ratio of the fusion inhibitor compound concentration in the TxF, TxL and TxH were 16.21, 13.91 and 20.83, respectively. The average epithelial lining fluid (ELF) to plasma ratios of the fusion inhibitor were 5.19 in the TxF, 4.19 in the TxL and 6.27 in the TxH. The replication inhibitor compound was less concentrated in the lung tissues and ELFs compared to the fusion inhibitor. The average lung to plasma ratios of the replication inhibitor in the TxNF, TxL and TxH were 2.54, 1.56 and 1.37, respectively. The replication inhibitor concentrations in the ELFs were low and undetectable in some samples. The average ELF to plasma ratios of replication inhibitor concentrations were 0.20 in the TxNF, 0.18 in the TxL and 0.25 in the TxH.

In the Phase II study, the C_{trough} level of fusion inhibitor and replication inhibitor in the plasma were maintained above the therapeutic levels demonstrated in the Phase I study (Fig

2). Both inhibitor compound plasma C_{trough} levels in the high dose combination administered at day 4 (TxH4) reached near the level of the low dose combination administered at day 3 (TxL3). The average level of the fusion inhibitor compound distribution in the lungs at day 6 in the TxL3 (ELF=19,526.92 ng/ml, lung=25,525 ng/g), TxH4 (ELF=17,187.94 ng/ml, lung=32,505 ng/g) and TxF3 (ELF=7,383.10 ng/ml, lung=24,890 ng/g) were measured. The level of the replication inhibitor compound distribution in the ELFs was low and undetected in two samples (1/5 in TxNF3 and 1/5 TxL3). The average level of replication inhibitor concentrations in the TxL3, TxH4 and TxNF3 were 2,966. 26 ng/ml, 3,057. 25 ng/ml and 1,179.34 ng/ml in the ELFs, and 8,596 ng/g, 13,785 ng/g and 8,651 ng/g in the lungs, respectively (Fig 2).

Viral Titer and Viral RNA detection in BALFs and Lung Tissues

The combination treatment of fusion protein inhibitor and non-fusion protein inhibitor significantly reduced the level of virions detected via FFU assay and RT-qPCR in the lung and BALF samples compared to the non-treatment group. The total level of virion RNA in BALF samples were reduced up to 28 times in the high dose combination treatment (TxH) and reduced by 11 times in the low dose combination treatment (TxL). Higher levels of viable viral reduction were demonstrated with the FFU assay up to 600 times in the high dose treatment group and 67 times with low dose treatment. This extreme reduction of viable virus with the FFU assay may have been influenced by a compound carry-over effect with this technique of virus quantification, although this may be unlikely due to the low dose of compound administered and the dilution steps that would reduce the compound residues below the activity range. The low dose combination administration appeared to reduce the number of virion in

BALF and lung at higher level compared to monotherapy of fusion and replication inhibitor compound. There was a significantly lower level of virions in the high dose combination treatment (TxH) with up to 4-times greater reduction of total virion RNA compared to fusion inhibitor monotherapy (TxF) ($p<0.05$) and 6-times greater reduction compared to non-fusion protein inhibitor monotherapy (TxNF) ($p<0.01$) (Fig 3a-d).

Administration of low dose combination therapy at 3 dpi (TxL3) ($p<0.001$), high dose at 4 dpi (TxH4) ($p<0.01$) and monotherapy of non-fusion inhibitor at 3 dpi (TxNF3) ($p<0.05$) significantly reduced the level of virus detected with BALF and lung samples compared to the non-treated hRSV infected group (RSV). The average level of virions detected in the BALF were reduced 195, 39 and 36 times in the TxL3 ($2.96x10^5$ virions/ml), TxH4 ($8.85x10^5$ virions/ml) and TxNF3 ($1.05x10^6$ virions/ml) treatment, respectively. Compared to monotherapy of fusion inhibitor at 3 dpi (TxF3), the level of virions in BALF were significantly lower in TxL3 ($p<0.0001$), TxH4 ($p<0.05$) and TxNF3 ($p<0.05$) treatment groups. The level of virions in the lung was significantly lower only in the TxL3 compared to TxF3 monotherapy treatment group. The virus titers were below the detection level of FFU assay in all treatment groups, although this may have been influenced by a compound carry-over effect as previously mentioned. No virions or viable virus were detected in both BALF and lung samples of the negative control group (Fig 4a-d).

Clinical Assessments and Lung Pathology

In both phases of the study, the clinical parameters including respiratory rate, heart rate and body temperature of all animals were in the normal range (Fig 5). The body weight gradually increased at a similar rate throughout the study period in all groups with the average

daily gain ranging from 177 to 217 g/day. One lamb in Phase I study (Lamb#3) from the TxH group was weak and bloating from the beginning of the study prior to viral inoculation. Later the animal appeared lethargic and was terminated before the end of the study period (4 dpi). At necropsy Lamb#3 had lesion of pulmonary edema associated with *in utero* fetal distress and failure to thrive. Evidence of hRSV-associated pneumonia was not observed at necropsy.

Macroscopic hRSV-associated lung lesions were diminished at 6 dpi in all treatment groups with lowest lung involvement percentage (lung%) in the high dose combination group (TxH) (0.17±0.61), followed by low dose combination treatment (TxL) (1.27±3.62), fusion inhibitor treatment (TxF) (2.76±5.64) and non-fusion inhibitor treatment group (TxR) (11.39±10.79), respectively (Fig 6). Histological pulmonary lesions of hRSV infected and treated lambs were diminished in a fashion similar to the macroscopic lesions where the overall histological consolidation score (CS) was zero in TxH and appeared with an increasing severity from TxL (0.21/4), TxF (0.25/4) and TxNF (0.71/4), respectively. Features of bronchiolitis, syncytial cells formation, bronchiolar epithelial necrosis and hyperplasia, neutrophilic infiltration and lymphoplasmacytic peribronchiolar and perivascular cuffs were present in the TxF and TxNF treatment groups. Certain histological features were not evident in combination treatment regimens; TxH lacked bronchiolitis, syncytial cell formation, bronchiolar epithelial necrosis and hyperplasia and neutrophilic infiltration, and TxL lacked syncytial cell formation, bronchiolar epithelial necrosis and hyperplasia (Fig 7).

With the delayed administration of antiviral treatment, the hRSV-associated pulmonary lesion appeared the lowest with combination treatment at 3 dpi (TxL3) (lung% = 1.06, CS = 0.05), followed by fusion inhibitor monotherapy at 3 dpi (TxF3) (lung% = 1.11, CS = 0.2), combination treatment at 4 dpi (TxH4) (lung% = 4.66, CS = 0.2) and the highest with

replication inhibitor monotherapy at 3 dpi (TxNF3) (lung% = 10.40, CS = 1.05). Microscopic features of syncytial cell formation and bronchiolar epithelial necrosis were lacking in all treatment regimens with absence of neutrophilic and perivascular lymphoplasmacytic cuffs in TxL3 and absence of bronchiolitis in TxH4 (Fig 9, 10).

Histological Detection of HRSV Antigen and RNA in Pulmonary Tissue

Localization of hRSV viral antigen with IHC and RNA with *in situ* hybridization determined that the virus was within intact and sloughed bronchiolar epithelial cells, and occasionally in scattered type II pneumocytes and pulmonary alveolar macrophages. The level of hRSV antigen detected with IHC in hRSV-infected, non-treatment group (RSV) was 3.08 in the bronchioles and 13.03 in the alveoli and the level of viral RNA was 41.25 in the bronchioles and 187.5 in the alveoli. The average viral RNA positive signal counts in the lung tissues in the RSV group were 73.5/400 μm^2 in the bronchioles and 340.4/400 μm^2 in the alveoli. The immunoreactivity and viral RNA positive signal were lower in all treatment groups compared to the hRSV-infected, non-treated group (RSV). Immunoreactivity of the viral antigen was quantified, and the average values appeared in a decreasing manner from TxNF (bronchioles=2.77, alveoli=7.46), TxF (bronchioles=0.27, alveoli=0), TxL (bronchioles=0.16, alveoli=0.16) and none were detected in high combination dosage, TxH. A similar trend was identified when virion RNA was detected with RNA *in situ* hybridization assessed by positive signal counts of the bronchioles and alveoli. The average positive viral RNA signal counts in the bronchioles per 400 μm^2 lung tissue area from TxNF, TxF, TxL and TxH treatment groups were 38.09, 14.14, 11.10 and 6.52, respectively. The positive signal

counts in the alveoli per 400 μm^2 lung tissue area from TxNF, TxF, TxL and TxH treatment groups were 216.57, 42.82, 27.90 and 29.95, respectively (Fig 8).

In the Phase II treatment time window study, the average hRSV immunoreactivity had highest detection in TxNF3 (bronchioles=2.46, alveoli=3.41), followed by TxH4 (bronchioles=0.60, alveoli=1.90), TxF3 (bronchioles=0.38, alveoli=0.68) and was not detected in TxL3 (Fig 11a-d). RNA *in situ* hybridization detected viral RNA in all treatment groups. The average positive signal viral RNA cell counts in the bronchioles and alveoli per 400 μm^2 lung tissue area corresponded with the IHC antigen detection, i.e. highest in TxNF3 (bronchioles=25.2, alveoli=76.1), followed by TxH4 (bronchioles=13.4, alveoli=45.9), TxF3 (bronchioles=10.5, alveoli=124.7) and TxL3 (bronchioles=16.0, alveoli=63.3), respectively. (Fig 11e-h). All samples from the negative control group lacked evidence of viral infection with IHC and RNA *in situ* hybridization.

The H score in the non-treatment hRSV-infected group was 12.09±3.257 with all treatment regimens having significantly lower level of H score (Fig 8, 11). The H score levels in the Phase I study were low in the combination treatments (TxH=0.25±0.27 and TxL=0.18±0.10) and fusion protein monotherapy (TxF=0.24±0.41). Slightly higher H scores were detected in replication inhibitor monotherapy (TxNF=2.07±0.98). The H score level was also evaluated for the Phase II treatment time window study with the lowest average score detected in low dose combination, 3 dpi treatment group (TxL3) (0.489±0.4199), followed by TxH4 (0.698±0.5330), TxF3 (1.186±1.799) and highest in TxNF3 (3.139±3.908). There were significant correlations ($p<0.0001$) of H score with viral levels detected by lung RT-qPCR (r=0.687), IHC bronchiole score (r=0.696), IHC alveolar score (r=0.698) and semi-quantitative scoring of RNA *in situ* hybridization in bronchioles (r=0.819) and alveoli (r=0.771).

Cytokine and CC10 mRNA Expression

Significant increase of mRNA levels of CXCL10 (IP10), CCL2 (MCP-1), CCL3 (MIP-1α), CD274 (PD-L1) and IFN-λ were present in M37 hRSV infected lambs (RSV) compared to non-infected group. Monotherapeutic administration of non-fusion inhibitor (TxNF) had significantly increased level of CCL3 (MIP-1α) and CD274 (PD-L1). No significant differences in mRNA expression of lung cytokines and chemokines were observed between treatment groups in the Phase II treatment time window study. There were no significant differences in RANTES, IL-13 and CC10 expression in the lung (Fig 12).

Discussion

The antiviral mechanisms of hRSV therapeutic compounds can be classified into two distinct groups: 1) compounds that target viral entry and 2) compounds that target non-entry mechanisms of hRSV [29, 30]. HRSV is part of the family Pneumoviridae (formerly subfamily of Paramyxoviridae) [31] which have viral envelopes composed of three glycoproteins: fusion (F) protein and attachment (G) protein that function in viral attachment and entry, and small hydrophobic (SH) protein that serves as an ion channel. Interestingly, previous testing has shown that fusion protein is indispensable for viral entry into the host cells while deletion of G protein produced a replication-competent viral mutant [32]. A major group of antiviral compounds, fusion protein inhibitors, have been developed to block viral infection. The mechanism of inhibition by these small molecule fusion protein inhibitors is through high affinity binding at the trimeric ectodomain pocket of prefusion F protein and restricting movement into the post-fusion conformation resulting in the blockage of fusion of the viral envelope to the host cell membrane [18, 19]. The capability of viral escape mutation from these fusion inhibitors has been identified in laboratory setting [33]. Furthermore, the most effective

time to administer this group of compounds is when given as a prophylactic treatment or within the first 24 hours after infection, since the mechanism of antiviral activity involves blocking the early steps of viral entry and fusion [19] although the results from this lamb study demonstrated pronounce reduction of hRSV-associated lung lesions and 5-fold reduction of virus in BALF samples when administered at 3 dpi.

Once the virus enters the cell, the non-entry antiviral hRSV replication inhibitors are prime therapeutic candidates for late-onset treatment of viral infection. Replication inhibitors target various specific machinery required for viral replication including nucleoside inhibitors [34] and nucleoprotein inhibitors [35, 36]. The hRSV replication inhibitor tested with the HuAEC model was found to be effective when administered at 72 hours post-infection which is a prolonged time window for treatment compared to the fusion inhibitor [20]. A non-fusion inhibitor anti-hRSV compound, JNJ-64166037, has also been tested in lamb model of hRSV and had pronounced antiviral activity with daily oral administration starting at 1h post infection [37]. Treatment with a fusion inhibitor that blocks the early phase of viral entry in combination with a replication inhibitor that prevents further viral replication would be beneficial in enhancing the reduction of viral load and useful in clinical settings where the infection timeline is imprecise. Administration of a combination of antiviral drugs with different modes of action has been shown to optimize following infection with influenza virus [38], hepatitis B virus [39], hepatitis C virus [40] and human immunodeficiency virus [41]. Reports describe the benefits of combination delivery of an immunotherapeutic compound and an antiviral nucleoside inhibitor for patients at high risk for hRSV infection [42, 43]. To the extent of our knowledge, this is the first preclinical *in vivo* experiment of combination small molecule antiviral therapy against hRSV infection.

In this lamb model study, lack of alterations in the plasma concentration of fusion and replication inhibitor compounds were observed in combination treatment compared to monotherapy treatment administered at the equivalent dose. There were appropriate distributions of both fusion and replication inhibitor compounds in the lung and epithelial lining fluid with minimal differences in distribution between combination and monotherapy treatment. This indicates that there is less likelihood of interference in absorption, distribution and biometabolism process of this combination therapy. Outside of the work in this study and previous *in vitro* assays, little is known about the dynamics of the combination of these two compounds and therefore, future investigations and additional work are needed in order to advance this treatment regimen toward clinical trials and approval. Such studies could include: the compatibility of the formulations, drug-drug interactions and binding to endogenous protein and other molecules that may alter the pharmacokinetics, toxicity level, and biometabolism rate.

Our findings demonstrate that the administration of a combination of a fusion inhibitor and replication inhibitor for hRSV reduced the viral load in the BALF and lung tissue samples and decreased the degree of hRSV-related lung lesions to a greater extent compared to fusion and replication inhibitor monotherapy. This result indicates the synergistic potential of combining these treatment compounds. The amount of virus and host inflammatory responses are the main factors contributing to the pathogenesis of hRSV infection and are associated with severity of the infection in human infants [44-47]. The quantification of hRSV viral level from BALF samples by RT-qPCR represents the entire lobe/lung airways and lacks drug carrying-over effect that may be apparent with cell culture based viral titration. Interestingly, there was a pronounced decrease in the viral load and reduced pulmonary lesions with combination

therapy when the first dosage was administered at 3 and 4 dpi compared with fusion inhibitor monotherapy delivered at 3 dpi. In addition, monotherapy of replication inhibitor given at 3 dpi significantly reduced the viral load, though the pulmonary lesions were decreased to a lesser extent compared to other therapeutic regimens. This indicates that there is an extended treatment time window of up to 4 days post-infection with anti-hRSV replication inhibitors and even more pronounced reduction of viral load and lesions when administering in combination with hRSV-fusion inhibitor. Thus, fusion and replication inhibitor combination therapy is a promising candidate for future treatment of hRSV infection.

An innate immune response in the lung is essential for defense against hRSV infection in infants since their adaptive immune response is not fully developed. The first-line of defense against hRSV infection is the mucociliary apparatus that serves a physical barrier and antimicrobial products that coat the airways such as surfactant proteins (SP-A, SP-D), uteroglobin (CC10), DUOX/LPO oxidative system, defensins and cathelicidins [47]. There is also activation of pattern recognition receptors that upregulate the cellular immune components and upregulate the production of cytokines. The cytokine components of hRSV infection are associated with regulating the balance of host immune response which is important in the disease outcome of hRSV infection [48]. A set of cytokines were analyzed in hRSV-infected lamb lungs at day 6 post-infection and we found significantly increased mRNA expression of CXCL10 (IP-10), CCL2 (MCP-1), CCL3 (MIP-1α), CD274 (PD-L1) and IFN-λ. The chemokines CXCL10 (IP-10), CCL2 (MCP-1), CCL3 (MIP-1α), CCL5 (RANTES) are responsible for chemoattraction of cellular inflammatory components in the lung which have shown increased levels in infants with severe hRSV bronchiolitis [49]. Overall, the chemokine profile of lambs infected with hRSV strain M37 in this study was consistent with previous

reported data of inflammatory response in neonatal lambs infected with hRSV strain A2 [50, 51]. Interestingly, CCL5 (RANTES) in hRSV-infected lambs did not appear to significantly decrease at 6 dpi. The explanation for a lack of RANTES (CCL5) expression could be due to a host defect in production or direct viral blockage, although this still remains inconclusive. The expression of T cell regulatory ligand, PD-L1 (CD274) was elevated in hRSV-infected neonatal lamb model at 6 dpi which was also consistent with previous reported data [50]. This elevation of PD-L1 (CD274) level may play a role in the inactivation of cytotoxic T cell response against hRSV infection which was observed in other model studies [52, 53].

The main method of immunomodulation mediated by hRSV is through the hRSV nonstructural protein (NS1/2) which reduces the signaling of type I interferon (IFNα/β) production [54]. Low levels or lack of IFNα/β was detected in nasal or bronchoalveolar lavages from infants infected with hRSV [55, 56]. Similar reports were observed in hRSV-infected neonatal lamb model [50]. Nevertheless, type III interferon (IFN-λ) had detectable increase with hRSV infection observed in well-differentiated pediatric primary bronchial epithelial cell cultures (WD-PBECs) [57], suggesting its role in antiviral response. A similar pattern of predominant type III interferon response was reported in other respiratory paramyxoviruses including measles and mumps in humans [58]. These results indicate the potential of hRSV-infected lamb model for studying viral interferon responses, effect of antiviral treatment on interferon response [59] and future antiviral interferon therapy.

Administration of combination drug therapy against hRSV has a promising potential candidate for the treatment option of both early and late detection of hRSV infection. This combined treatment had potent antiviral effects in the hRSV-infected lamb model and demonstrated an extended time window for treatment up to 4 days after infection. The

combination treatment regimen also offers a potential barrier to the evolution of escape mutants compared to monotherapies. Furthermore, the neonatal lamb model of hRSV infection appears useful for testing antiviral therapeutic compounds.

Acknowledgments

We would like to thank Janssen Infectious Diseases & Vaccines, Janssen Pharmaceutica NV, Beerse, Belgium for the funding in this study. We also would like to thank the Iowa State University, Veterinary Pathology Histology Laboratory technicians, Toni Christofferson, Deborah Moore, Diane Gerjets, and Virginia Montgomery, and Laboratory Animal Resources and Livestock Infectious Disease Isolation Facility staff, Diane McDonald, Kathleen Mullin, and Dale Hinderaker for their help and support.

Declaration of Conflicting Interests

This study was funded by Janssen Infectious Diseases & Vaccines, Janssen Pharmaceutica NV, Beerse, Belgium.

References

1. Shi T, McAllister DA, O'Brien KL, Simoes EAF, Madhi SA, Gessner BD, et al. Global, regional, and national disease burden estimates of acute lower respiratory infections due to respiratory syncytial virus in young children in 2015: a systematic review and modelling study. Lancet. 2017;390(10098):946-58. Epub 2017/07/07. doi: 10.1016/S0140-6736(17)30938-8. PubMed PMID: 28689664; PubMed Central PMCID: PMCPMC5592248.

2. Jain S, Finelli L, Team CES. Community-acquired pneumonia among U.S. children. N Engl J Med. 2015;372(22):2167-8. doi: 10.1056/NEJMc1504028. PubMed PMID: 26017833.

3. Falsey AR, Hennessey PA, Formica MA, Cox C, Walsh EE. Respiratory syncytial virus infection in elderly and high-risk adults. N Engl J Med. 2005;352(17):1749-59. doi: 10.1056/NEJMoa043951. PubMed PMID: 15858184.

4. Falsey AR, McElhaney JE, Beran J, van Essen GA, Duval X, Esen M, et al. Respiratory syncytial virus and other respiratory viral infections in older adults with moderate to severe influenza-like illness. J Infect Dis. 2014;209(12):1873-81. Epub 2014/01/29. doi: 10.1093/infdis/jit839. PubMed PMID: 24482398; PubMed Central PMCID: PMCPMC4038137.

5. Thompson WW, Shay DK, Weintraub E, Brammer L, Cox N, Anderson LJ, et al. Mortality associated with influenza and respiratory syncytial virus in the United States. JAMA. 2003;289(2):179-86. PubMed PMID: 12517228.

6. Johnson S, Oliver C, Prince GA, Hemming VG, Pfarr DS, Wang SC, et al. Development of a humanized monoclonal antibody (MEDI-493) with potent in vitro and in vivo activity against respiratory syncytial virus. J Infect Dis. 1997;176(5):1215-24. PubMed PMID: 9359721.

7. Homaira N, Rawlinson W, Snelling TL, Jaffe A. Effectiveness of Palivizumab in Preventing RSV Hospitalization in High Risk Children: A Real-World Perspective. Int J Pediatr. 2014;2014:571609. Epub 2014/12/04. doi: 10.1155/2014/571609. PubMed PMID: 25548575; PubMed Central PMCID: PMCPMC4274815.

8. Santos RP, Chao J, Nepo AG, Butt S, Stellrecht KA, Pearce JM, et al. The use of intravenous palivizumab for treatment of persistent RSV infection in children with leukemia. Pediatrics. 2012;130(6):e1695-9. Epub 2012/11/12. doi: 10.1542/peds.2011-1768. PubMed PMID: 23147965.

9. Marcelin JR, Wilson JW, Razonable RR, Services MCHOaTID. Oral ribavirin therapy for respiratory syncytial virus infections in moderately to severely immunocompromised patients. Transpl Infect Dis. 2014;16(2):242-50. Epub 2014/03/13. doi: 10.1111/tid.12194. PubMed PMID: 24621016.

10. Ventre K, Randolph AG. Ribavirin for respiratory syncytial virus infection of the lower respiratory tract in infants and young children. Cochrane Database Syst Rev. 2007;(1):CD000181. Epub 2007/01/24. doi: 10.1002/14651858.CD000181.pub3. PubMed PMID: 17253446.

11. Nouvini R, Kiner B, Yarovikova M, Strachan P. Ribavirin Treatment for Respiratory Syncytial Virus in Immunocompromised Hosts. Blood. 2016;128(22):2210-.

12. Krilov LR. Safety issues related to the administration of ribavirin. Pediatr Infect Dis J. 2002;21(5):479-81. PubMed PMID: 12150196.

13. Aliprantis A, Wolford D, Caro L, Maas B, Ma H, Vora K, et al. 1971. A Randomized, Double-Blind, Placebo-Controlled Trial to Assess the Safety and Tolerability of a Respiratory Syncytial Virus (RSV) Neutralizing Monoclonal Antibody (MK-1654) in Healthy Subjects. *Open Forum Infectious Diseases*. 2018;5(Suppl 1):5572. doi: 10.1093/ofid/ofy210.1627.

14. DeVincenzo JT, D., Oluwayi O, Mori J, Thomas E, Mathews N, Harland R, et al. Safety and Efficacy of Oral RV521 in a Human Respiratory Syncytial Virus (RSV) Phase 2a Challenge Study. American Thoracic Society 2018 International Conference; San Diego, California: American Journal of Respiratory and Critical Care Medicine; 2018.

15. Israel S, Rusch S, DeVincenzo J, Boyers A, Fok-Seang J, Huntjens D, et al. Effect of Oral JNJ-53718678 (JNJ-678) on Disease Severity in Healthy Adult Volunteers Experimentally Inoculated With Live Respiratory Syncytial Virus (RSV): A Placebo-Controlled Challenge Study. Open Forum Infectious Diseases. 2016;3(suppl_1).

16. Rhodin M, editor EDP-938, a Novel Non-Fusion Replication Inhibitor of RSV, Displays a High Barrier to Resistance In Vitro. 11th International Respiratory Syncytial Virus Symposium; 2018 Oct 31- Nov 4, 2018; Asheville, NC, USA.

17. Coates M, Brookes D, Kim YI, Allen H, Fordyce EAF, Meals EA, et al. Preclinical Characterization of PC786, an Inhaled Small-Molecule Respiratory Syncytial Virus L Protein Polymerase Inhibitor. Antimicrob Agents Chemother. 2017;61(9). Epub 2017/08/24. doi: 10.1128/AAC.00737-17. PubMed PMID: 28652242; PubMed Central PMCID: PMCPMC5571287.

18. Battles MB, Langedijk JP, Furmanova-Hollenstein P, Chaiwatpongsakorn S, Costello HM, Kwanten L, et al. Molecular mechanism of respiratory syncytial virus fusion inhibitors. Nat Chem Biol. 2016;12(2):87-93. Epub 2015/12/07. doi: 10.1038/nchembio.1982. PubMed PMID: 26641933; PubMed Central PMCID: PMCPMC4731865.

19. Roymans D, Alnajjar SS, Battles MB, Sitthicharoenchai P, Furmanova-Hollenstein P, Rigaux P, et al. Therapeutic efficacy of a respiratory syncytial virus fusion inhibitor. Nat Commun. 2017;8(1):167. Epub 2017/08/01. doi: 10.1038/s41467-017-00170-x. PubMed PMID: 28761099.

20. Mirabelli C, Jaspers M, Boon M, Jorissen M, Koukni M, Bardiot D, et al. Differential antiviral activities of respiratory syncytial virus (RSV) inhibitors in human airway epithelium. J Antimicrob Chemother. 2018. Epub 2018/03/27. doi: 10.1093/jac/dky089. PubMed PMID: 29596680; PubMed Central PMCID: PMCPMC6005027.

21. Derscheid RJ, Ackermann MR. Perinatal lamb model of respiratory syncytial virus (RSV) infection. Viruses. 2012;4(10):2359-78. Epub 2012/10/23. doi: 10.3390/v4102359. PubMed PMID: 23202468; PubMed Central PMCID: PMCPMC3497056.

22. Ackermann MR. Lamb model of respiratory syncytial virus-associated lung disease: insights to pathogenesis and novel treatments. ILAR J. 2014;55(1):4-15. doi: 10.1093/ilar/ilu003. PubMed PMID: 24936027; PubMed Central PMCID: PMCPMC4158344.

23. Grosz DD, van Geelen A, Gallup JM, Hostetter SJ, Derscheid RJ, Ackermann MR. Sucrose stabilization of Respiratory Syncytial Virus (RSV) during nebulization and experimental infection. BMC Res Notes. 2014;7:158. Epub 2014/03/18. doi: 10.1186/1756-0500-7-158. PubMed PMID: 24642084; PubMed Central PMCID: PMCPMC3995326.

24. Derscheid RJ, van Geelen A, McGill JL, Gallup JM, Cihlar T, Sacco RE, et al. Human respiratory syncytial virus Memphis 37 grown in HEp-2 cells causes more severe disease in lambs than virus grown in Vero cells. Viruses. 2013;5(11):2881-97. Epub 2013/11/22. doi: 10.3390/v5112881. PubMed PMID: 24284879; PubMed Central PMCID: PMCPMC3856420.

25. Larios Mora A, Detalle L, Van Geelen A, Davis MS, Stohr T, Gallup JM, et al. Kinetics of Respiratory Syncytial Virus (RSV) Memphis Strain 37 (M37) Infection in the Respiratory Tract of Newborn Lambs as an RSV Infection Model for Human Infants. PLoS One. 2015;10(12):e0143580. Epub 2015/12/07. doi: 10.1371/journal.pone.0143580. PubMed PMID: 26641081; PubMed Central PMCID: PMCPMC4671688.

26. Derscheid RJ, van Geelen A, Gallup JM, Kienzle T, Shelly DA, Cihlar T, et al. Human respiratory syncytial virus memphis 37 causes acute respiratory disease in perinatal lamb lung. Biores Open Access. 2014;3(2):60-9. doi: 10.1089/biores.2013.0044. PubMed PMID: 24804166; PubMed Central PMCID: PMCPMC3994985.

27. Gallup JM, Ackermann MR. The 'PREXCEL-Q Method' for qPCR. Int J Biomed Sci. 2008;4(4):273-93. PubMed PMID: 19759920; PubMed Central PMCID: PMC2744046.

28. Wang F, Flanagan J, Su N, Wang LC, Bui S, Nielson A, et al. RNAscope: a novel in situ RNA analysis platform for formalin-fixed, paraffin-embedded tissues. J Mol Diagn. 2012;14(1):22-9. doi: 10.1016/j.jmoldx.2011.08.002. PubMed PMID: 22166544; PubMed Central PMCID: PMCPMC3338343.

29. Jorquera PA, Tripp RA. Respiratory syncytial virus: prospects for new and emerging therapeutics. Expert Rev Respir Med. 2017;11(8):609-15. Epub 2017/06/14. doi: 10.1080/17476348.2017.1338567. PubMed PMID: 28574729.

30. Olszewska W, Openshaw P. Emerging drugs for respiratory syncytial virus infection. Expert Opin Emerg Drugs. 2009;14(2):207-17. doi: 10.1517/14728210902946399. PubMed PMID: 19453286; PubMed Central PMCID: PMCPMC2705842.

31. Rima B, Collins P, Easton A, Fouchier R, Kurath G, Lamb RA, et al. ICTV Virus Taxonomy Profile: Pneumoviridae. J Gen Virol. 2017;98(12):2912-3. Epub 2017/10/31. doi: 10.1099/jgv.0.000959. PubMed PMID: 29087278; PubMed Central PMCID: PMCPMC5775899.

32. Karron RA, Buonagurio DA, Georgiu AF, Whitehead SS, Adamus JE, Clements-Mann ML, et al. Respiratory syncytial virus (RSV) SH and G proteins are not essential for viral replication in vitro: clinical evaluation and molecular characterization of a cold-passaged, attenuated RSV subgroup B mutant. Proc Natl Acad Sci U S A. 1997;94(25):13961-6. PubMed PMID: 9391135; PubMed Central PMCID: PMCPMC28415.

33. Yan D, Lee S, Thakkar VD, Luo M, Moore ML, Plemper RK. Cross-resistance mechanism of respiratory syncytial virus against structurally diverse entry inhibitors. Proc Natl Acad Sci U S A. 2014;111(33):E3441-9. Epub 2014/08/04. doi: 10.1073/pnas.1405198111. PubMed PMID: 25092342; PubMed Central PMCID: PMCPMC4143008.

34. Wang G, Deval J, Hong J, Dyatkina N, Prhavc M, Taylor J, et al. Discovery of 4'-chloromethyl-2'-deoxy-3',5'-di-O-isobutyryl-2'-fluorocytidine (ALS-8176), a first-in-class RSV polymerase inhibitor for treatment of human respiratory syncytial virus infection. J Med Chem. 2015;58(4):1862-78. Epub 2015/02/10. doi: 10.1021/jm5017279. PubMed PMID: 25667954.

35. Challa S, Scott AD, Yuzhakov O, Zhou Y, Tiong-Yip CL, Gao N, et al. Mechanism of action for respiratory syncytial virus inhibitor RSV604. Antimicrob Agents Chemother. 2015;59(2):1080-7. Epub 2014/12/01. doi: 10.1128/AAC.04119-14. PubMed PMID: 25451060; PubMed Central PMCID: PMCPMC4335855.

36. Gottlieb J, Zamora MR, Hodges T, Musk AW, Sommerwerk U, Dilling D, et al. ALN-RSV01 for prevention of bronchiolitis obliterans syndrome after respiratory syncytial virus infection in lung transplant recipients. J Heart Lung Transplant. 2016;35(2):213-21. Epub 2015/09/03. doi: 10.1016/j.healun.2015.08.012. PubMed PMID: 26452996.

37. Sitthicharoenchai P, Gallup J, Riquax P, Roymans D, Lançois D, Larios-Mora A, et al., editors. Efficacy of the non-fusion human respiratory syncytial virus (hRSV) replication inhibitor JNJ-64166037 in hRSV

infected lamb model. 11th International Respiratory Syncytial Virus Symposium; 2018 Oct 21 - Nov 4, 2018; Asheville, NC, USA.

38. Dunning J, Baillie JK, Cao B, Hayden FG, (ISARIC) ISARaEIC. Antiviral combinations for severe influenza. Lancet Infect Dis. 2014;14(12):1259-70. Epub 2014/09/08. doi: 10.1016/S1473-3099(14)70821-7. PubMed PMID: 25213733.

39. Paul N, Han SH. Combination Therapy for Chronic Hepatitis B: Current Indications. Curr Hepat Rep. 2011;10(2):98-105. Epub 2011/02/19. doi: 10.1007/s11901-011-0095-1. PubMed PMID: 21654909; PubMed Central PMCID: PMCPMC3085106.

40. Poordad F, Lawitz E, Kowdley KV, Cohen DE, Podsadecki T, Siggelkow S, et al. Exploratory study of oral combination antiviral therapy for hepatitis C. N Engl J Med. 2013;368(1):45-53. doi: 10.1056/NEJMoa1208809. PubMed PMID: 23281975.

41. Maenza J, Flexner C. Combination antiretroviral therapy for HIV infection. Am Fam Physician. 1998;57(11):2789-98. PubMed PMID: 9636341.

42. Chávez-Bueno S, Mejías A, Merryman RA, Ahmad N, Jafri HS, Ramilo O. Intravenous palivizumab and ribavirin combination for respiratory syncytial virus disease in high-risk pediatric patients. Pediatr Infect Dis J. 2007;26(12):1089-93. doi: 10.1097/INF.0b013e3181343b7e. PubMed PMID: 18043443.

43. Liu V, Dhillon GS, Weill D. A multi-drug regimen for respiratory syncytial virus and parainfluenza virus infections in adult lung and heart-lung transplant recipients. Transpl Infect Dis. 2010;12(1):38-44. Epub 2009/09/15. doi: 10.1111/j.1399-3062.2009.00453.x. PubMed PMID: 19761558.

44. El Saleeby CM, Bush AJ, Harrison LM, Aitken JA, Devincenzo JP. Respiratory syncytial virus load, viral dynamics, and disease severity in previously healthy naturally infected children. J Infect Dis. 2011;204(7):996-1002. doi: 10.1093/infdis/jir494. PubMed PMID: 21881113; PubMed Central PMCID: PMCPMC3203391.

45. El Saleeby CM, Devincenzo JP. Respiratory syncytial virus load and disease severity in the community. J Med Virol. 2011;83(5):904-5. doi: 10.1002/jmv.22039. PubMed PMID: 21412798.

46. DeVincenzo JP, El Saleeby CM, Bush AJ. Respiratory syncytial virus load predicts disease severity in previously healthy infants. J Infect Dis. 2005;191(11):1861-8. Epub 2005/04/21. doi: 10.1086/430008. PubMed PMID: 15871119.

47. Openshaw PJM, Chiu C, Culley FJ, Johansson C. Protective and Harmful Immunity to RSV Infection. Annu Rev Immunol. 2017;35:501-32. Epub 2017/02/06. doi: 10.1146/annurev-immunol-051116-052206. PubMed PMID: 28226227.

48. Derscheid RJ, Ackermann MR. The innate immune system of the perinatal lung and responses to respiratory syncytial virus infection. Vet Pathol. 2013;50(5):827-41. Epub 2013/03/25. doi: 10.1177/0300985813480216. PubMed PMID: 23528938.

49. McNamara PS, Flanagan BF, Hart CA, Smyth RL. Production of chemokines in the lungs of infants with severe respiratory syncytial virus bronchiolitis. J Infect Dis. 2005;191(8):1225-32. Epub 2005/03/14. doi: 10.1086/428855. PubMed PMID: 15776367.

50. Sow FB, Gallup JM, Olivier A, Krishnan S, Patera AC, Suzich J, et al. Respiratory syncytial virus is associated with an inflammatory response in lungs and architectural remodeling of lung-draining lymph nodes of newborn lambs. Am J Physiol Lung Cell Mol Physiol. 2011;300(1):L12-24. Epub 2010/10/08. doi: 10.1152/ajplung.00169.2010. PubMed PMID: 20935230; PubMed Central PMCID: PMCPMC3023288.

51. Sow FB, Gallup JM, Derscheid R, Krishnan S, Ackermann MR. Ontogeny of the immune response in the ovine lung. Immunol Invest. 2012;41(3):304-16. Epub 2011/11/28. doi: 10.3109/08820139.2011.631657. PubMed PMID: 22122502; PubMed Central PMCID: PMCPMC3812944.

52. Telcian AG, Laza-Stanca V, Edwards MR, Harker JA, Wang H, Bartlett NW, et al. RSV-induced bronchial epithelial cell PD-L1 expression inhibits CD8+ T cell nonspecific antiviral activity. J Infect Dis. 2011;203(1):85-94. doi: 10.1093/infdis/jiq020. PubMed PMID: 21148500; PubMed Central PMCID: PMCPMC3086441.

53. Yao S, Jiang L, Moser EK, Jewett LB, Wright J, Du J, et al. Control of pathogenic effector T-cell activities in situ by PD-L1 expression on respiratory inflammatory dendritic cells during respiratory syncytial virus infection. Mucosal Immunol. 2015;8(4):746-59. Epub 2014/12/03. doi: 10.1038/mi.2014.106. PubMed PMID: 25465101; PubMed Central PMCID: PMCPMC4632244.

54. Lo MS, Brazas RM, Holtzman MJ. Respiratory syncytial virus nonstructural proteins NS1 and NS2 mediate inhibition of Stat2 expression and alpha/beta interferon responsiveness. J Virol. 2005;79(14):9315-9. doi: 10.1128/JVI.79.14.9315-9319.2005. PubMed PMID: 15994826; PubMed Central PMCID: PMCPMC1168759.

55. Hall CB, Douglas RG, Simons RL, Geiman JM. Interferon production in children with respiratory syncytial, influenza, and parainfluenza virus infections. J Pediatr. 1978;93(1):28-32. PubMed PMID: 206677.

56. Scagnolari C, Midulla F, Pierangeli A, Moretti C, Bonci E, Berardi R, et al. Gene expression of nucleic acid-sensing pattern recognition receptors in children hospitalized for respiratory syncytial virus-associated acute bronchiolitis. Clin Vaccine Immunol. 2009;16(6):816-23. Epub 2009/04/22. doi: 10.1128/CVI.00445-08. PubMed PMID: 19386802; PubMed Central PMCID: PMCPMC2691037.

57. Villenave R, Broadbent L, Douglas I, Lyons JD, Coyle PV, Teng MN, et al. Induction and Antagonism of Antiviral Responses in Respiratory Syncytial Virus-Infected Pediatric Airway Epithelium. J Virol. 2015;89(24):12309-18. Epub 2015/09/30. doi: 10.1128/JVI.02119-15. PubMed PMID: 26423940; PubMed Central PMCID: PMCPMC4665230.

58. Okabayashi T, Kojima T, Masaki T, Yokota S, Imaizumi T, Tsutsumi H, et al. Type-III interferon, not type-I, is the predominant interferon induced by respiratory viruses in nasal epithelial cells. Virus Res. 2011;160(1-2):360-6. Epub 2011/07/26. doi: 10.1016/j.virusres.2011.07.011. PubMed PMID: 21816185.

59. McCutcheon KM, Jordan R, Mawhorter ME, Noton SL, Powers JG, Fearns R, et al. The Interferon Type I/III Response to Respiratory Syncytial Virus Infection in Airway Epithelial Cells Can Be Attenuated or Amplified by Antiviral Treatment. J Virol. 2016;90(4):1705-17. Epub 2015/11/25. doi: 10.1128/JVI.02417-15. PubMed PMID: 26608311; PubMed Central PMCID: PMCPMC4733981.

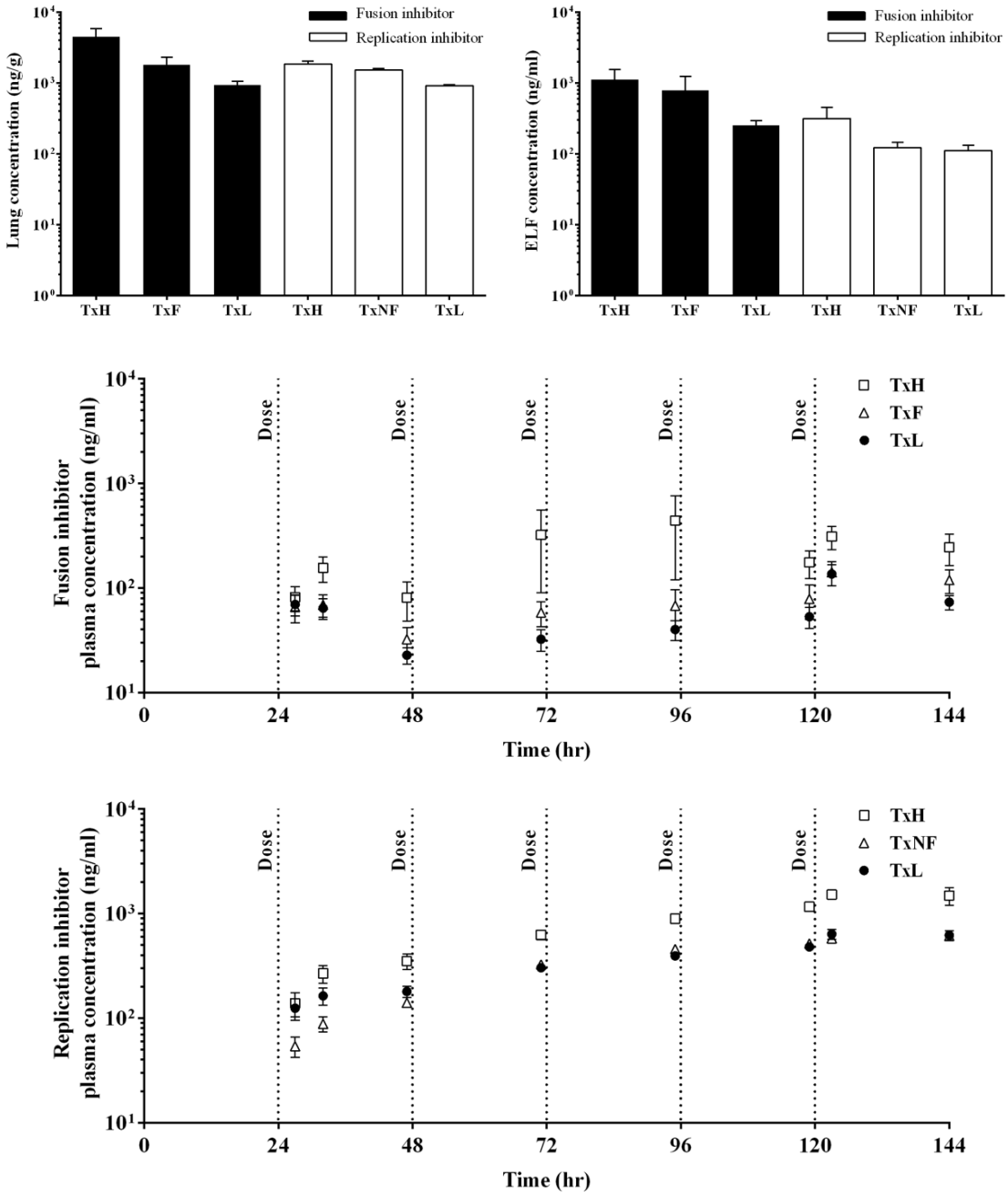

Figure 1: Pharmacokinetics of fusion and replication inhibitors in Phase I combination efficacy study

The small molecule inhibitor compound levels were measured in the lung (top left) and epithelial lining fluid (ELF) (top right) at day 6 post-infection. The fusion (middle) and replication (bottom) inhibitor concentrations in the plasma of treatment groups were evaluated at different time points. The time of treatment administration is indicated by the dotted lines.

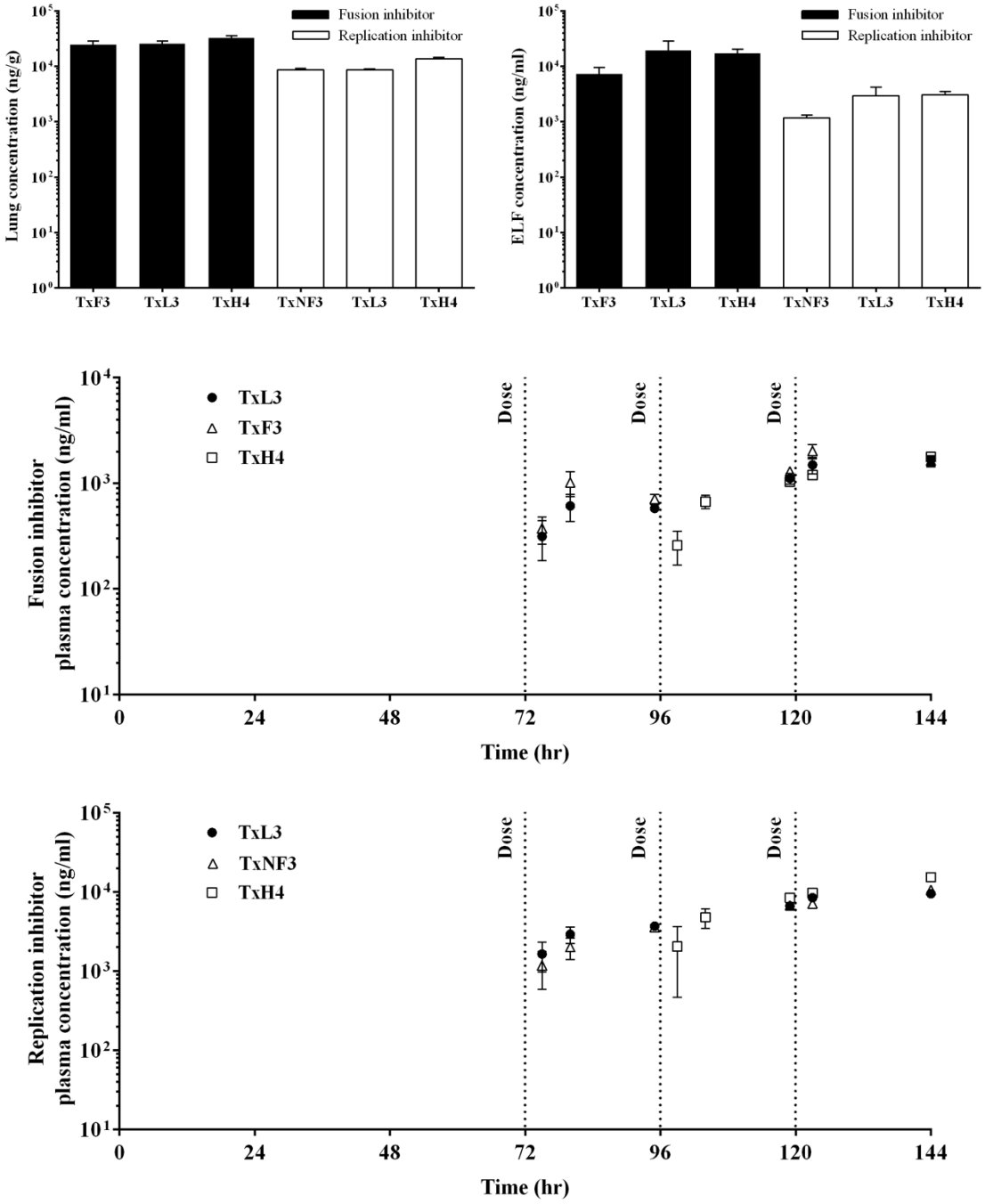

Figure 2: Pharmacokinetics of fusion and replication inhibitors in Phase II treatment time window study

The small molecule inhibitor compound levels were measured in the lung (top left) and epithelial lining fluid (ELF) (top right) at day 6 post-infection. The fusion (middle) and replication (bottom) inhibitor concentrations in the plasma of treatment groups were evaluated at different time points. The time of treatment administration is indicated by the dotted lines.

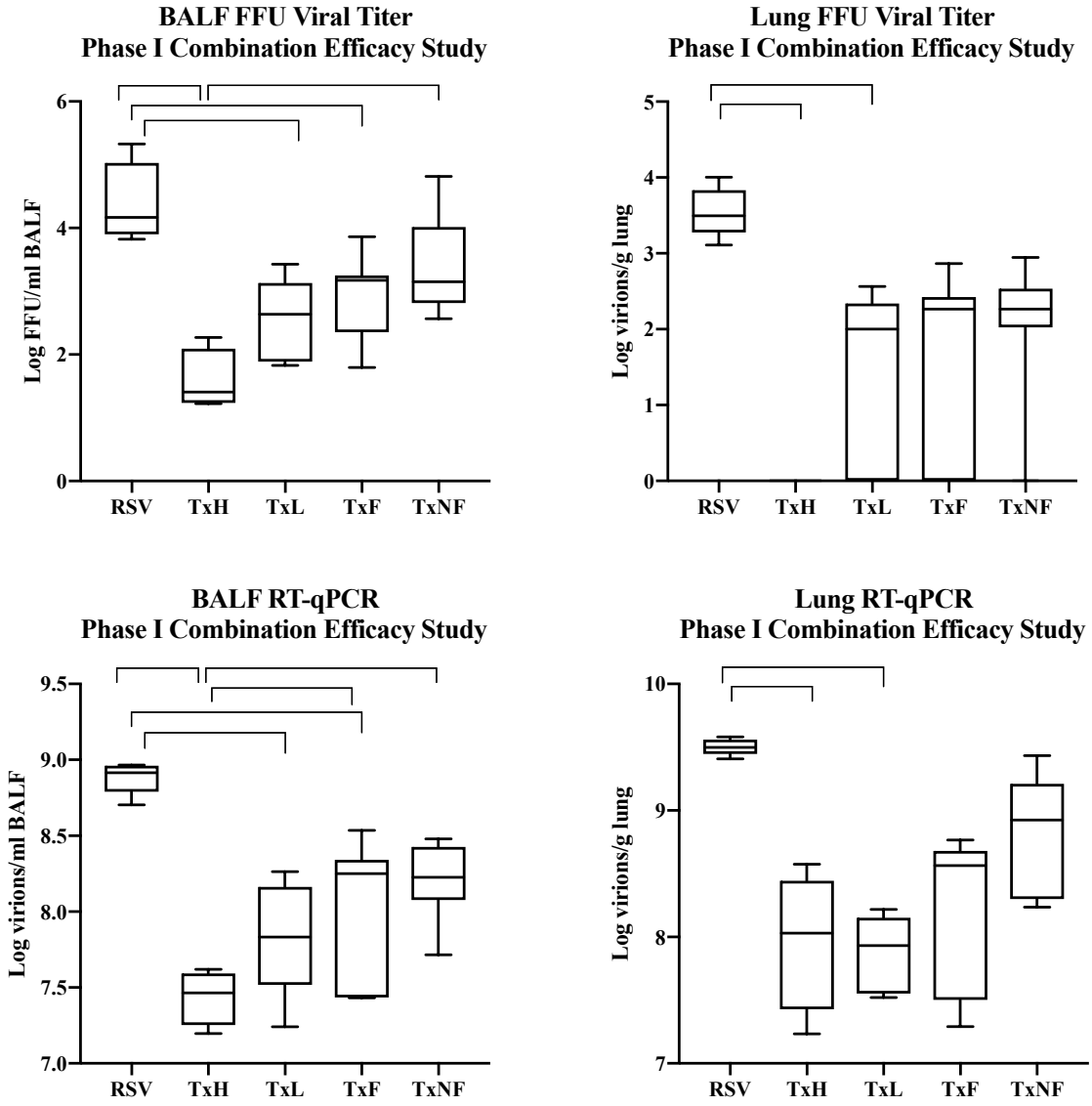

Figure 3: Phase I combination efficacy study viral titer in BALF and lung detected by FFU and RT-qPCR

Levels of viral titer in BALF (top left) and lung (top right) detected by FFU and viral RNA detected in BALF (bottom left) and lung (bottom right) by RT-qPCR in different treatment groups of Phase I combination treatment efficacy study.

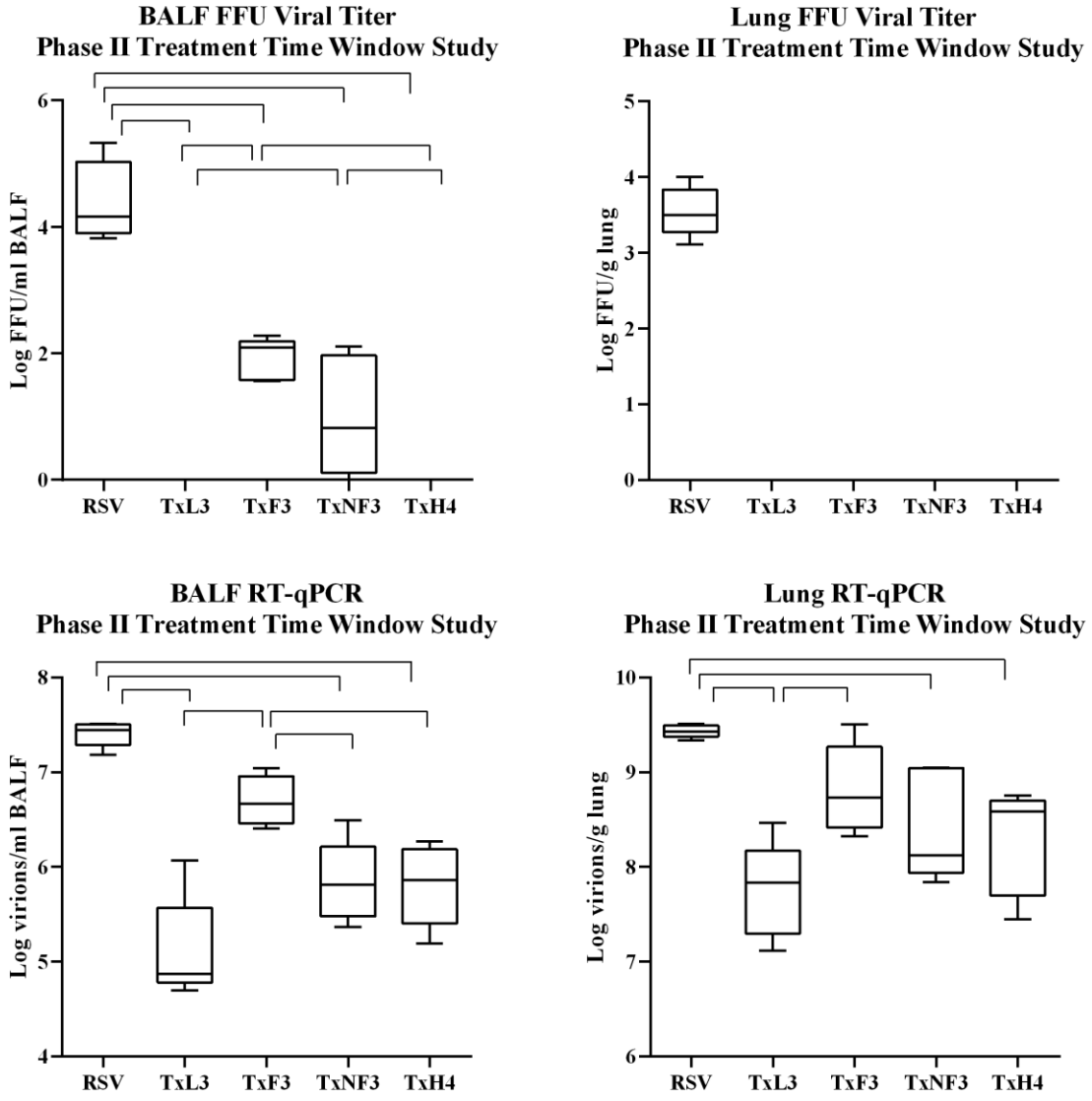

Figure 4: Phase II treatment time window study viral titer in BALF and lung detected by FFU and RT-qPCR

Levels of viral titer in BALF (top left) and lung (top right) detected by FFU and viral RNA detected in BALF (bottom left) and lung (bottom right) by RT-qPCR in different treatment groups of Phase II treatment time window study.

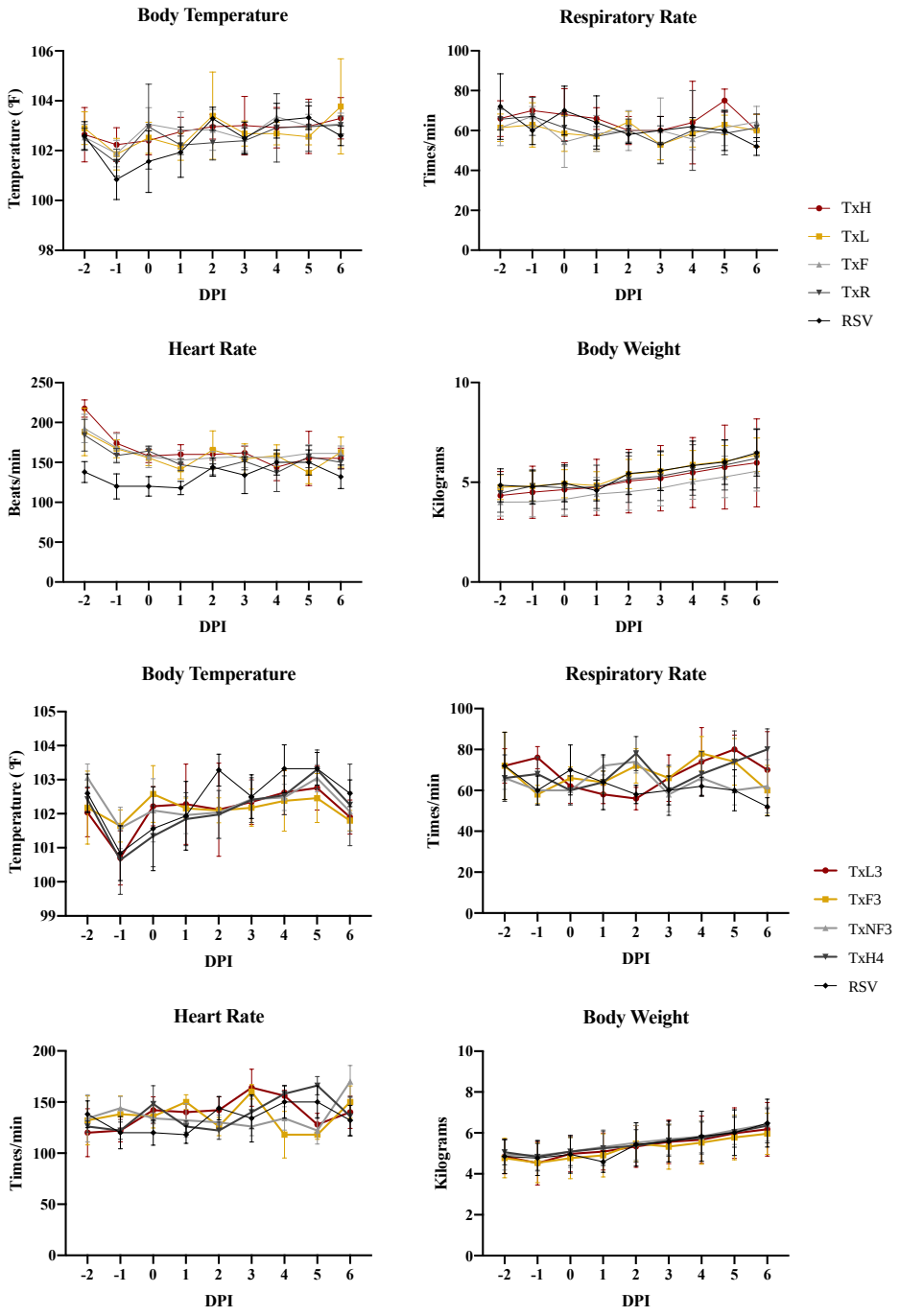

Figure 5: Clinical parameters assessment in Phase I and Phase II combination study

Mean±SD of body temperature, respiratory rate, heart rate and body weight of the lambs measure once daily throughout the Phase I efficacy study (top); combination high dose (TxH), combination low dose (TxL), fusion inhibitor (TxF), non-fusion inhibitor (TxR) and RSV-infected non-treatment group (RSV), and Phase II treatment time window study (bottom); low dose combination given at 3 dpi (TxL3), fusion inhibitor given at 3 dpi (TxF3), non-fusion inhibitor given at 3 dpi (TxNF3) and high dose combination given at 4 dpi (TxH4).

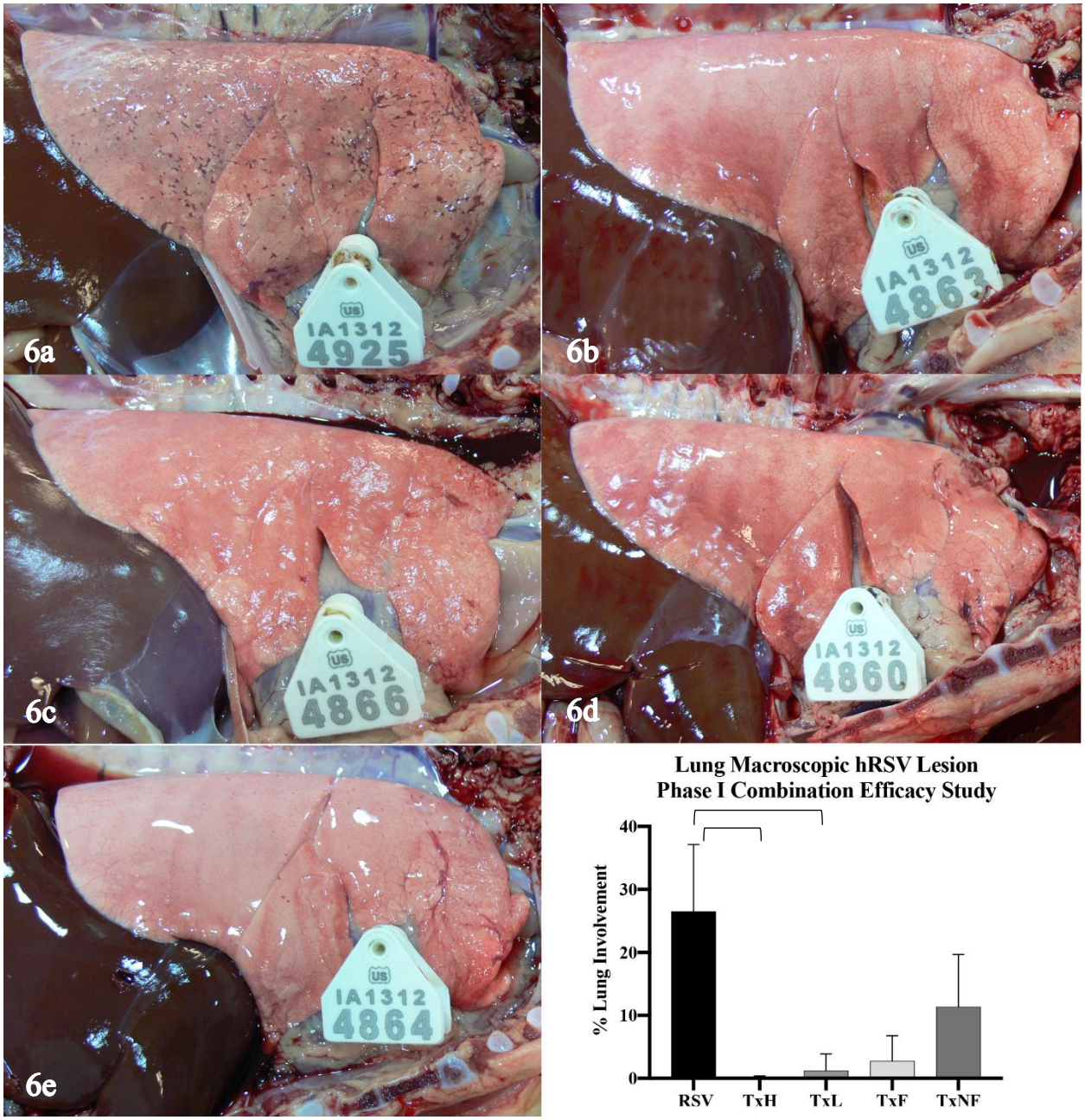

Figure 6: Macroscopic lesions of lungs from Phase I combination efficacy study

Macroscopic lesions of lungs from the combination efficacy study (Phase I); (6a) RSV, (6b) TxH, (6c) TxL, (6d) TxF, and (6e) TxNF. Average percentages of lung lesion are compared in the graph (bottom right).

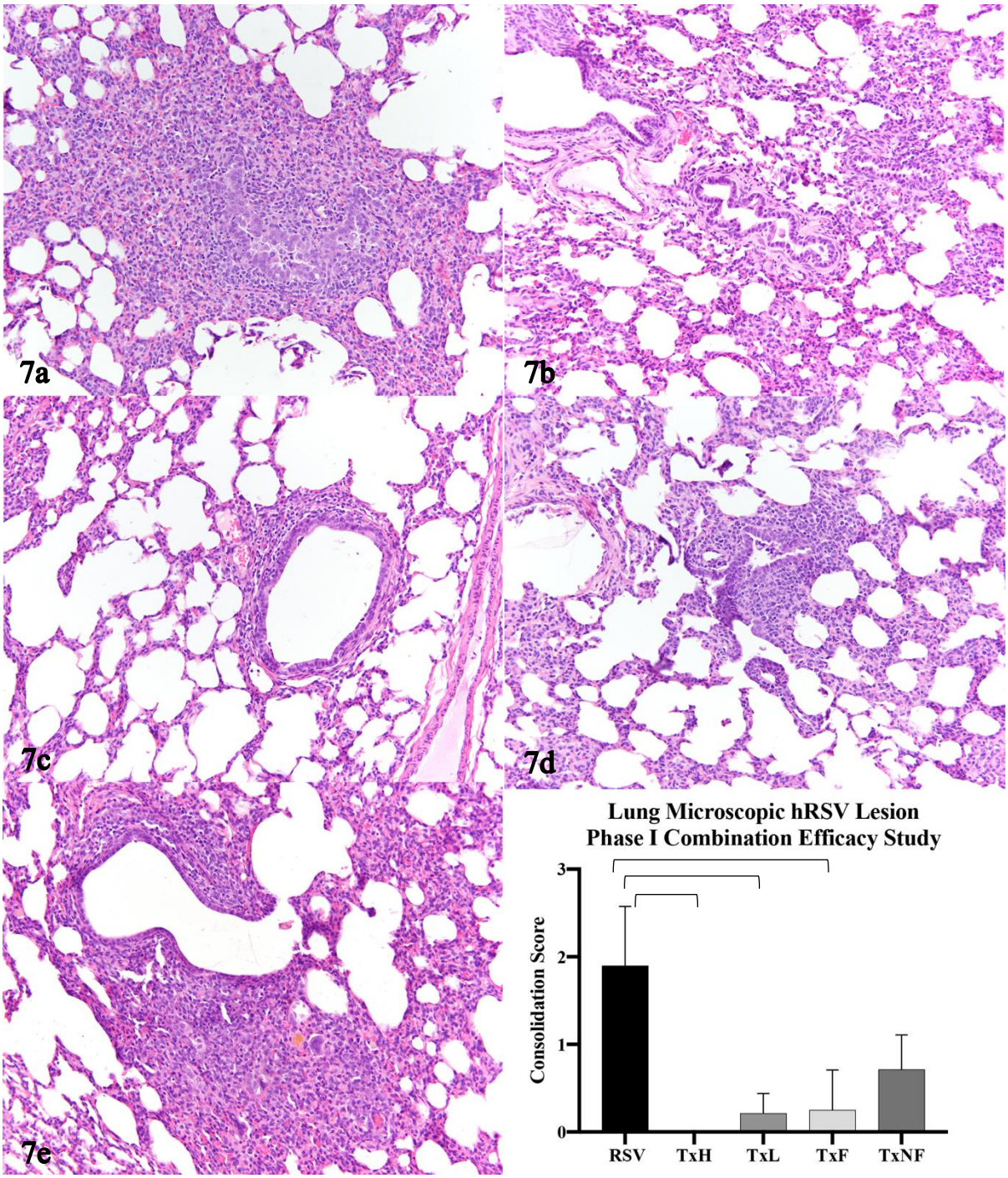

Figure 7: Microscopic lesion in lungs of Phase I combination efficacy study

Pulmonary histopathological changes in lungs from the combination efficacy study (Phase I); (7a) RSV, (7b) TxH, (7c) TxL, (7d) TxF, and (7e) TxNF. Average percentages of microscopic lung consolidation score are compared in the graph (bottom right).

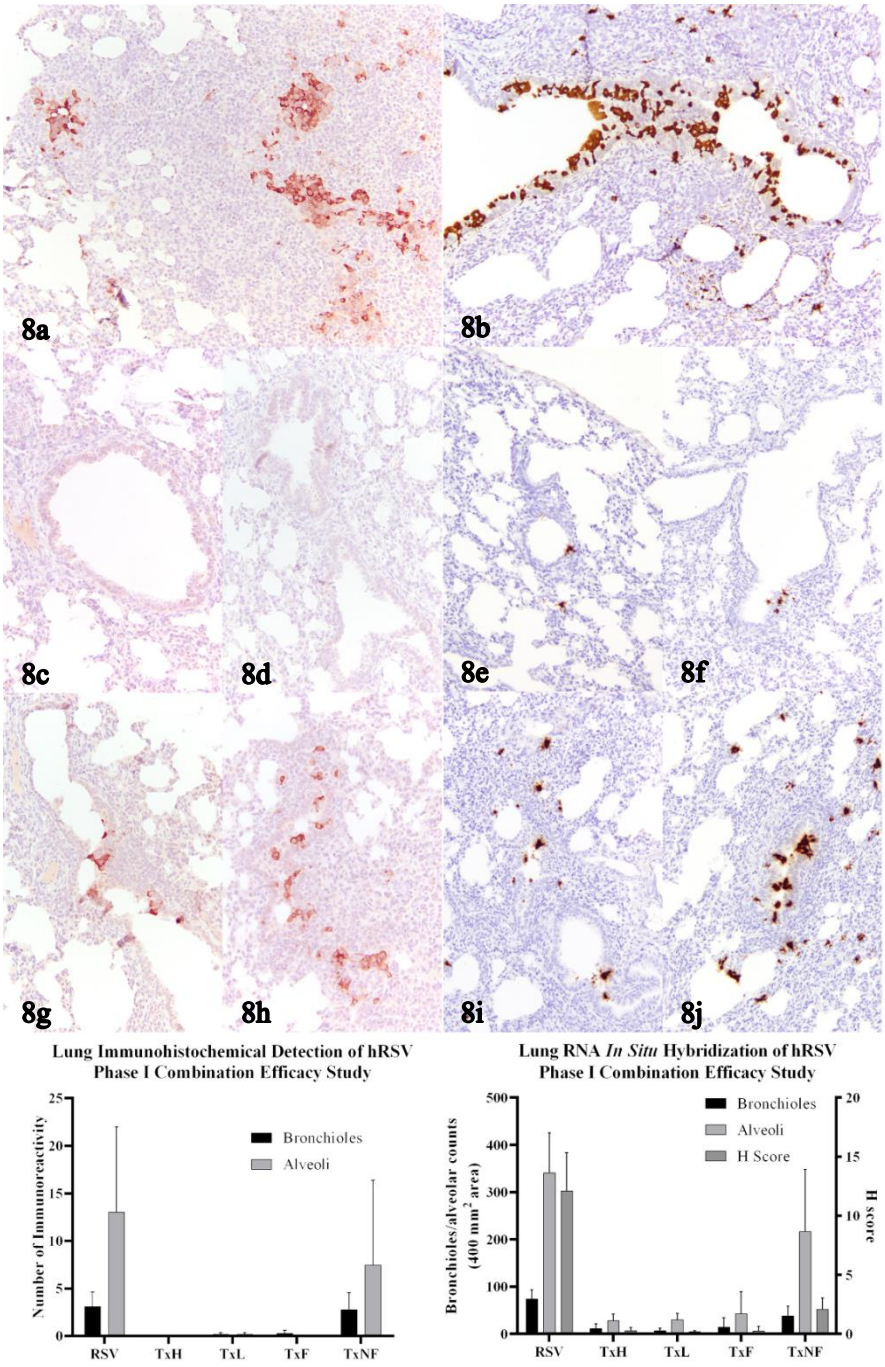

Figure 8: Immunohistochemical detection of RSV antigen and *in situ* hybridization detection of hRSV mRNA in lamb lungs from Phase I combination efficacy study

Immunohistochemical (8a, 8c, 8d, 8g, 8f) and RNA *in situ* hybridization (8b, 8e, 8f, 8i, 8j) of hRSV in different treatment group of Phase I combination efficacy study; RSV (8a, 8b), TxH (8c, 8e), TxL (8d, 8f), TxF (8g, 8i), and TxNF (8h, 8j). The average level of hRSV detected with immunohistochemistry (bottom left) and RNA *in situ* hybridization (bottom right) is compared between different treatment groups.

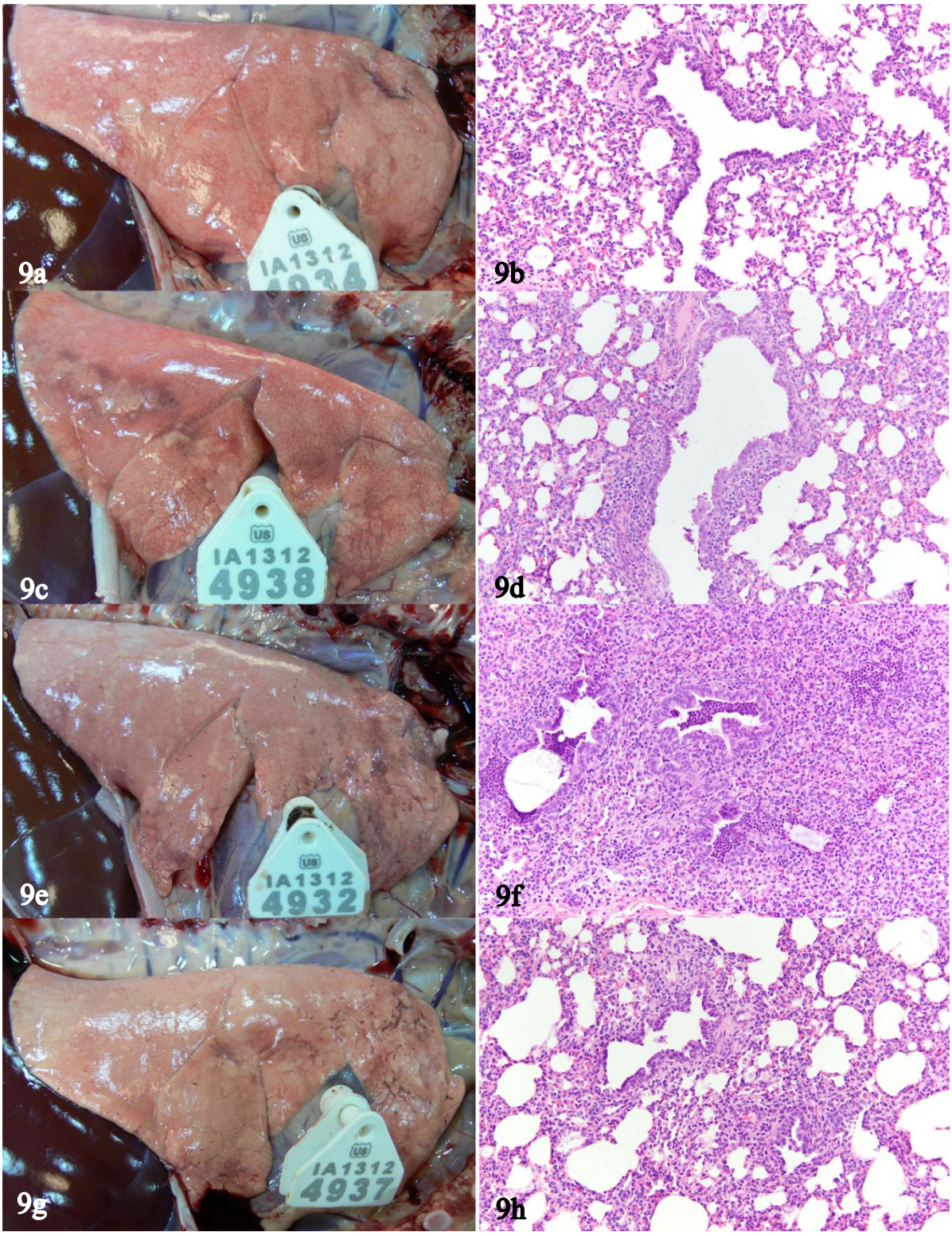

Figure 9: Morphological lesions in the lung from Phase II treatment time window study

Morphological lesions in the lung from the treatment time window study (Phase II); (9a, 9b) TxL3, (9c, 9d) TxF3, (9e, 9f) TxNF3, and (9g, 9h) TxH4.

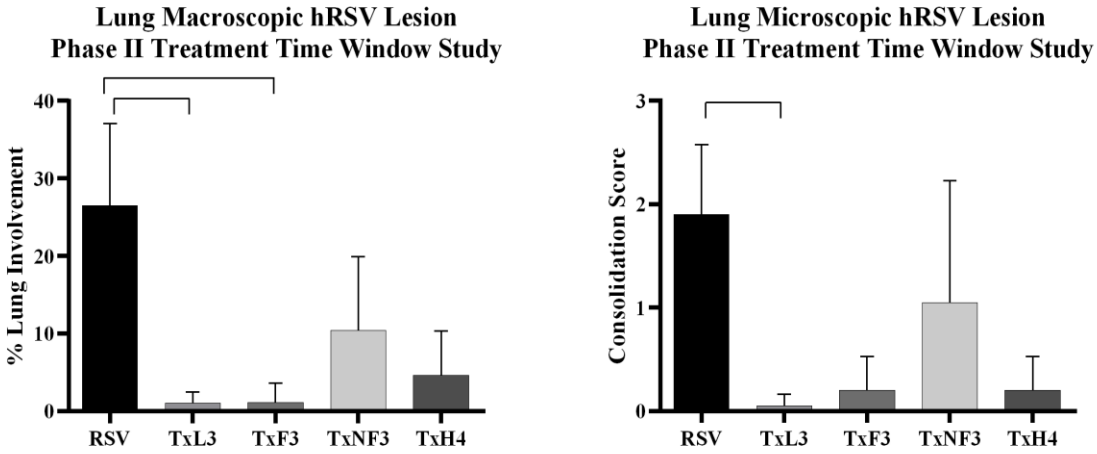

Figure 10: Macroscopic and microscopic hRSV-associated lung lesion from Phase II treatment time window study

The degree of macroscopic (left) and microscopic (right) hRSV-associated lesion of different treatment groups evaluated at 6 days post-infection from the treatment time window study (Phase II).

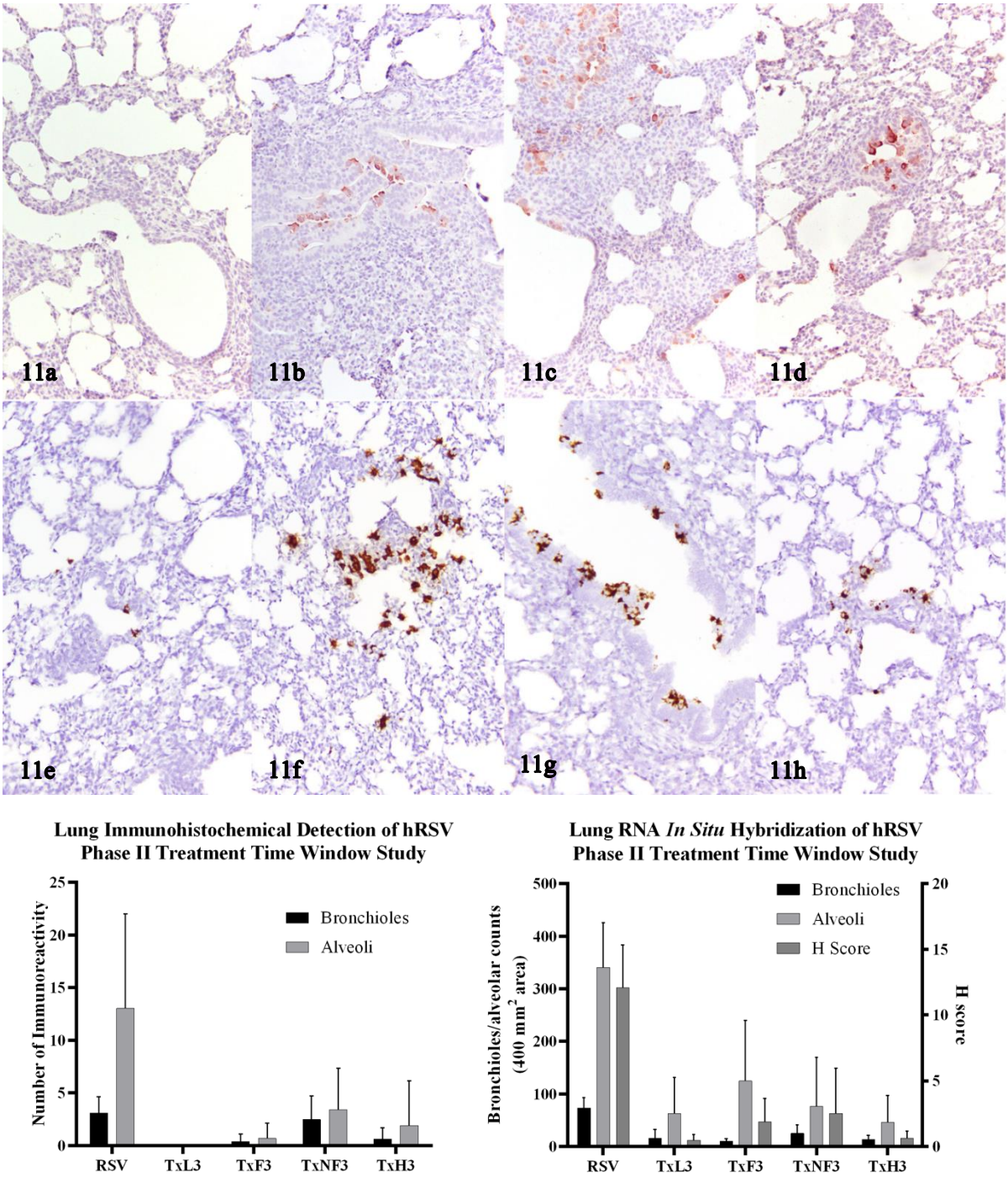

Figure 11: Immunohistochemical detection of RSV antigen *in situ* hybridization detection of hRSV mRNA in lamb lungs from Phase II treatment time window study

Immunohistochemical (11a-d) and RNA *in situ* hybridization (11e-h) of hRSV antigen detected in different treatment group of treatment time window study (Phase II); (11a, 11e) TxL3, (11b, 11f) TxF3, (11c, 11g) TxNF3, and (11d, 11h) TxH4. The average level of hRSV viral antigen detected with immunohistochemistry (bottom left) and RNA *in situ* hybridization (bottom right) is compared between different treatment groups.

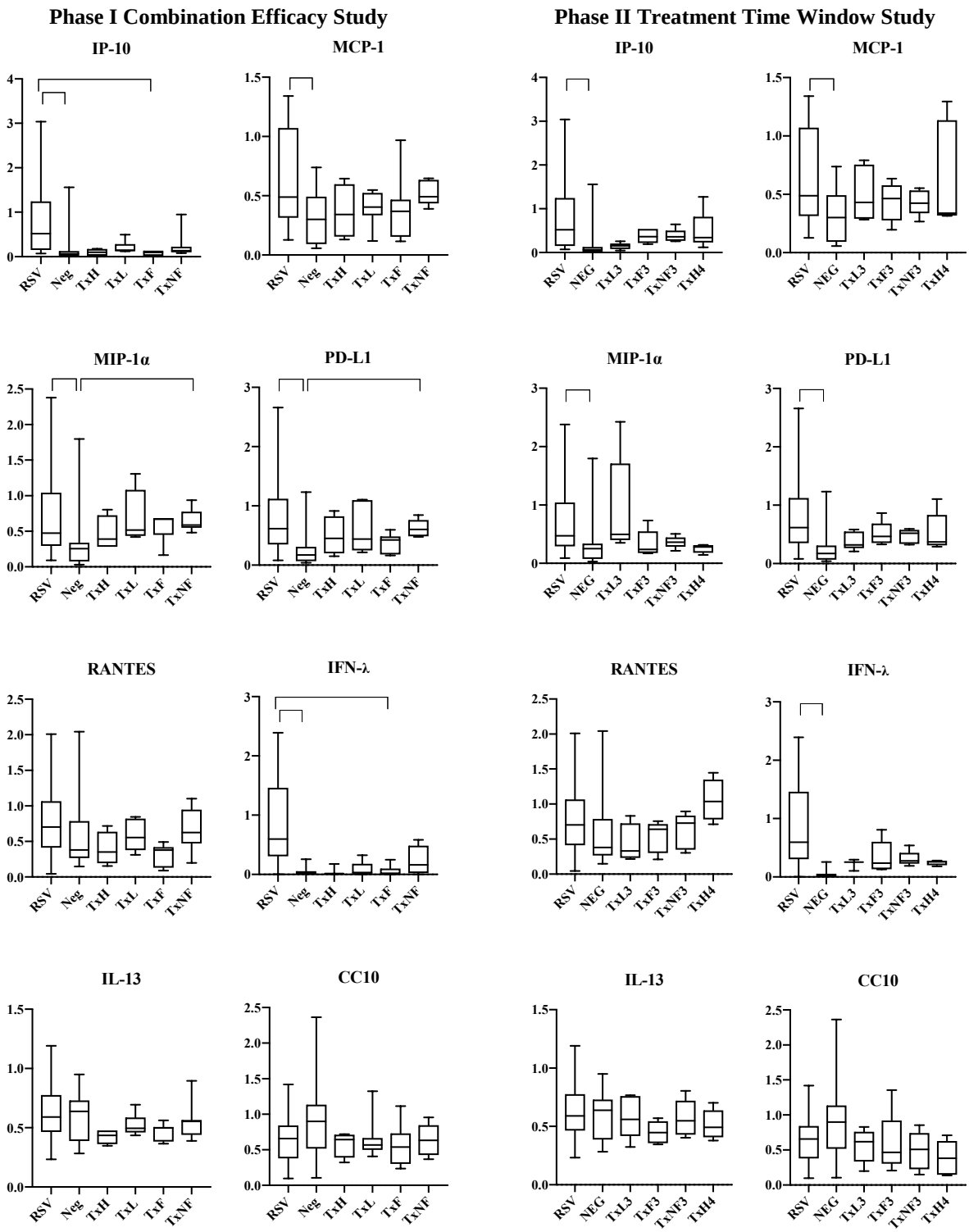

Figure 12: Cytokine and chemokine mRNA expression (IP-10, MCP-1, MIP-1α, PD-L1, RANTES, IFN-λ, IL-13 and CC110) from Phase I and Phase II combination study.

Supplementary Table 1: Microscopic scoring criteria of hRSV infected lung evaluated. Two representative histological sections taken from each right cranial lobe, left cranial lobe, left middle lobe and left caudal lobe were examined per lamb.

Score	1	2	3	4
Microscopic alveolar consolidation (CS)*	1-9% of the evaluated region presented with alveolar consolidation	10-39% of evaluated region presented with alveolar consolidation	40-69% of evaluated region presented with alveolar consolidation	More than or equal to 70% of evaluated region presented with alveolar consolidation
Bronchiolitis (BR)	Minimal detectable lesion (epithelial degeneration) in one or a few bronchioles per 200X field	Epithelial degeneration involving less than 10% of the airway lumen; minimal neutrophils, cell debris; adventitial lymphocytes in multiple bronchioles	Epithelial degeneration involving >10-50% of the airway lumen with cell debris, neutrophils; adventitial lymphocytes; multiple bronchioles	Circumferential bronchiolitis with dense adventitial lymphocytes; multiple bronchioles affected
Syncytial formation (SYN)	One distinct syncytial cell	Up to three in three 200x fields	More than three in three fields	Numerous
Epithelial necrosis (EN)	Minimally detectable in one or a few per 20x per field	10% in multiple airways per field	10-50% in multiple airways per field	Circumferential in multiple airways
Epithelial hyperplasia (EH)	Minimally detectable in one or a few airways per 20X field	10% of airway per field	10-50% in multiple airways per field	Circumferential
Neutrophil infiltrates (NEU)	Minimally detectable	10 or less neutrophils in one or a few airways/alveoli	10 or more neutrophils in several airways/alveoli	10 or more involving many/most airways/alveoli
Peribronchiolar lymphoplasmacytic infiltrates (BN)	Earliest detectable lymphocytic infiltrates in the adventitia	Segmental to circumferential infiltrates	Circumferential infiltrates that expand more than three cells wide	Circumferential infiltrates that for nodules.
Perivascular lymphoplasmacytic infiltrates (VN)	Earliest detectable lymphocytic infiltrates in the adventitia	Segmental to circumferential infiltrates	Circumferential infiltrates that expand more than three cells wide	Circumferential infiltrates that for nodules.

* CS scoring is based on evaluation of 20, 200X field per slide (field number 22) with a single slide containing two lung sections representing each lung lobe.

Supplementary Table 2: List of RT-qPCR forward primers, reverse primers and probes sequences for each target.

Target	Forward primers	Reverse primers	Probes
RSV M37	5'-GCTCTTAGCAAAGTCAAGTTGAACGA	5'-TGCTCCGTTGGATGGTGTATT	6FAM-ACACTCAACAAAGATCAACTTCTGTCATCCAGC-TAMRA
IP-10	5'-CACCCTGAGCTGTTCAGTAGTGA	5'-GCGCCCCGGTATAGCTTAC	6FAM-CCCTGGCACTGTGAC-MGBNFQ
MIP-1α	5'-CAGCAGCCAGTGCTCCAA	5'-ACCTGCCGGCCTTTTTTG	6FAM-CCTGGTGTCATCTTCCAGA-MGBNFQ
PD-L1	5'-TGGTCATCCCAGAACCATATCTAG	5'-CCCAGAGTCACCAAGTGATTCC	6FAM-TCCAGCAAAAAAG-MGBNFQ
MCP-1	5'-GCTGTGATTTTCAAGACCATCCT	5'-GGGCGGGAGATATAGGCAAA	6FAM-AAAGAGTTTTGTGCAGACCCCAACC-TAMRA
RANTES	5'-TGCTTCTGCCTCCCCATATG	5'-GGGCGGGAGATATAGGCAAA	6FAM-CACCACGCCCTGCT-MGBNFQ
IL-13	5'-CAGCCCTGGACTCCCTGAT	5'-CCTCTTGGTCCTGTGGATGAC	6FAM-AGCATCTCCAACTGC-MGBNFQ
IFN-λ	5'-TCCCAGGACTGCCTCGAA	5'-GGGTGAGGAGGCGGAAGA	6FAM-CCTCCGTGATGTTCA-MGBNFQ
CC10	5'-GCTGCCCTGGAACCTTTCA	5'-CCTTCAGCTGTCTTGTTGCTTCT	6FAM-CCCTGACGAAGACATG-MGBNFQ

CHAPTER 5. GENERAL CONCLUSIONS

Suitable methods for prevention, treatment and control of human respiratory syncytial virus (hRSV) infection are needed. Currently, no vaccine or therapy has proven to be fully successful and none have advanced pass all required clinical trials. In hopes for future disease alleviation, many antiviral compounds have been tested in laboratory settings and animal models to identify promising drug candidates for hRSV treatment. The main goal of this dissertation was to assess the therapeutic efficacy of orally administered small molecule inhibitor(s) against hRSV in newborn lambs as a model of hRSV infection and bronchiolitis infants.

In Chapter 2, we described in detail the method for evaluating orally administered small molecule antiviral compound to hRSV-infected lambs and demonstrated the therapeutic efficacy of hRSV fusion protein inhibitor, JNJ-53718678. We identified a reduction of pulmonary viral load and lung lesions in a dose-dependent manner and demonstrated a profound reduction with appropriate dosage when administered within the 24 hours post infection (hpi). This potent antiviral compound has good potential as a drug candidate and had advanced into the clinical trial phase.

In Chapter 3 we explored another therapeutic target for the treatment of hRSV infection that inhibits viral replication. The small molecule replication inhibitor, JNJ-64166037, was administered orally to hRSV-infected lambs at 1 hpi. This compound effectively reduced viral load and pulmonary lesions in a dose-dependent manner, thus characterizing another potential antiviral therapeutic compound that inhibits a different stage of viral infection specifically at the viral replication cycle. In addition to the routine viral isolation assay, molecular assay and immunohistochemical staining to quantify and localize the hRSV antigen in the lungs of our

lambs, we performed a recently developed technique, RNA *in situ* hybridization (RNAscope®) analysis on the lung tissues in order to identify cellular localization of RSV mRNA and estimate the density of virus in each cell. We were able to modify an RNAscope® evaluation method (H scoring) using image analyzer software to efficiently quantify the amount of hRSV mRNA present in the lung tissue samples.

The last part of this dissertation, Chapter 4, we administered combination antiviral treatment of fusion and replication inhibitors in lambs infected with hRSV in order to first, investigate the therapeutic efficacy compared to that of monotherapy, and second, to evaluate the treatment time window of compound administration. We determined that the combination treatment at 24 hpi was able to decrease the average viral load and lung lesion more extensively than single administration of fusion and replication inhibitors. In addition, administering the combination therapy at 3- and 4-days post-infection (dpi) demonstrated significant reduction of viral load and pulmonary lesions compared to monotherapy of fusion inhibitor at 3 dpi, indicating a wider window for treatment which is more practical in clinical settings. A new approach of cytokine expression analysis was applied in this study for the hRSV Memphis 37 infected lambs, by combining the cytokines mRNA expression in the lung from multiple studies in the hRSV-infected positive control and non-infected negative control animals at 6 dpi to create a profile and baseline of cytokines expression for future pathogenesis studies and comparison with treated animals.

The research completed in this dissertation has shed some light towards potential treatments for hRSV infection and further demonstrated the potential of hRSV infected lambs as a model of hRSV infection in infants. Questions remain on the potency, dosage, safety, possible drug interactions when these compounds are administered with other compounds.

There are potential adverse drug reactions of these hRSV small molecule inhibitors when used in humans and infants as for any medication. These issues may be assessed and elucidated with advancement through multiple phases of clinical trials. Lambs infected with hRSV mimics hRSV infection in infants, but immunological responses by lambs could be further characterized through a complete kinetic assessment of cytokine profile response for different strains of hRSV and also the type of cellular immune response [1, 2], and long-term immunological changes in lamb lungs previously infected with hRSV. Moreover, some immunologic responses may prime lungs for asthma later in life and allergic reactions, both of which are reported in human infants [3-7]. Lambs may also be suitable for studies of other respiratory viral pathogens such as metapneumovirs, adenovirus, parainfluenza virus and bacterial infections.

References

1. McGill JL, Rusk RA, Guerra-Maupome M, Briggs RE, Sacco RE. Bovine Gamma Delta T Cells Contribute to Exacerbated IL-17 Production in Response to Co-Infection with Bovine RSV and Mannheimia haemolytica. PLoS One. 2016;11(3):e0151083. Epub 2016/03/04. doi: 10.1371/journal.pone.0151083. PubMed PMID: 26942409; PubMed Central PMCID: PMCPMC4778910.

2. McGill JL, Sacco RE. γδ T cells and the immune response to respiratory syncytial virus infection. Vet Immunol Immunopathol. 2016;181:24-9. Epub 2016/02/21. doi: 10.1016/j.vetimm.2016.02.012. PubMed PMID: 26923879.

3. Knudson CJ, Varga SM. The relationship between respiratory syncytial virus and asthma. Vet Pathol. 2015;52(1):97-106. Epub 2014/02/10. doi: 10.1177/0300985814520639. PubMed PMID: 24513802.

4. Sigurs N, Bjarnason R, Sigurbergsson F, Kjellman B. Respiratory syncytial virus bronchiolitis in infancy is an important risk factor for asthma and allergy at age 7. Am J Respir Crit Care Med. 2000;161(5):1501-7. doi: 10.1164/ajrccm.161.5.9906076. PubMed PMID: 10806145.

5. Sigurs N, Gustafsson PM, Bjarnason R, Lundberg F, Schmidt S, Sigurbergsson F, et al. Severe respiratory syncytial virus bronchiolitis in infancy and asthma and allergy at age 13. Am J Respir Crit Care Med. 2005;171(2):137-41. Epub 2004/10/29. doi: 10.1164/rccm.200406-730OC. PubMed PMID: 15516534.

6. Sigurs N, Aljassim F, Kjellman B, Robinson PD, Sigurbergsson F, Bjarnason R, et al. Asthma and allergy patterns over 18 years after severe RSV bronchiolitis in the first year of life. Thorax. 2010;65(12):1045-52. Epub 2010/06/27. doi: 10.1136/thx.2009.121582. PubMed PMID: 20581410.

7. Wu P, Hartert TV. Evidence for a causal relationship between respiratory syncytial virus infection and asthma. Expert Rev Anti Infect Ther. 2011;9(9):731-45. doi: 10.1586/eri.11.92. PubMed PMID: 21905783; PubMed Central PMCID: PMCPMC3215509.